



OKLAHOMA TRANSPORTATION CENTER

ECONOMIC ENHANCEMENT THROUGH INFRASTRUCTURE STEWARDSHIP

REAL-TIME MEASUREMENT OF QUALITY DURING THE COMPACTION OF SUBGRADE SOILS

**SESH COMMURI, PH.D.
MUSHARRAF ZAMAN, PH.D., P.E.
MANIK BARMAN
MOEEN NAZARI
SYED IMRAN
FARES BEAINY**

OTCREOS10.1-11-F

Oklahoma Transportation Center
2601 Liberty Parkway, Suite 110
Midwest City, Oklahoma 73110

Phone: 405.732.6580
Fax: 405.732.6586
www.oktc.org

DISCLAIMER

The contents of this report reflect the views of the authors, who are responsible for the facts and accuracy of the information presented herein. This document is disseminated under the sponsorship of the Department of Transportation University Transportation Centers Program, in the interest of information exchange. The U.S. Government assumes no liability for the contents or use thereof.

TECHNICAL REPORT DOCUMENTATION PAGE

1. REPORT NO. OTCREOS10.1-11-F	2. GOVERNMENT ACCESSION NO.	3. RECIPIENTS CATALOG NO.	
4. TITLE AND SUBTITLE Real-time measurement of quality during the compaction of subgrade soils		5. REPORT DATE December 31, 2012	
		6. PERFORMING ORGANIZATION CODE	
7. AUTHOR(S) Sesh Commuri, Musharraf Zaman, Manik Barman, Moeen Nazari, Syed Imran, Fares Beainy		8. PERFORMING ORGANIZATION REPORT	
9. PERFORMING ORGANIZATION NAME AND ADDRESS The University of Oklahoma 110 W. Boyd Street, DEH 432 Norman, Oklahoma 73019		10. WORK UNIT NO.	
		11. CONTRACT OR GRANT NO. DTRT06-G-0016	
12. SPONSORING AGENCY NAME AND ADDRESS Oklahoma Transportation Center (Fiscal)– 201 ATRC– Stillwater, OK 74078 (Technical) 2601 Liberty Parkway, Suite 110 Midwest City, OK 73110		13. TYPE OF REPORT AND PERIOD COVERED Final June 01, 2010-December 31, 2012	
		14. SPONSORING AGENCY CODE	
15. SUPPLEMENTARY NOTES University Transportation Center			
16. ABSTRACT <p>Conventional quality control of subgrade soils during their compaction is usually performed by monitoring moisture content and dry density at a few discrete locations. However, randomly selected points do not adequately represent the entire compacted area and could leave soft spots undetected. If not rectified, these soft spots can adversely affect the performance and longevity of the asphalt pavements constructed on top of the prepared subgrade soil. This report presents the findings of a study investigating the ability of the Intelligent Asphalt Compaction Analyzer (IACA), developed at The University of Oklahoma, to estimate the resilient modulus (M_r) of cementitiously stabilized subgrade soils in real-time during their compaction. Preliminary feasibility studies were carried out at two different sites in Year One of the study. These results were then used to develop calibration and estimation procedures for the IACA. The validation of the IACA was carried out at two different project sites in Year Two of the study. Virgin soil and additives from each of these sites were first collected and their properties were studied in the laboratory. Regression models were then developed to analyze the dependence of the subgrade stiffness (M_r) on the soil properties and level of compaction. Tests using Falling Weight Deflectometer (FWD) and Nuclear Density Gauge were conducted at select locations on the stabilized subgrade after compaction. IACA estimated M_r values were then compared with FWD backcalculated moduli and M_r values predicted using the regression models. The results of these tests reveal that the calibrated IACA can be used to estimate the resilient modulus of the soil in real time during compaction with an accuracy that is suited for quality control applications.</p>			
17. KEY WORDS Intelligent Compaction, Soil Subgrade, Stiffness, Resilient Modulus		18. DISTRIBUTION STATEMENT No restrictions. This publication is available at www.oktc.org and from the NTIS.	
19. SECURITY CLASSIF. (OF THIS REPORT) Unrestricted	20. SECURITY CLASSIF. (OF THIS PAGE) Unrestricted	21. NO. OF PAGES 89 + covers	22. PRICE

SI (METRIC) CONVERSION FACTORS

Approximate Conversions to SI Units				
Symbol	When you know	Multiply by	To Find	Symbol
LENGTH				
in	inches	25.40	millimeters	mm
ft	feet	0.3048	meters	m
yd	yards	0.9144	meters	m
mi	miles	1.609	kilometers	km
AREA				
in ²	square inches	645.2	square millimeters	mm ²
ft ²	square feet	0.0929	square meters	m ²
yd ²	square yards	0.8361	square meters	m ²
ac	acres	0.4047	hectares	ha
mi ²	square miles	2.590	square kilometers	km ²
VOLUME				
fl oz	fluid ounces	29.57	milliliters	mL
gal	gallons	3.785	liters	L
ft ³	cubic feet	0.0283	cubic meters	m ³
yd ³	cubic yards	0.7645	cubic meters	m ³
MASS				
oz	ounces	28.35	grams	g
lb	pounds	0.4536	kilograms	kg
T	short tons (2000 lb)	0.907	megagrams	Mg
TEMPERATURE (exact)				
°F	degrees Fahrenheit	(°F-32)/1.8	degrees Celsius	°C
FORCE and PRESSURE or STRESS				
lbf	poundforce	4.448	Newtons	N
lbf/in ²	poundforce per square inch	6.895	kilopascals	kPa

Approximate Conversions from SI Units				
Symbol	When you know	Multiply by	To Find	Symbol
LENGTH				
mm	millimeters	0.0394	inches	in
m	meters	3.281	feet	ft
m	meters	1.094	yards	yd
km	kilometers	0.6214	miles	mi
AREA				
mm ²	square millimeters	0.00155	square inches	in ²
m ²	square meters	10.764	square feet	ft ²
m ²	square meters	1.196	square yards	yd ²
ha	hectares	2.471	acres	ac
km ²	square kilometers	0.3861	square miles	mi ²
VOLUME				
mL	milliliters	0.0338	fluid ounces	fl oz
L	liters	0.2642	gallons	gal
m ³	cubic meters	35.315	cubic feet	ft ³
m ³	cubic meters	1.308	cubic yards	yd ³
MASS				
g	grams	0.0353	ounces	oz
kg	kilograms	2.205	pounds	lb
Mg	megagrams	1.1023	short tons (2000 lb)	T
TEMPERATURE (exact)				
°C	degrees Celsius	9/5+32	degrees Fahrenheit	°F
FORCE and PRESSURE or STRESS				
N	Newtons	0.2248	poundforce	lbf
kPa	kilopascals	0.1450	poundforce per square inch	lbf/in ²

ACKNOWLEDGEMENTS

The field demonstration presented in this report would not have been possible without the unparalleled support of Haskell Lemon Construction Company (HLCC), Oklahoma City, Oklahoma and Silver Star Construction Company, Moore, Oklahoma. Access to HLCC's construction sites and equipment as well as their technical staff has been vital to the success of this project. In particular, the authors wish to thank Jay Lemon (Chief Executive Officer, HLCC), Bob Lemon (Chief Operations Officer, HLCC), and Craig Parker (Vice-President, Silver Star Construction Company) for their vision and unqualified support of the research team. Their partnership with OU has been critical for the success of this project.

The authors also wish to acknowledge the financial support of Oklahoma Transportation Center. The financial support and technical partnership with Volvo Construction Equipment (VCE), Shippensburg, PA has been central to the OU's research in Intelligent Compaction. The assistance of Burgess Engineering, Moore, Oklahoma in conducting spot tests for pavement quality is also greatly appreciated.

CONTINUOUS REAL TIME MEASUREMENT OF PAVEMENT QUALITY DURING CONSTRUCTION

Research Project

**Sesh Commuri†
Gerald Tuma Presidential Professor**

**Musharraf Zaman††
David Ross Boyd Professor and Aaron Alexander Professor
Associate Dean for Research and Graduate Programs**

**Manik Barman†††
Research Fellow**

**Moeen Nazari †††
Ph. D. Student**

**Syed Asif Imran†
Ph. D. Student**

**Fares Beainy†
Research Fellow**

†School of Electrical and Computer Engineering
The University of Oklahoma
110 W. Boyd, Street, DEH 432
Norman, Oklahoma 73019

††College of Engineering
The University of Oklahoma
202 W. Boyd, Street, CEC 106
Norman, Oklahoma 73019

†††School of Civil Engineering and Environmental Sciences
The University of Oklahoma
202 W. Boyd, Street, CEC 334
Norman, Oklahoma 73019

**Oklahoma Transportation Center
2601 Liberty Parkway, Suite 110
Midwest City, Oklahoma 73110**

TABLE OF CONTENTS

1. EXECUTIVE SUMMARY	x
2. INTRODUCTION	1
3. GOALS OF THE PROPOSED RESEARCH	5
4. RESULTS OF THE RESEARCH PROJECT	6
4.1 Rock Creek Road, Norman, Oklahoma	9
4.2 Hefner Road, Edmond, Oklahoma	16
4.3 60 th Street, Norman, OK.....	17
4.4 Apple Valley, Oklahoma City, OK.....	36
4.5 Generic Regression Models	55
5. OUTCOMES OF THE RESEARCH AND CONCLUSIONS	58
5. RECOMMENDATIONS AND SCOPE FOR FUTURE WORK.....	60
7. TECHNOLOGY TRANSFER SUCESSSES	62
8. REFERENCES	63
APPENDIX A	66

LIST OF FIGURES

Figure 1. Flowchart of the activities involved in estimation of pavement stiffness by the IACA (Commuri And Zaman, 2008).....	4
Figure 2. Stabilization of soil subgrade with fly-ash using a Terex RS-500C stabilizer. 10	
Figure 3. Compaction of the stabilized subgrade using Ingersoll-Rand SD115F compactor.	11
Figure 4. Prepared soil subgrade.	11
Figure 5. Moisture content vs dry density relationship for the raw soil.	13
Figure 6. Comparison between the IACA estimated density of the stabilized subgrade and the density of asphalt layer constructed on top of the stabilized subgrade.....	15
Figure 7. Comparison of compaction of soil subgrade and asphalt base layers at the 12 test stations.	17
Figure 8. Particle size distribution of soil.	19
Figure 9. Proctor test results for the raw soil.	19
Figure 10. Proctor test results for 10% CKD-mixed soil.	20
Figure 11. M_r as a function of stress state at moisture content = OMC-2%,.....	22
Figure 12. M_r as a function of stress state at moisture content = OMC-2%,.....	22
Figure 13. M_r as a function of stress state at moisture content = OMC-2%,.....	23
Figure 14. M_r as a function of stress state at moisture content = OMC,	23
Figure 15. M_r as a function of stress state at moisture content = OMC,	24
Figure 16. M_r as a function of Stress state at moisture content = OMC,	24
Figure 17. M_r as a function of stress state at moisture content = OMC -2%, Specimen No. 1.....	25
Figure 18. M_r as a function of stress state at moisture content = OMC -2%.....	26
Figure 19. M_r as a function of stress state at moisture content = OMC -2%,.....	26
Figure 20. M_r as a function of stress state at moisture content = OMC, Specimen No. 4.	27
Figure 21. M_r as a function of stress state at moisture content = OMC,	27
Figure 22. M_r as a function of stress state at moisture content = OMC,	28
Figure 23. Actual vs predicted M_r at 0-day curing period.....	30
Figure 24. Actual vs predicted M_r at 28-day curing period.....	30
Figure 25. Predictability of the regression model developed for relating the 0- and 28-day M_r	31
Figure 26. Correlation between FWD backcalculated 28-day moduli and IACA predicted 0-day M_r	34
Figure 27. Correlation between FWD backcalculated 0-day Moduli and IACA estimated 0-day M_r	35
Figure 28. IACA estimated M_r and FWD backcalculated moduli of subgrade at 0-day at different stations.	36
Figure 29. Particle size distribution of soil.	38
Figure 30. Moisture content and dry density relationship for raw soil.	38
Figure 31. Moisture content and dry density relationship for CKD mixed soil.....	39
Figure 32. M_r as a function of stress state at moisture content = OMC-2%,.....	41
Figure 33. M_r as a function of stress state at moisture content = OMC-2%,.....	42
Figure 34. M_r as a function of stress state at moisture content = OMC-2%,.....	42

Figure 35. M_r as a function of stress state at moisture content = OMC,	43
Figure 36. M_r as a function of stress state at moisture content = OMC-2%,.....	44
Figure 37. M_r as a function of stress state at moisture content = OMC-2%,.....	44
Figure 38. M_r as a function of stress state at moisture content = OMC-2%,.....	45
Figure 39. M_r as a function of stress state at moisture content = OMC,	45
Figure 40. M_r as a function of stress state at moisture content = OMC, Specimen No.5.	46
Figure 41. M_r as a function of stress state at moisture content = OMC, Specimen No.6.	46
Figure 42. Predicted vs actual M_r values at 0-day curing period.	48
Figure 43. Predicted vs actual M_r values at 28-day curing period.	49
Figure 44. Predictability of the regression model developed for relating the 0-day M_r and 28-day M_r	50
Figure 45. Correlation between the IACA estimated 0-day M_r and laboratory model predicted 28-day M_r	53
Figure 46. Correlation between the IACA estimated 0-day M_r and laboratory model predicted 0-day M_r	53
Figure 47. IACA estimated M_r and laboratory model predicted M_r at different stations.	54
Figure 48. Validation of the generic regression model for 28-day M_r	57

LIST OF TABLES

Table 1. Summary of soil properties.....	13
Table 2. Densities of the soil subgrade and asphalt base layer at the different test stations.....	14
Table 3. Field moisture contents and degree of compactions at the twelve stations.....	20
Table 4. Moisture contents, dry densities and degree of compactions for the resilient modulus specimens.....	21
Table 5. Value of coefficients in the constitutive model for 0-day curing period.....	28
Table 6. Value of coefficients in the constitutive model for 28-day curing period.....	28
Table 7. IACA estimated moduli for the 9 test stations considered in the analysis.....	32
Table 8. FWD moduli for the 9 test stations considered in the analysis.....	33
Table 9. Moisture contents, dry densities and degree of compaction at.....	40
Table 10. Moisture content, dry density and degree of compaction for the resilient modulus test specimens.....	40
Table 11. Value of the coefficients in the constitutive model for 0-day curing.....	47
Table 12. Value of the coefficients in the constitutive model for 28-day curing.....	47
Table 13. Predicted 28-day resilient modulus at the twelve stations.....	51
Table 14. Predicted 0-day resilient modulus at the twelve stations.....	51
Table 15. IACA measured modulus for the 12 test stations.....	52
Table 16. Comparison of the moduli obtained through different methods.....	52
Table 17. Comparison of the moduli obtained through different methods.....	56

1. EXECUTIVE SUMMARY

The long term performance of an asphalt pavement depends on the quality of the supporting subgrade. A well designed and compacted subgrade would drain well, have high strength, and have adequate load bearing capacity to support the pavement layers. Preparation of the soil subgrade layer for an asphalt pavement typically requires stabilization of the soil using additives, usually cement kiln dust (CKD) or lime, and subsequent compaction using vibratory rollers. Quality control during the preparation of the subgrade is usually limited to taking spot readings of density and moisture using a Nuclear Density Gauge (NDG). In some instances, additional Dynamic Cone Penetration (DCP), Falling Weight Deflectometer (FWD) test or similar tests are conducted to determine the stiffness/modulus of the compacted subgrade. However, these tests are cumbersome to perform and often do not reveal deficiencies in the preparation of the site. Intelligent Compaction techniques have been proposed to continuously monitor the stiffness of the subgrade during the compaction process and to alter the machine parameters to ensure uniformity in the compaction. In the future, these Intelligent Compaction technologies will have the ability to estimate the modulus of the pavement continuously during its construction. In this research project, OU's Intelligent Asphalt Compaction Analyzer (IACA) was modified to enable the determination of the quality of compaction of cementitiously stabilized subgrade soils during their construction.

In the first year of the research presented in this report, the IACA technology was modified to classify the vibrations of the vibratory compactor during the compaction of cementitiously stabilized soil subgrades that support the other layers of HMA pavements. Raw soil and bulk CKD were collected from the construction site and analyzed in the lab to determine the soil classification. The optimum moisture content (OMC) and maximum dry density (MDD) of the raw soil and the soil modified with CKD were also determined. The resilient modulus and unconfined compressive strength of the raw and modified soil were also experimentally determined. These values were used to establish target compaction values for the calibration of the IACA.

Two sites involving the construction of full-depth asphalt pavements were identified for studying the ability of the IACA to estimate the level of compaction of the cementitiously stabilized soil subgrades. The first investigation was carried out during the extension of Rock Creek Road between Porter and 12th Street NE in Norman, OK. The second investigation was carried out during the rehabilitation of a six mile section of the Heffner Road between Broadway Extension and Sooner Road in Edmond, OK. The following are the observations from the research carried out in the first year of the project.

1. The current study was limited to the use of the IACA on a smooth steel drum vibratory compactor. It was found that the sensors and the computational hardware of the IACA used to estimate stiffness of asphalt pavements could be used for soil compaction without significant modification. The IACA software, on the other hand, had to be modified to account for the differences in the calibration method for the soil and the analysis of the vibration data.
2. The IACA can be used to observe and classify the vibrations of the soil compactor during the compaction of the subgrade soil. Density measurements taken at specific locations of the compacted subgrade using a Nuclear Density Gauge (NDG) were used to calibrate the IACA. The estimated density of the compacted subgrade was verified through NDG measurements at several locations on the compacted subgrade.
3. The effect of the subgrade on the density achieved in the HMA base layer was studied. It was found that lower compaction (density) of the base affects the density that is achieved in the HMA layers constructed on top of the base.
4. The use of steel drum roller makes the IACA technology ideally suited for 'proof rolling' the soil base prior to the construction of HMA pavement layers.

These results were then used to develop calibration and estimation procedures for the IACA. The validation of the IACA was carried out at two different project sites in Year Two of the study. Virgin soil and additives from each of these sites were first collected and their properties were studied in the laboratory. Regression models were then developed to analyze the dependence of the subgrade stiffness (M_r) on the soil properties and level of compaction. Tests using Falling Weight Deflectometer (FWD)

and Nuclear Density Gauge were conducted at select locations on the stabilized subgrade after compaction. IACA estimated M_r values were then compared with FWD backcalculated moduli and M_r values predicted using the regression models. These tests revealed that the IACA estimated modulus correlated well with the FWD-backcalculated subgrade modulus ($R^2 = 0.63$; error = $\pm 15\%$) as well as with the laboratory measured M_r ($R^2 = 0.59$; error = $\pm 15\%$). The results of the project confirm that after calibration, the IACA can be used to estimate the resilient modulus of the soil in real time during compaction with an accuracy that is suited for quality control applications.

The research team is working with its industry partner to commercialize the IACA technology. Current efforts are focused on determining the stiffness of cementitiously stabilized soil subgrades and multiple layers of asphalt pavements during their construction. Future research will include the extension of IACA to the compaction of soil subgrades with lime / fly ash additives, compaction of cohesive soils, and closed-loop control of vibratory compactors during Intelligent Compaction of soils and asphalt pavements.

2. INTRODUCTION

The long term performance of an asphalt pavement depends on the quality of the supporting subgrade. A well designed and compacted subgrade would need to drain well, exhibit good strength, and possesses an adequate load bearing capacity. Compaction is a process of densification of soil by the reduction of air voids and is generally achieved through the use of pad foot and/or smooth drum vibratory compactors. The application of vibratory energy results in an increase in the density and load bearing capacity of the subgrade. Compaction also reduces the potential for changes in moisture to significantly alter the strength of the subgrade (Lambe, 1969). Often, the virgin soil at the site of construction lacks the strength to withstand traffic loads even after compaction. In such cases, it is common practice to add stabilizing agents such as Cement Kiln Dust (CKD), lime, and then perform compaction. During this process, the stabilizing agent is mixed with the virgin soil to the specified depth using reclaimers/stabilizers such as Terex RS-500C. The stabilized soil is then hydrated to optimum moisture level and compacted using padfoot and/or smooth steel drum rollers.

The current state of practice for setting the compaction parameters for the stabilized subgrade is through laboratory testing. The type of stabilizer (or additives) and the amount required for a given soil is determined through tests in the laboratory. For example, Oklahoma DOT (Department of Transportation) selects optimal additive percentage on the basis of pH and 7-day unconfined compressive strength (UCS) test for lime and cement kiln dust (CKD) / Fly-ash (FA), respectively (OHD L-50, 2009). Implementation of the Mechanistic-Empirical Pavement Design Guide (MEPDG) (ARA 2004) requires strength and deformation parameters for critical performance of stabilized soil layer to be considered during the design of pavement layers. One of the important measures of performance to be considered during the design is the stiffness of the subgrade and is specified in terms of the 28-day resilient modulus (M_r).

A review of previous studies (Little,1996; Siekmeier et al., 2000; Lenke et al. 2001; Nazarian et al., 2003; Hoffman et al. 2004; Camargo et al. 2006; Mooney and Rinehart,

2007) reveals that no widely accepted field procedure to evaluate the in-situ Mr values of cementitiously stabilized subgrade soils is available. Dynamic Cone Penetrometer (DCP), Soil Stiffness Gauge (SSG), Plate Loading Test (PLT), Clegg Impact Hammer (CIH), California Bearing Ratio (CBR), Falling Weight Deflectometer (FWD) and Light Weight Deflectometer (LWD) tests were conducted in these studies to evaluate the quality of stabilized subgrade layer. However, a major shortcoming of these devices is that they are spot-testing devices that typically assess much less than 1% of the constructed subgrade (Mooney and Rinehart, 2007). The importance of developing an in-situ test that will measure strength and stiffness of stabilized subgrade layer has been highlighted by Petry et al. (2002) and in the Transportation Research Board Research Needs Statement (TRB, 2009). The ability to ascertain the modulus of soil subgrade during compaction will enable the identification and remediation of soft spots in the subgrade prior to the construction of asphalt overlays. Uniform and well compacted subgrade can reduce early deterioration of pavements. In the study reported in this report, the development of intelligent compaction techniques to estimate resilient modulus of cementitiously stabilized subgrades was investigated.

The Intelligent Asphalt Compaction Analyzer (IACA) is a roller mountable device that can sense the vibrations of the roller during the compaction of a pavement and using the knowledge of the asphalt mix and the pavement design, can estimate the achieved level of compaction of the asphalt mix. The IACA technology was developed at the University of Oklahoma during 2003-2006 with support from the Oklahoma Center for the Advancement of Science and Technology (OCAST) (Commuri and Zaman, 2008). During 2006-2009, the use of the IACA in determining the density of asphalt pavements was demonstrated during the construction of asphalt pavements across the United States. The results of these tests showed that the IACA was able to estimate the density of the asphalt pavement during its construction to within $\pm 1.5\%$ of the actual density. This is comparable to the accuracy of spot density measurement tools currently being used by the paving industry and by the transportation agencies such as Oklahoma Department of Transportation (ODOT). However, the IACA additionally provides instantaneous complete coverage of the pavement which can help in the elimination of over/under compaction of the pavement. During 2008-2010, the IACA

technology was enhanced to allow for the estimation of the dynamic modulus of an asphalt pavement during its construction. In the project jointly funded by the Oklahoma Transportation Center (OTCREOS7.1-10) and Volvo Construction Equipment Company (VCE) Shippensburg, PA, the ability of the IACA to estimate the stiffness of asphalt pavement was demonstrated during the construction of Interstate I-35 in Norman, OK. For the first time, the estimated stiffness was validated through FWD tests conducted on the completed pavement. The enhancement of the IACA to estimate the stiffness (resilient modulus) of cementitiously stabilized soil subgrades that form the foundation for asphalt pavements is the subject of the research presented in this report.

The IACA is based on the hypothesis that the vibratory roller and the underlying pavement form a mechanically coupled system. The response of the roller is determined by the frequency of the vibratory motors and the natural vibratory modes of the coupled system. The vibration of the roller varies with the stiffness of the underlying pavement layer. The analysis of the vibration spectra of the roller can therefore be used to estimate the stiffness of the pavement layer(s) on which it rests. The IACA is mounted on a vibratory roller and is equipped with a measurement system that can continuously record the compaction level of the layer underneath. A global positioning system (GPS) based documentation system is also installed for continuous recording of the spatial position of the roller. An user interface is incorporated to display the real time operational parameters like compaction level, temperature of pavement, roller pass, direction of roller, GPS location of the roller, and a color coded map of compaction level at each location.

The functional modules of the IACA are shown in Figure 1. The sensor module (SM) in the IACA consists of accelerometer(s) for measuring the vibrations of the compactor during the operation. An user interface for specifying the amplitude and frequency of the vibration motors and for recording the soil type is also a part of the SM. The feature extraction (FE) module computes the Fast Fourier Transform of the input signal and extracts the features corresponding to vibrations at different salient frequencies. The Artificial Neural Network (ANN) classifier is a multi-layer Neural Network that is trained to classify the extracted features so that each class represents a vibration pattern

specific to a pre-specified level of compaction. The Compaction Analyzer (CA) then post-processes the output of the ANN and estimates the stiffness in real time.

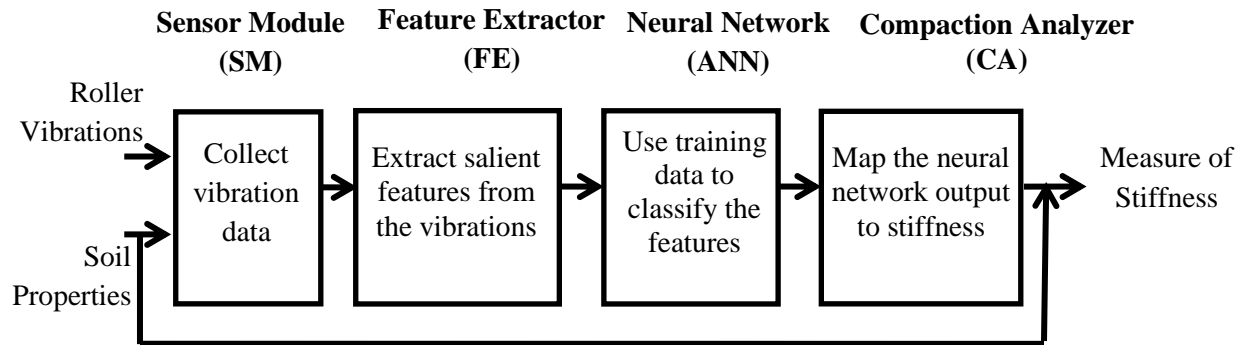


Figure 1. Flowchart of the activities involved in estimation of pavement stiffness by the IACA (Commuri And Zaman, 2008).

In order to extend the IACA to estimate the stiffness of cementitiously stabilized subgrade soil, the IACA has to be first trained to extract salient features of the vibration spectra of the roller during compaction. Further, the neural network has to be trained to classify the observed features into predetermined groups. Finally, the compaction analyzer should be designed such that it can take into account parameters such as the soil type and gradation, the type and quantity of the additive used, moisture content, dry density of the soil, etc., to relate the classified features into a modulus value representing the stiffness of the compacted subgrade. The procedure that was designed to accomplish this goal and the verification of the proposed technique are discussed in the following sections of the report.

3. GOALS OF THE PROPOSED RESEARCH

The main goals of the study reported in this paper are as follows:

- a) Study the feasibility of using the IACA to determine the stiffness of cementitiously stabilized subgrade during compaction,
- b) Perform soil characterization tests and resilient modulus tests in the laboratory to determine the relationship between different parameters such as soil type, its particle size distribution, stabilizing agent used, moisture content, dry density, curing time, etc., and the resilient modulus of stabilized soil specimens,
- c) Develop calibration procedures for the IACA and evaluate the accuracy of IACA estimated modulus by comparing with the values measured through in-situ tests.

In order to accomplish the goals of the project, research was planned as a two-step process. The first step (Year One of the study) involved the investigation of the feasibility of using the IACA during compaction of cementitiously stabilized soil subgrades. The results of the investigation will then be used to develop calibration and estimation procedures for the IACA. The validation of the IACA will be carried out at two different project sites in Year Two of the study. Virgin soil and additives from each of these sites will be collected and their properties will be studied in the laboratory. Regression models will then be developed to analyze the dependence of the subgrade stiffness (M_r) on the soil properties and level of compaction. Tests using Falling Weight Deflectometer (FWD) and Nuclear Density Gauge will be conducted at select locations on the stabilized subgrade after compaction. IACA estimated M_r values will be compared with FWD backcalculated moduli and M_r values predicted using the regression models. It is expected that the two step process will maximize the adaption of the IACA for estimating the resilient modulus of cementitiously stabilized soil subgrades during the compaction process. Further, the use of regression models for estimating the modulus will provide an elegant way to validate the compaction quality achieved during field compaction when it is not feasible to conduct detailed FWD tests.

4. RESULTS OF THE RESEARCH PROJECT

The ability of the IACA in predicting the compaction level was studied by calibrating and validating the IACA at four different project sites. In the first two sites, the ability of IACA in determining the in-situ density of the subgrade was studied. From these two projects, the issues involved in installing the IACA, measuring and recording the vibration data, and effectiveness of the calibration process were studied. The IACA output was correlated with the in-situ densities. In the two projects conducted in Year Two, a comprehensive study was performed for calibration and validation of the IACA in terms of resilient modulus (M_r). Extensive laboratory and field studies were conducted for correlating the IACA estimated M_r with FWD backcalculated modulus and laboratory determined M_r .

In each project, the general testing and data collection procedures involved both field tests, as well as laboratory investigations. While similar procedures were followed at each site, the location of the construction sites and the construction schedule followed by the contractor resulted in minor variations in the schedule of tests performed. Below are the steps adopted for achieving the goals of the project.

1) *Collection of soil and additive samples*

Virgin soil and bulk CKD were collected from each the construction sites prior to the construction.

2) *Characterization of raw and stabilized soils*

Properties of the raw and stabilized soil were studied in the lab. The particle size distribution and Atterberg's limits tests were performed on the collected soil to determine the classification of soil. The particle size distribution was determined by checking the percentage passing through US Standard sieve numbers 4, 10, 40 and 200. To determine the fractions of clay (% finer than 0.002 mm) and silt (% coarser than 0.002 mm and finer than 0.075 mm) hydrometer test was conducted on soil according to AASHTO-M145 specifications (AASHTO- M145, 2008). Proctor test was used to establish the relationships between moisture content and dry density for the raw and

stabilized soils. This relationship was then used to determine the optimum moisture content (OMC) and maximum dry density (MDD) for the stabilized soils. It may be noted that in all the projects sites incorporated in this study the subgrade was stabilized using CKD.

3) *Resilient modulus test on the stabilized soils*

In the two projects conducted in Year Two of the study, the resilient modulus test (AASHTO T307-99) was performed on a number of precompacted specimens. In order to match the composition of the subgrade soil in the field, specimen for resilient modulus tests were prepared by mixing the corresponding additive that was used to stabilize the subgrade in the field. Stabilized soil mixture was compacted in a mold of 101.6 mm (4.0 in) diameter and 203.2 mm (8.0 in) height to produce specimen for conducting resilient modulus tests. The test was conducted using a Material Testing System (MTS) machine in accordance with AASHTO T307-99 test procedure. Total 15 stress sequences were applied to the compacted specimen using a cyclic haversine-shaped load pulse with a loading period of 0.1 seconds and a rest period of 0.9 second duration. The resilient modulus was calculated based on the recorded vertical displacements at last five successive load cycles for each test sequence. The required load was applied using a 22.3 kN (5000 lb) load cell. The vertical displacements were measured using two loose core linear variable differential transformers (LVDTs) that were attached to the specimens. The resilient modulus for each sequence was calculated from the average recoverable strain and average load from last five cycles using *Equation 1*.

$$M_r = \sigma_d / \epsilon_r \quad \text{Equation 1}$$

Where σ_d is repeated cyclic deviatoric stress, and ϵ_r is recoverable strain measured in the MTS machine.

Resilient modulus tests were conducted at two different curing periods. The first set of tests were conducted immediately after the compaction. These test results are referred to as the resilient modulus at 0-day curing period, or simply 0-day M_r . Then, after the completion of the 0-day test, specimens were stored for curing at a temperature equal

to 23.0 ± 2 °C and a relative humidity equal to approximately 96%. Specimens were cured for 28 days and then tested for 28-day resilient modulus (or simply 28-day M_r).

4) *Regression models for resilient modulus:*

Based on the resilient modulus test results, regression relationship for the resilient modulus was developed so that M_r could be predicted for any moisture content (M_c) and dry density (γ_d) (within a feasible range). A number of constitutive models are available in literature for prediction of resilient modulus (AASHTO 1993, NCHRP 1-28 1997, Andrei et al. 2004, AASHTO 2004). Using these constitutive models, the resilient modulus can be predicted from the knowledge of stress state, atmospheric pressure and soil properties. In the present work, the following constitutive model (AASHTO, 1993) was adopted.

$$M_r = k_1 p_a \left(\frac{\theta}{p_a} \right)^{k_2} \left(\frac{\sigma_d}{p_a} \right)^{k_3} \quad \text{Equation 2}$$

where M_r is the resilient modulus; k_1 , k_2 and k_3 are the regression coefficients in the constitutive model; p_a is the atmospheric pressure; θ is the bulk stress and σ_d is the deviatoric stress. The laboratory resilient modulus test results, the applied stress state and atmospheric pressure were utilized to backcalculate k_1 , k_2 and k_3 coefficients. Total 75 to 80% of the laboratory test data was used to determine these coefficients as a function of moisture content and dry density. The accuracy of the regression models were then validated by using the remaining 20 to 25% of the test data.

5) *Calibration of IACA in Field*

In each project, after the stabilized soil was compacted using a pad foot roller, a smooth steel drum vibratory compactor equipped with the IACA was used to first compact a 10 meter long test strip. The vibrations of the roller were recorded during the proof rolling process. The GPS coordinates at these test locations were also recorded. After the proof rolling was completed, NDG readings were taken at three locations (3 meter apart) on the control strip in the direction of the roller travel.

The vibration of the roller is considered as to be a function of stiffness of the soil.

Calibration of the IACA was performed using the laboratory estimated M_r values at 0-day curing period. This was because the IACA readings in the field were also taken at 0-day curing period (at the time of construction). Based on the variability of dry densities and moisture contents of the stabilized subgrade at different stations, the maximum and minimum M_r values were estimated using the empirical model that was developed for determining the resilient modulus. The neural network was used to calculate the level of compaction at these test locations. The model predicted M_r values were then mapped to the neural network outputs of the corresponding highest and lowest compaction region of the test bed to calculate the calibration parameters.

6) *Validation of IACA measured stiffness*

Once the IACA was calibrated, it was used to estimate and record the stiffness of the entire subgrade during proof rolling. In each project, several test stations were marked on the prepared subgrade. Moisture content and dry density were measured at each of the stations with the NDG. The GPS coordinates of each station were also recorded. FWD test was considered for the validation of IACA. However, in some cases, the construction schedule does not permit the performance of FWD tests. In such cases, the laboratory predicted M_r results can be used for validating the IACA. The modulus estimated from the NDG measurements on the marked stations were compared with the IACA estimated M_r at the corresponding stations to study the accuracy of the IACA estimates.

The following sections present a comprehensive discussion of the test sites and results obtained at each of the four project sites.

4.1 Rock Creek Road, Norman, Oklahoma

The ability of the IACA in determining the stiffness of a subgrade during its compaction was studied during the extension of Rock Creek Road between Porter Street and 12th street NE in Norman, Oklahoma. The site was prepared by first removing the existing vegetation and then grading the soil. The soil was stabilized by mixing 15% fly ash to a depth of 203.3 mm (8 inches) and then compacting it using an Ingersoll-Rand SD-115F

PRO PAC/CS-563C compactor. A 76.2 mm (3 inches) thick asphalt base course was then compacted on top of the prepared subgrade. The asphalt base course constructed with a S3 PG 64-22 mix. The nominal maximum aggregate size was 19 mms (0.75 inches). Figure 2 shows a Terex RS-500C stabilizer mixing fly-ash into the soil subgrade to begin the roadway foundation. Figure 3 shows a subgrade being compacted with an Ingersoll-Rand SD-115F compactor. The prepared subgrade is shown in Figure 4.



Figure 2. Stabilization of soil subgrade with fly-ash using a Terex RS-500C stabilizer.



Figure 3. Compaction of the stabilized subgrade using Ingersoll-Rand SD115F compactor.



Figure 4. Prepared soil subgrade.

Soil Description

The subgrade soil at this site primarily consists of Doolin-Pawhuska complex, with 0-3% slopes (Soil Survey of Cleveland County, Oklahoma, 1987). Typically, the surface layer is brown silt loam (CL, CL-ML) about 203.3 mm (8 inches) thick, with liquid limit (LL) and plasticity index (PI) varying from 22 to 37% and 2 and 14%, respectively. The subsoil is dark grayish brown and grayish brown silty clay (CL, CH) to a depth of about 1295.4 mm (51 inches), having a LL of 37 to 70% and a PI of 15 to 40%. There is coarsely mottled light brownish gray and brownish yellow silty clay to a depth of 1930 mm (76 inches), and reddish yellow silty clay loam (CL, CH) to a depth of 2033 mm (80 inches). The soil in this region has LL and PI in the range of 37 to 70% and 15 to 40%, respectively.

Laboratory Investigation

The particle size distribution and Atterberg's limits of the collected soil indicated that the soil could be classified as CL with a LL of 24% and a PI of approximately 10%. The particle size distribution showed the percentage passing through US Standard sieve numbers 4, 10, 40 and 200 were 100, 98, 81 and 58%, respectively. The amount of clay fraction (% finer than 0.002 mm) and silt (% coarser than 0.002 mm and finer than 0.075 mm) (AASHTO- M145, 2008) were found to be 35 and 23%, respectively.

The moisture content versus the dry density relationship is given in Figure 5. The OMC for the raw soil was found to be 15.1%, whereas, it was 18% for the soil stabilized with 15% of fly ash. The MDD of raw soil and stabilized soil were 17.5 and 16.7kN/m³, respectively. A summary of the soil properties determined in the laboratory are presented in

Table 1.

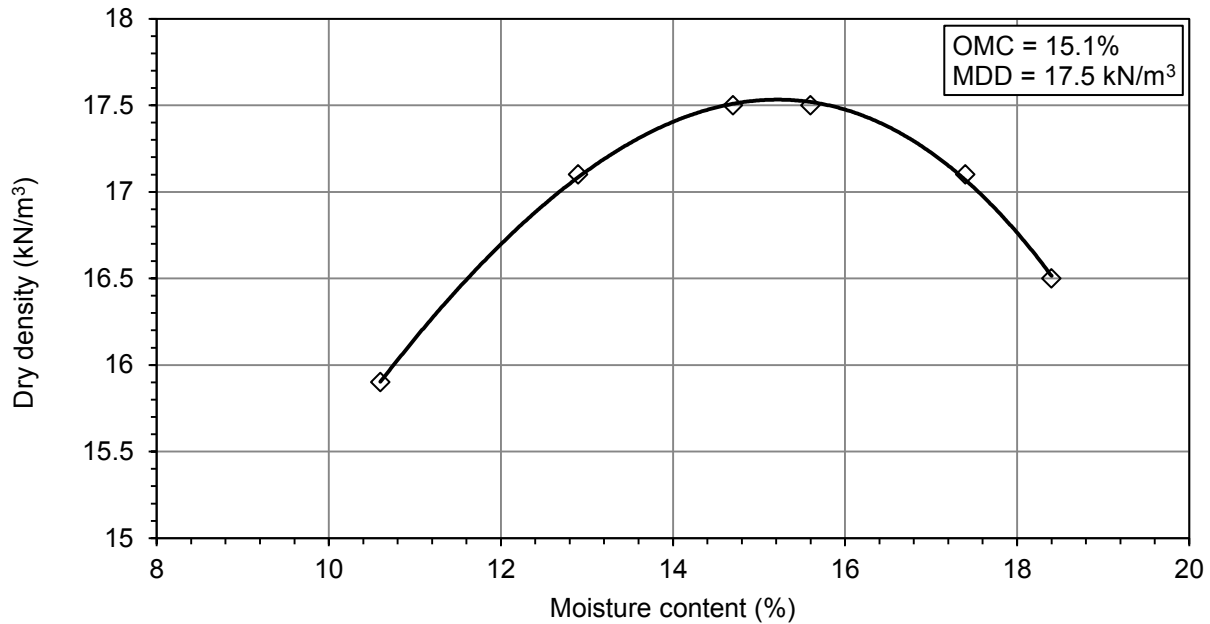


Figure 5. Moisture content vs dry density relationship for the raw soil.

Table 1. Summary of soil properties.

Parameter	Value
Unified Soil Classification System(UCSD)	CL
% finer than 0.075 mm	58
% finer than 0.002 mm	35
LL (%)	24
PI (%)	10
Specific gravity	2.63
Optimum moisture content (OMC) (%)	15.1 (raw soil), 18 (soil + 15 % fly-ash)
Maximum dry density (MDD) (kN/m ³)	17.5 (raw soil), 16.7 (soil + 15 % fly-ash)

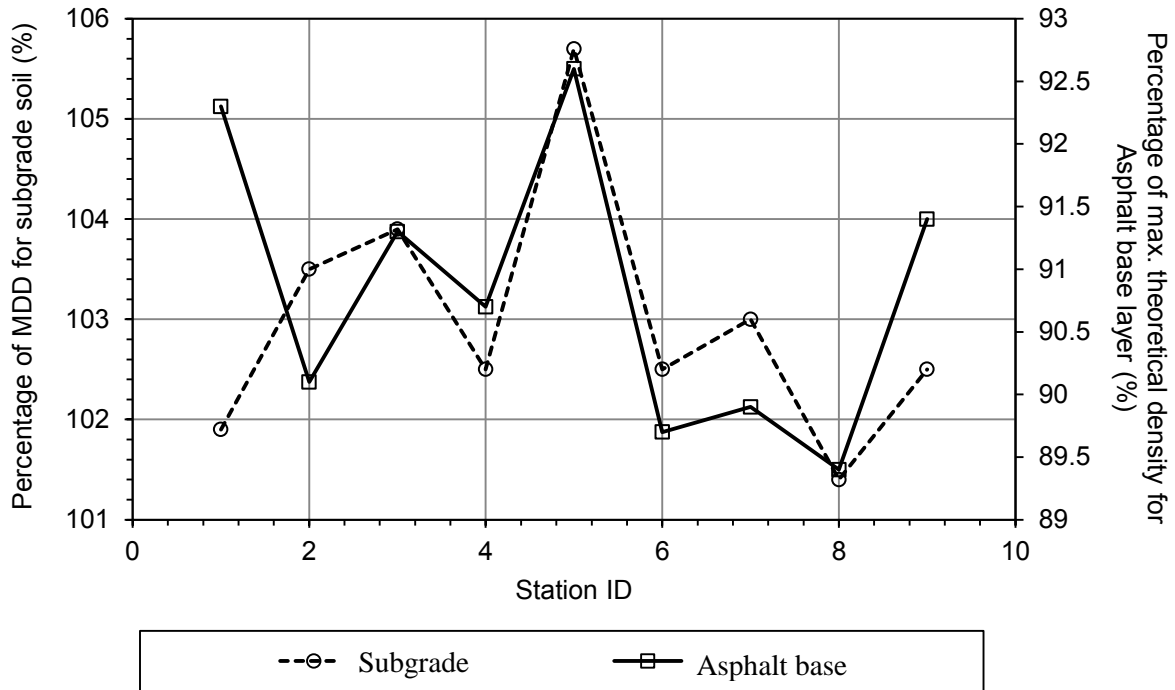
Field Investigation

The IACA was installed on the CS-563C single drum vibratory compactor used for finish rolling of the compacted subgrade. The vibration data was collected over several roller passes. This data was then used to train the IACA to recognize the features in the vibratory signal corresponding to the different levels of compaction. The target compaction values determined in the laboratory were used to perform raw calibration of the IACA. The calibration parameters were then refined to minimize the error between the IACA estimated density and NDG density at selected stations on the compacted subgrade.

Nine test stations were marked on the compacted subgrade. The stations were uniformly spaced at 6.1 m (20 feet) interval. The density and the in-situ moisture content were recorded at each station using an NDG. Table 2 shows the densities of the subgrade and the asphalt base layer at each of the test station. It may be noted that the percentage of maximum dry density for the subgrade is also referred to as degree of compaction. Results in Table 2 show that the IACA estimated density of the soil subgrade compares well with the density measured by the NDG. Further, it can be seen in Figure 6 that the density achieved in the asphalt layer is affected by the support offered by the underlying subgrade.

Table 2. Densities of the soil subgrade and asphalt base layer at the different test stations.

Test Stations	Soil Subgrade		Core location number	Asphalt base	
	NDG estimated degree of compaction (%)	IACA estimated degree of compaction (%)		Core density (% of max. theoretical density)	IACA estimated density (% of max. theoretical density)
F1	100.5	101.9	R0	90.31	92.3
F2	101.7	103.5	R2	92.26	90.1
F3	103.0	103.9	R4	91.56	91.3
F4	98.6	102.5	R6	92.81	90.7
F5	101.4	105.7	R8	93.44	92.6
F6	100.3	102.5	L2	91.93	89.7
F7	101.7	103	L4	92.6	89.9
F8	103.4	101.4	L6	91.3	89.4
F9	103.4	102.5	L8	91.76	91.4



Note: The densities of asphalt layers are the percentage of maximum theoretical density.

Figure 6. Comparison between the IACA estimated density of the stabilized subgrade and the density of asphalt layer constructed on top of the stabilized subgrade.

The comparison of estimated and actual densities in Table 2 and Figure 6 show that the IACA is able to estimate the density of the subgrade within a close range of what had been measured by the NDG. Further, the comparison of the IACA estimated densities in several test stations of the stabilized subgrade and the corresponding estimated densities of asphalt layer, constructed on top of the stabilized subgrade, showed that the IACA was able to capture the influence of the compaction level of the subgrade on the overlaid asphalt layers. The results of this investigation provided a preliminary indication of the applicability of IACA to the compaction of cementitious stabilized soil subgrades.

4.2 Hefner Road, Edmond, Oklahoma

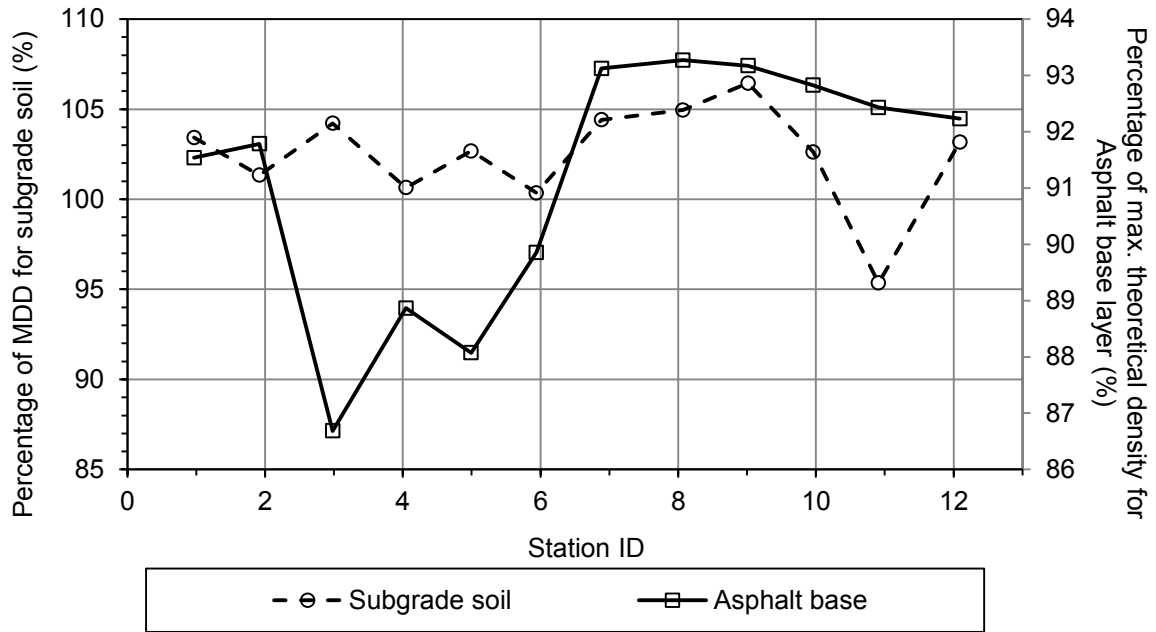
The ability of the IACA to determine the density of a subgrade during its compaction was studied during the construction of a 9.6 kilometers (6 miles) (2 lanes) stretch on E.Hefner Road. The stretch is located between Broadway Extension (HWY 77) to N. Midwest Blvd in Edmond, OK. The subgrade soil was stabilized by mixing 15% fly-ash to a depth of 304.8mm (12 inches) and then compacting with an Ingersoll-Rand SD-105DX compactor. A 76.2 mm (3 inches) asphalt base course was then compacted on top of the prepared soil subgrade using a HMA S3 (PG 70-28 OK) mix. The nominal maximum size of the aggregate was a 19mm (0.75 inch). The surface course was 50.8mm (2 inches) thick and was constructed with a 12.5mm (0.5 inch) HMA S4 (PG 70-28OK) mix.

Soil Description

The subgrade soil at this site primarily consists of ashport silt loam, with a very mild (0-1%) slope. Typically, the surface layer is about 250.4 mm (10 inches) thick and comprises of reddish brown silt loam (ML, CL, CL-ML). The LL and PI are in the range of 22 to 37%, and 2 to 13%, respectively. The upper part of the subsoil is reddish brown silty clay loam (CL) to a depth of 1625.6 mm (64 inches); the LL and the PI in this zone vary from 30 to 43, and 8 to 20, respectively. (Soil Survey of Oklahoma County, Oklahoma, 2003)

Field Investigation

The performance of the IACA was tested during the construction of this project. The density and moisture content of the stabilized subgrade were recorded at 12 stations using a NDG. Several cores were also extracted and their density was determined according to the AASHTO T-166. Figure 7 shows a comparison between the percentage of maximum dry density of the subgrade and the percentage of maximum theoretical density of the asphalt base. It can be seen from this figure, that inadequate compaction of the subgrade invariably affects the compaction achieved in the asphalt base constructed on top of the subgrade.



Note: The densities of asphalt layers are the percentage of maximum theoretical density.

Figure 7. Comparison of compaction of soil subgrade and asphalt base layers at the 12 test stations.

Similar to the evaluation on Rock Creek Road in Norman, OK, the applicability of the IACA in characterizing the subgrade stabilization was clearly demonstrated during this evaluation as well. It was observed that the dry density of the soil subgrade and the density asphalt base layer at 12 test stations followed a similar pattern. This indicates that an inadequate compaction of the subgrade invariably affects the compaction achieved in the asphalt layers constructed on top of the subgrade. Continuous monitoring of the level of compaction of the subgrade can help identify under compacted regions and provide timely information to the roller operator. Such information could be used to remedy compaction issues in the subgrade and improve the overall performance and longevity of the pavement.

4.3 60th Street, Norman, OK

The ability of the IACA in determining the density and resilient modulus of a subgrade during its compaction was studied during the construction of a 3.4 kilometers (2.127 miles) stretch full-depth asphalt pavement on 60th Street, Norman, OK. The stretch is located in between Tecumseh Road and Franklin road in NW Norman. The subgrade

soil was stabilized by mixing 10% CKD to a depth of 200 mm (8 inches). Ingersoll-Rand SD-105DX compactor was used for mechanical compaction. The base layer over the subgrade was constructed with two separate lifts. The thickness of both the lifts was 90mm (3.5 inch). The first layer was constructed using a S3 asphalt mix that had PG64-22 OK asphalt binder. The second layer was also constructed using a S3 asphalt mix but that had PG76-28 OK binder. The surface course was a 51 mm (2 inch) thick layer comprising of S4 asphalt mix with PG76-28OK asphalt binder.

Laboratory and Field Investigation

Figure 8 shows grain size distribution of collected soil. The LL and plastic limit (PL) tests were conducted on raw soil. The LL, PL and PI were found to be 23,19 and 4%, respectively. As per the Unified Soil Classification System (USCS), this soil could be classified as CL-ML. Figure 9 and Figure 10 present the relationship between moisture content and dry density for raw and CKD-stabilized (10% CKD) soil, respectively. The OMC for raw soil was found to be 13.5%, whereas, it was determined as 14.6% for CKD-stabilized soil. MDD of raw and CKD-stabilized soil were determined as 18.0 and 17.3 kN/m³, respectively.

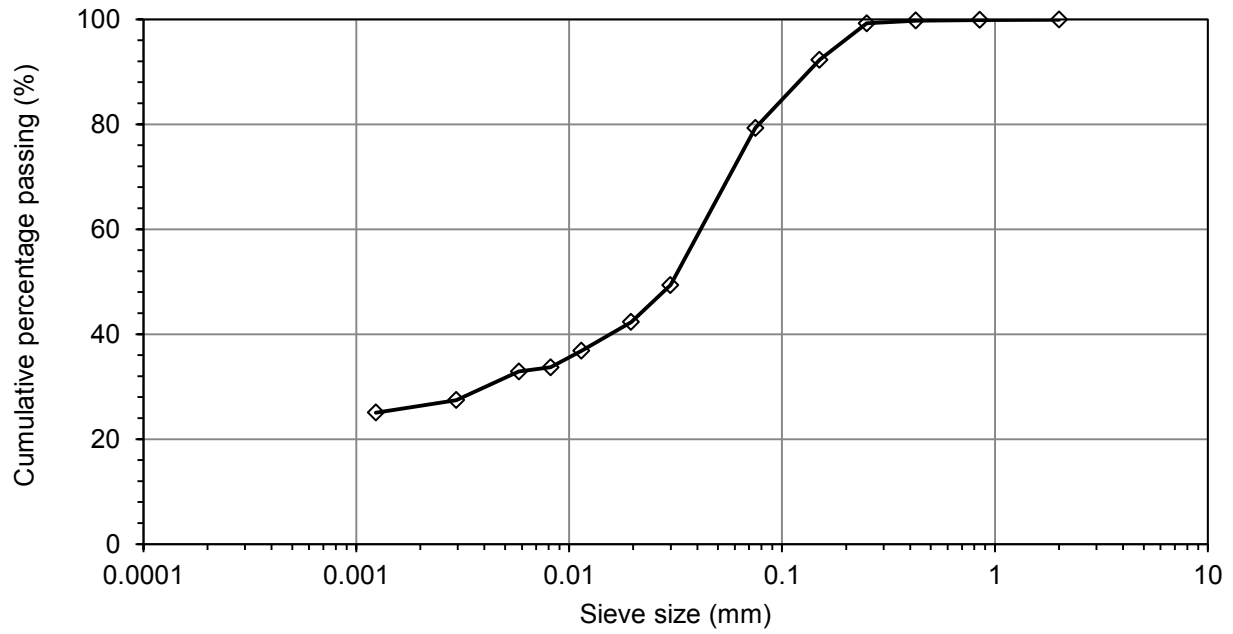


Figure 8. Particle size distribution of soil.

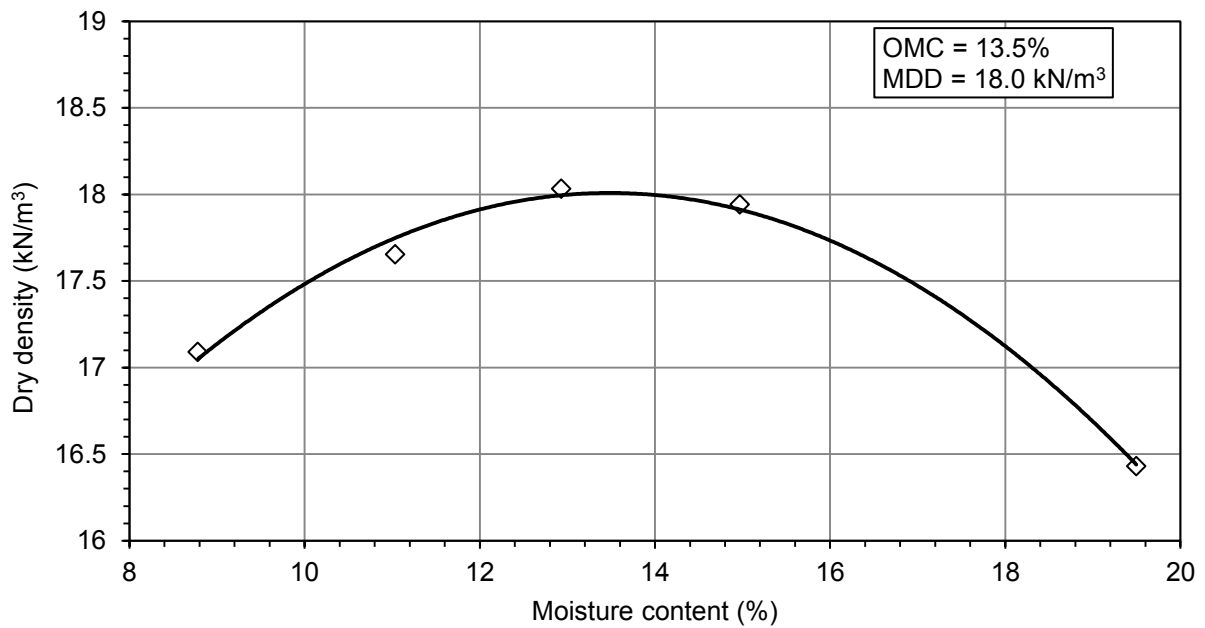


Figure 9. Proctor test results for the raw soil.

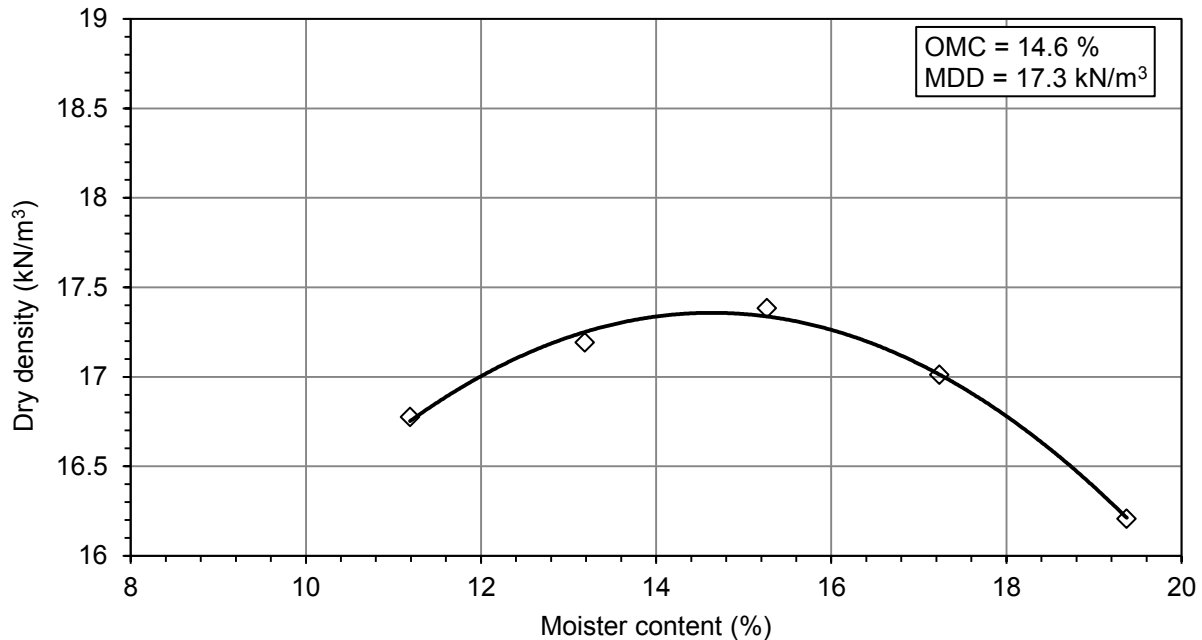


Figure 10. Proctor test results for 10% CKD-mixed soil.

Table 3. Field moisture contents and degree of compactions at the twelve stations.

Test stations	Moisture content (%)	Dry density (kN/m ³)	Degree of compaction (% of MDD)
M1	14.2	16.6	96.0
M2	13.2	16.8	97.1
M3	12.3	17.6	101.7
M4	13.2	17.2	99.4
M5	13.9	16.9	97.7
M6	13.8	16.7	96.5
M7	15.1	17.3	100.0
M8	13.7	17.0	98.3
M9	16.0	17.1	98.8
M10	16.7	16.9	97.7
M11	17.1	16.6	96.0
M12	15.1	17.1	98.8

Moisture content and density measured in the field

Twelve different stations were marked on the CKD-stabilized subgrade layer, at an approximately 15.24 meter (50 feet) interval. The degree of compaction in each station was determined using the laboratory determined MDD for CKD-stabilized soil (i.e., 17.3kN/m³) and the measured dry density by NDG. The degree of compactions and the measured field moisture contents for the twelve stations are presented in Table 3. It can

be seen that the degree of compaction ranged from 96 to 101.7%, while the moisture content ranged from 12.3 to 17.1%. It should be noted here that the OMC of CKD-stabilized soil was determined as 14.6%, but the measured field moisture contents were both above and below the OMC.

Laboratory resilient modulus

In this study, the resilient modulus test was performed on six specimens. To match with the composition of the subgrade in the field, resilient modulus samples were prepared with 10% CKD, by weight of the soil. Out of six specimens, three specimens were prepared at OMC and the other three were prepared at OMC-2%.

Table 4 lists the moisture content and degree of compaction for each compacted specimen.

Table 4. Moisture contents, dry densities and degree of compactions for the resilient modulus specimens.

Specimen No.	Moisture content (%)	Dry density (kN/m ³)	Degree of compaction (% of MDD)
1	12.1	17.3	100.0
2	12.4	17.1	98.8
3	12.1	17.2	99.4
4	14.7	17.4	100.6
5	14.6	17.5	101.2
6	14.8	17.6	101.7
OMC = 14.6% , MDD = 17.3 kN/m ³			

The resilient modulus results are presented in a graphical form in Figures 11-16. M_r values with respect to different stress state is presented in each graph. Tests were conducted at three different confining pressures (41.34, 27.56 and 13.78 kPa). Figure 11 through Figure 16 show the graphs for resilient moduli at 0-day curing for all the six specimens. As was expected, the M_r values decrease with the increase in the deviatoric stress. It can also be seen that at higher confining pressures, specimens exhibit a higher M_r . For specimens compacted at OMC, the influence of confining pressure is more than that of those which were compacted at OMC-2%. A closer look at all the graphs can reveal that the range of variation of the M_r in all the graphs are similar, except the specimen No. 5 (Figure 15). In this case, the M_r values for all the test

sequences was low indicating possible defect in the specimen. The 0-day M_r test results for this specimen have therefore been discarded from the analysis.

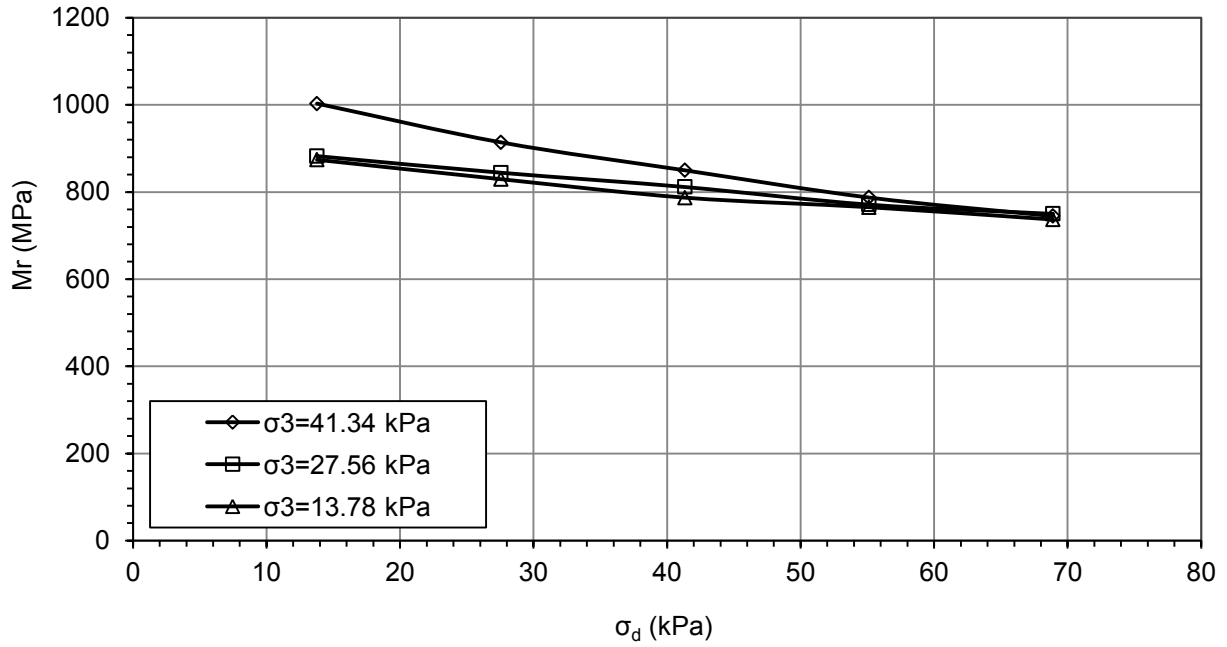


Figure 11. M_r as a function of stress state at moisture content = OMC-2%, Specimen No.1.

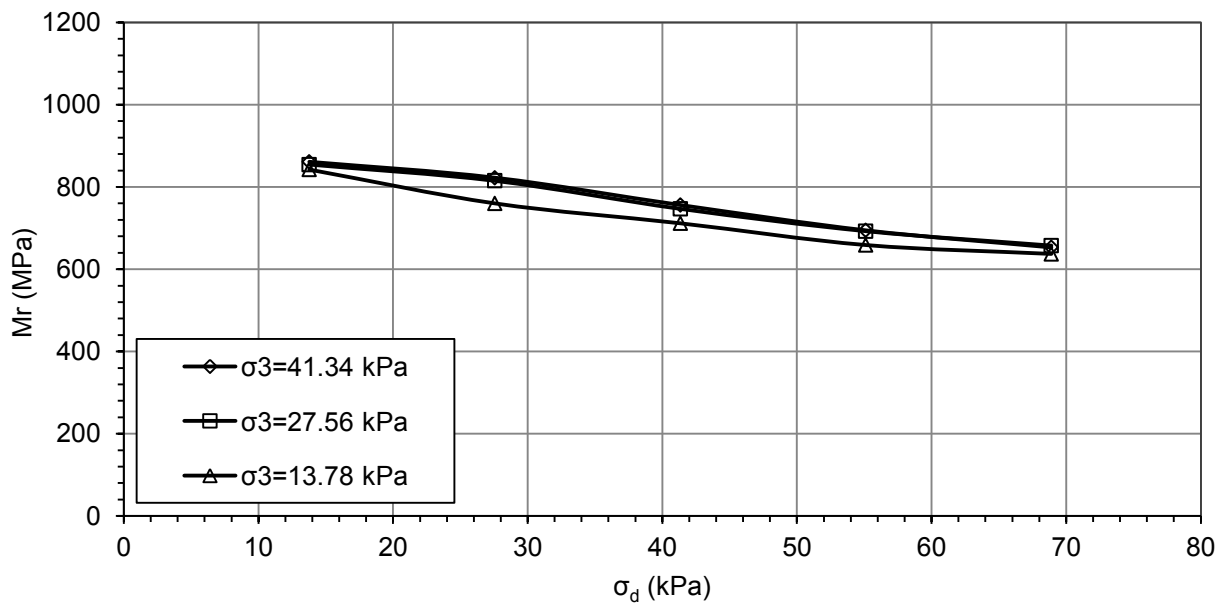


Figure 12. M_r as a function of stress state at moisture content = OMC-2%,

Specimen No. 2.

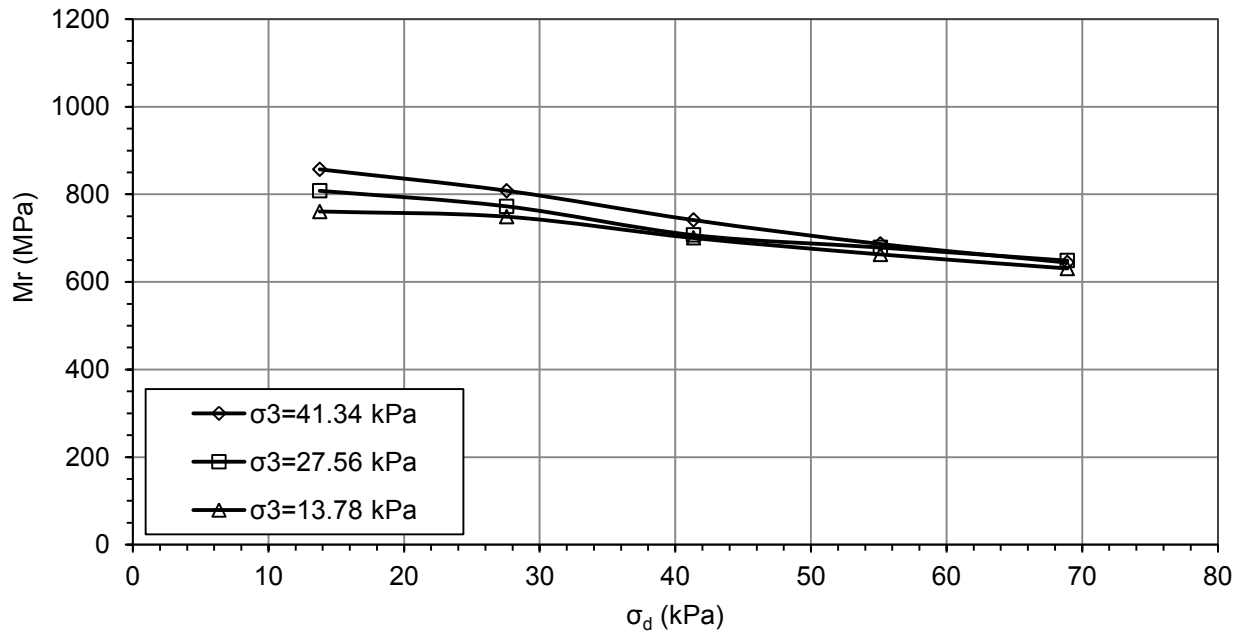


Figure 13. M_r as a function of stress state at moisture content = OMC-2%, Specimen No. 3.

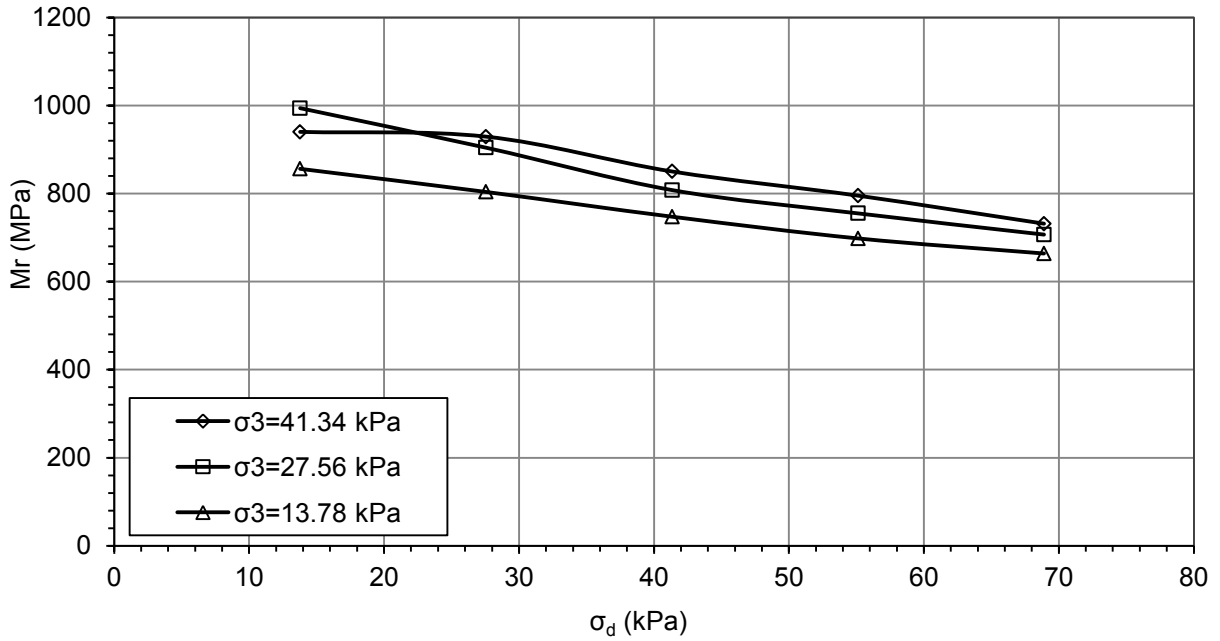


Figure 14. M_r as a function of stress state at moisture content = OMC, Specimen No. 4.

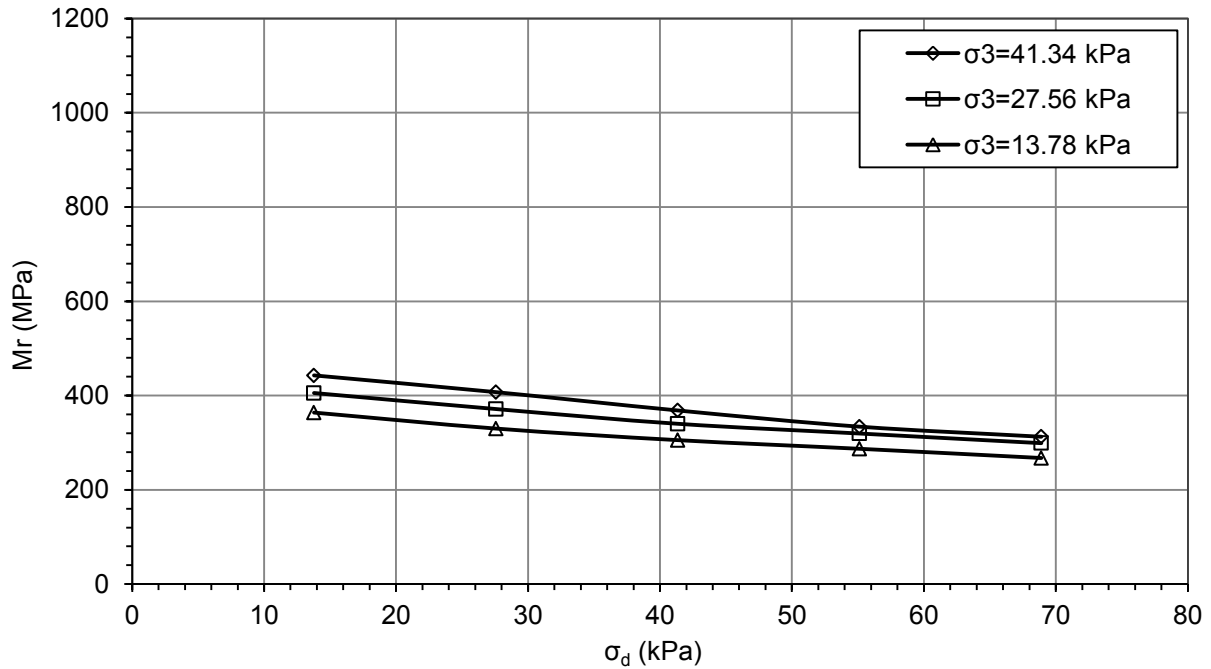


Figure 15. M_r as a function of stress state at moisture content = OMC, Specimen No. 5.

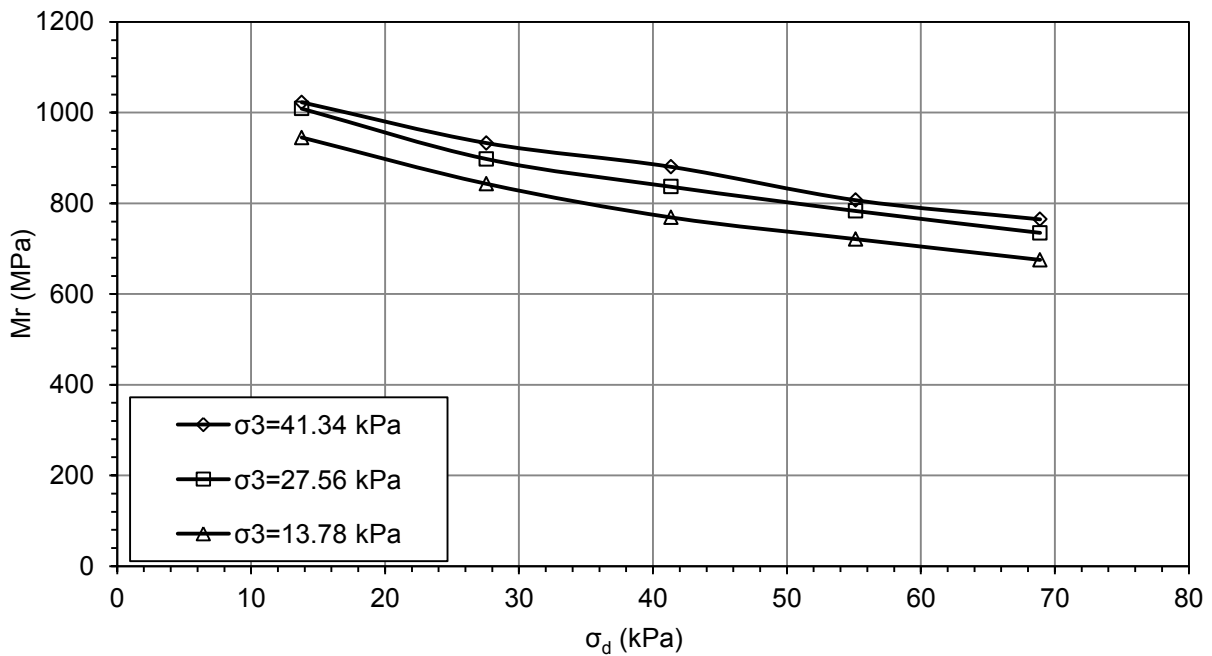


Figure 16. M_r as a function of Stress state at moisture content = OMC, Specimen No. 6.

Figure 17 through Figure 22 present the M_r test results at 28-day curing period. As it can be seen that the M_r considerably increases after 28 days of curing regardless the

applied stress state. This may be attributed due to the influence of hydarion of CKD. The CKD, which is a pozzolanic material is expected to gain a good amount of strength in about four weeks. The plots also show that the M_r of specimens do not considerably change with the deviatoric stress and confining pressure. Moreover, a distinct trend for M_r vs state stress is not obtaiend. The variation of M_r , both at 0 and 28-day curing period, with respect to the bulk stress (θ) has also been studied. The Appendix A of this report includes the plots showing the variation of M_r as a function of bulk stress and confining stress. It can be seen that the dependency of the M_r on the bulk stress is higher when the specimens were tested at 0-day curing period compared to that of 28-day curing period.

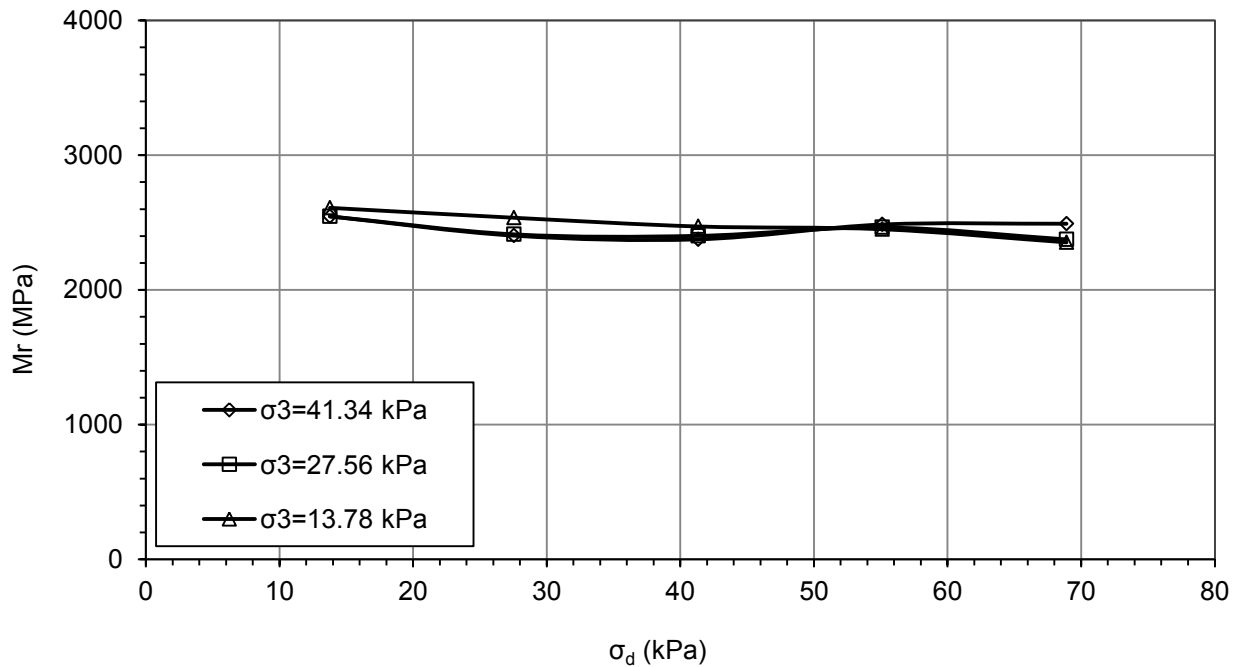


Figure 17. M_r as a function of stress state at moisture content = OMC -2%, Specimen No. 1.

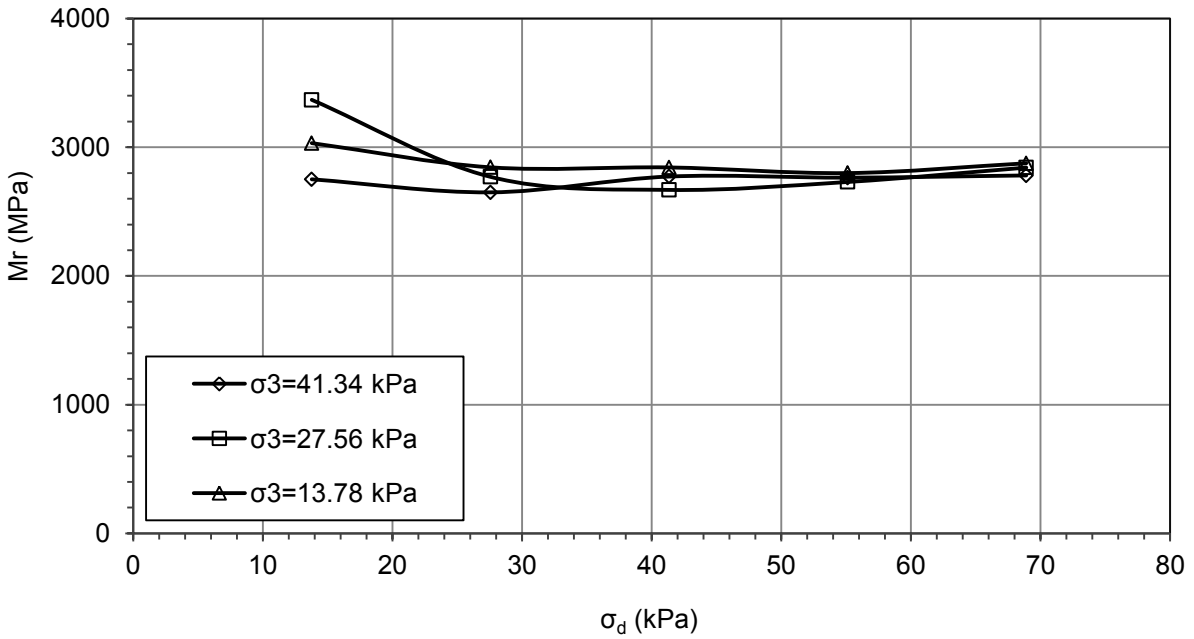


Figure 18. M_r as a function of stress state at moisture content = OMC -2%
Specimen No. 2.

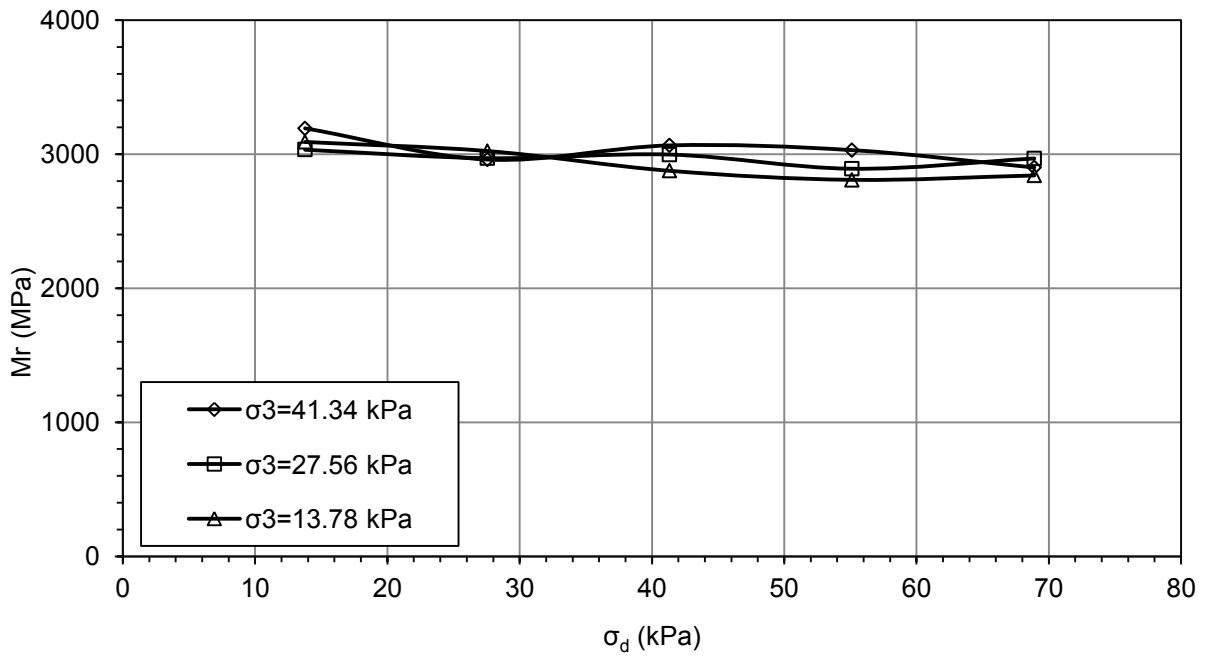


Figure 19. M_r as a function of stress state at moisture content = OMC -2%,
Specimen No. 3.

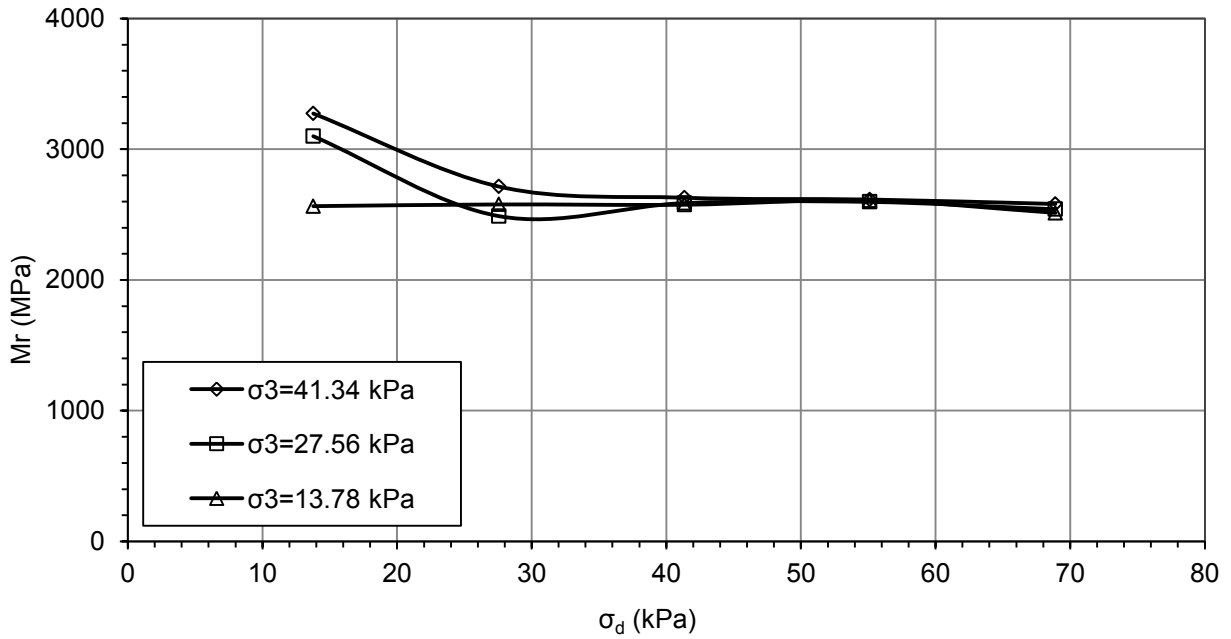


Figure 20. M_r as a function of stress state at moisture content = OMC, Specimen No. 4.

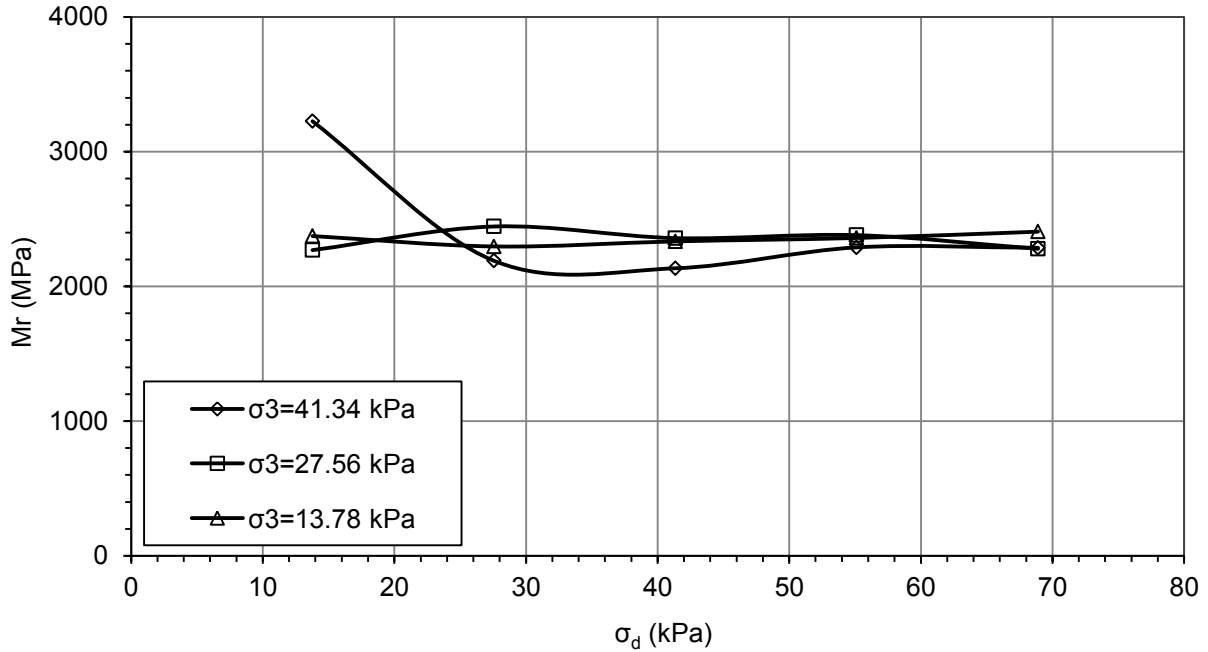


Figure 21. M_r as a function of stress state at moisture content = OMC, Specimen No. 5.

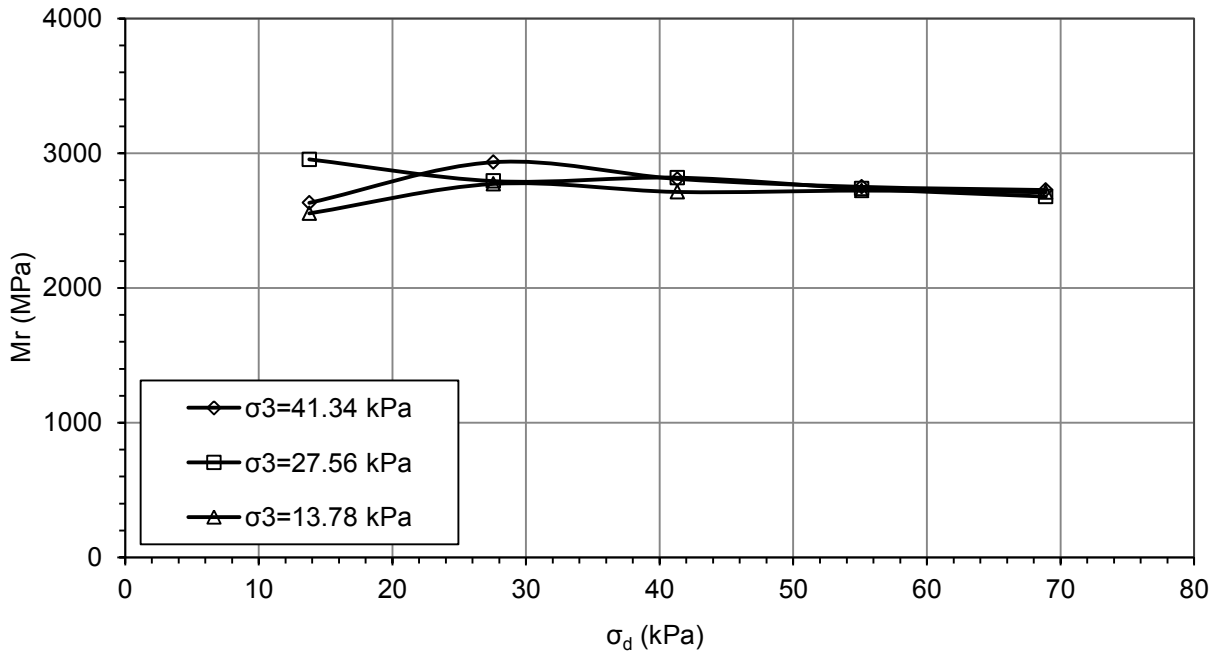


Figure 22. M_r as a function of stress state at moisture content = OMC, Specimen No. 6.

Regression models for the empirical determination of the resilient modulus

As previously discussed, the coefficients k_1 , k_2 and k_3 were numerically derived for each test specimen. Table 5 and Table 6 present the values of the regression coefficients for the 0- and 28-day curing periods, respectively.

Table 5. Value of coefficients in the constitutive model for 0-day curing period.

Specimen No.	k_1	k_2	k_3
1	6511.07	0.082	-0.154
2	5830.80	0.091	-0.194
3	6310.23	0.082	-0.163
4	5926.52	0.173	-0.257
5	--	--	--
6	6346.92	0.177	-0.241

Table 6. Value of coefficients in the constitutive model for 28-day curing period.

Specimen No.	k_1	k_2	k_3
1	25692.93	-0.005	-0.021
2	27308.96	-0.029	-0.030
3	26252.80	-0.013	-0.023
4	24893.09	0.006	-0.054
5	24105.58	0.017	-0.050
6	23627.74	0.024	-0.051

Since, the coefficients are function of moisture content and dry density, and are different for different tested specimens, regression models are developed so that these coefficients can be derived as a function of moisture content and density. Using these regression models, the coefficients (k_1 , k_2 and k_3) for any moisture content and dry density (within a reasonable range) can be determined, for a similar type of soil. The regression equations for 0- and 28-day curing period are given in *Equation 3 to Equation 8*.

Models for regression coefficients k_1 , k_2 and k_3 at 0-day curing:

$$k_1 = -53060.478 - 482.317(MC) + 3790.046(\gamma_d) \quad \text{Equation 3}$$

$$k_2 = -0.467 + 0.034(MC) + 0.008(\gamma_d) \quad \text{Equation 4}$$

$$k_3 = -2.553 - 0.052(MC) + 0.175(\gamma_d) \quad \text{Equation 5}$$

Models for regression coefficients k_1 , k_2 and k_3 at 28-day curing:

$$k_1 = 203060.877 + 410.151(MC) - 10565.166(\gamma_d) \quad \text{Equation 6}$$

$$k_2 = -2.547 - 0.006(MC) + 0.151(\gamma_d) \quad \text{Equation 7}$$

$$k_3 = -0.402 - 0.0149(MC) + 0.033(\gamma_d) \quad \text{Equation 8}$$

Figure 23 and Figure 24 show the predictability of the regression models developed for 0-day and 28-day curing periods, respectively. In these two figures, the actual and predicted resilient moduli are compared. In each figure, the resilient modulus data (80%) that was used to develop the model and the rest of the data (20%) that were used to validate the model are included. The actual resilient moduli depicted in the graphs refer to the laboratory test results. The predicted moduli are the calculated

values using the constitutive model presented in

$$M_r = k_1 p_a \left(\frac{\theta}{p_a} \right)^{k_2} \left(\frac{\sigma_d}{p_a} \right)^{k_3}$$

Equation 2. The corresponding values of k_1 , k_2 and k_3 were calculated using the developed regression models (Equation 3 to Equation 8). It can be seen in Figure 23

that the predictability of the 0-day curing models is quite good with a $R^2 = 0.81$ (for the data used to validate the model). In the case of 28-day curing, although the R^2 was low, M_r values could be predicted with an error less than 15%.

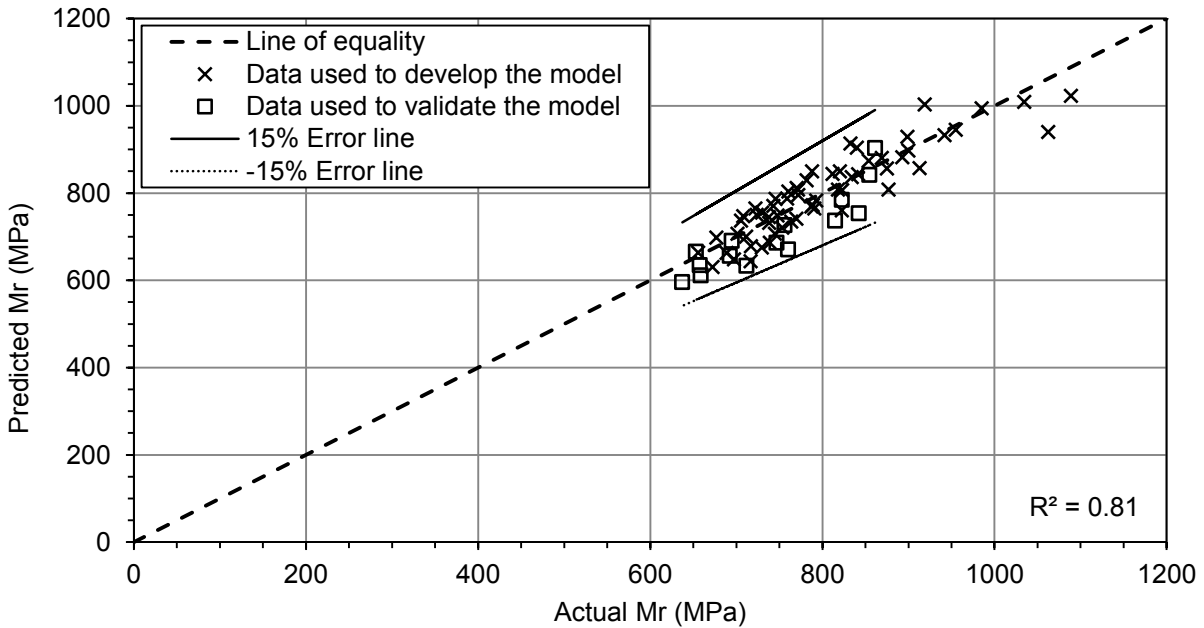


Figure 23. Actual vs predicted M_r at 0-day curing period.

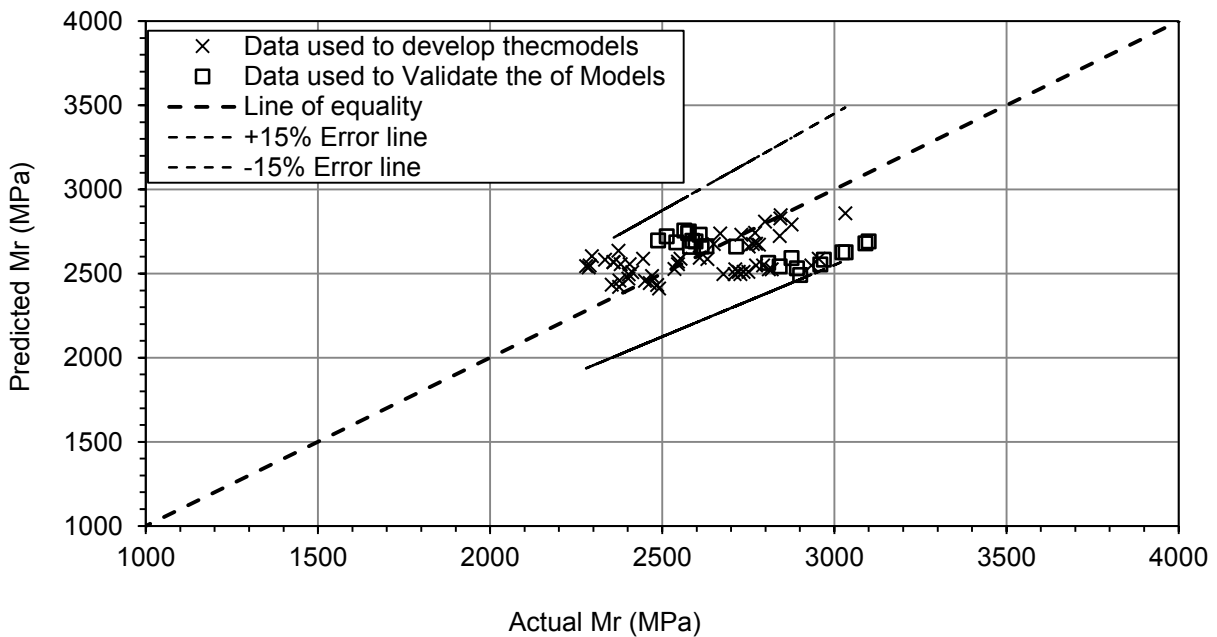


Figure 24. Actual vs predicted M_r at 28-day curing period.

Relationship between 0-day and 28-day predicted resilient moduli

A regression relationship between the 0- and 28-day resilient moduli was developed based on the 0- and 28-day laboratory resilient modulus test results. The ratio of the 28-day M_r to 0-day M_r , denoted as “x”, is correlated with the stress state and 0-day M_r . This relationship can be used to predict the 28-day M_r from the knowledge of 0-day M_r , and the vice versa. The regression model is given in *Equation 9*.

$$x = -0.0091(\sigma_3) + 0.0289(\sigma_d) + 0.0032(Mr_{0\text{-day}}) \quad \text{Equation 9}$$

where x is the ratio of 28-day M_r to 0-day M_r ; σ_3 is the confined pressure; σ_d is the deviatoric test and $Mr_{0\text{-day}}$ is resilient modulus of the specimen at 0-day curing period. The predictability of the regression model is shown in Figure 25. It can be seen that the 28-day M_r was predicted from the 0-day M_r with an error less than 20%.

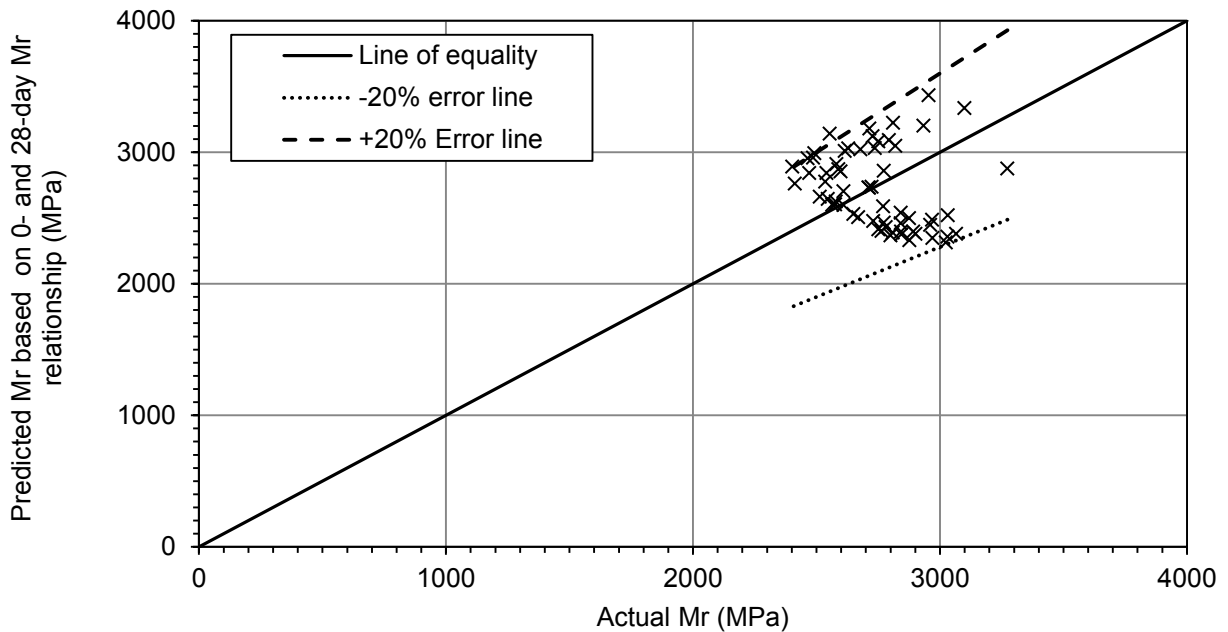


Figure 25. Predictability of the regression model developed for relating the 0- and 28-day M_r .

Estimation of the M_r for the IACA Calibration

As mentioned earlier, moisture content and dry density were measured at the calibration points. These moisture content, dry density information and the stress state were plugged into the regression models developed for coefficients k_1 , k_2 and k_3 . The actual stress state at the field is usually not known, therefore the maximum stress state applied in the resilient modulus test was used in calculating the coefficients k_1 , k_2 and k_3 using

$$M_r = k_1 p_a \left(\frac{\theta}{p_a} \right)^{k_2} \left(\frac{\sigma_d}{p_a} \right)^{k_3}$$

Equation 3 to Equation 8. Subsequently, using

Equation 2, the 0-day and 28-day resilient moduli were estimated. These moduli values were used in the calibration of the IACA.

IACA measured modulus

Table 7 presents the estimated resilient modulus for 0-day curing period at 12 different stations. It is to be noted that the NDG readings at IACA estimated moduli were found to be erroneous at 3 stations (Stations M2, M4 and M8) and hence, these were not used in the validation.

Table 7. IACA estimated moduli for the 9 test stations considered in the analysis.

Test stations	IACA estimated 0-day modulus (MPa)
M1	429
M2	453
M3	408
M4	344
M5	312
M6	228
M7	314
M8	420
M9	380
M10	374
M11	334
M12	363

FWD measured modulus

In this project, FWD testing was performed on the 12 selected stations. The validation of the IACA was performed with the FWD backcalculated modulus. The FWD test was

conducted on top of the asphalt overlays approximately four weeks after the compaction of the subgrade. The FWD deflection values and the thicknesses (measured from cores) of different layers were used to backcalculate the asphalt layer moduli and subgrade resilient moduli at all the 12 stations. Table 8 presents backcalculated FWD moduli of the compacted subgrade. Since the FWD moduli were obtained 28 days after the subgrade was compacted, the backcalculated moduli were converted to equivalent 0-day FWD moduli. The relationship developed between the 0-day and 28-day resilient moduli based on the laboratory resilient modulus test results (Equation 9) was used for this conversion. It was assumed that the relationship between the 0-day and 28-day FWD moduli could be considered as similar to the relationship between the 0-day and 28-day laboratory resilient moduli. Table 8 also included the equivalent 0-day FWD moduli for the 12 selected stations.

Table 8. FWD moduli for the 9 test stations considered in the analysis.

Test stations	0-day FWD modulus (MPa)	28-day FWD modulus (MPa)
M1	451	1384
M2	939	4360
M3	519	1707
M4	556	1896
M5	358	993
M6	174	380
M7	333	894
M8	274	685
M9	391	1125
M10	363	1012
M11	244	586
M12	246	593

Comparison between the IACA predicted M_r and FWD backcalculated moduli

Figure 26 shows the correlation between the IACA predicted 0-day M_r and FWD backcalculated 28-day moduli. It can be seen that the IACA estimates correlate well with the FWD backcalculated modulus ($R^2 = 0.60$). Finally, for a logical comparison, the 28-day FWD backcalculated moduli were converted to 0-day equivalent FWD moduli using Equation 9. The comparison between the 0-day FWD Moduli and the 0-day IACA estimated M_r is shown in Figure 27. The comparison reveals a good correlation between

IACA predicted M_r and FWD backcalculated moduli ($R^2 = 0.63$). This finding indicates that the IACA can predict the subgrade resilient modulus with a reasonable accuracy.

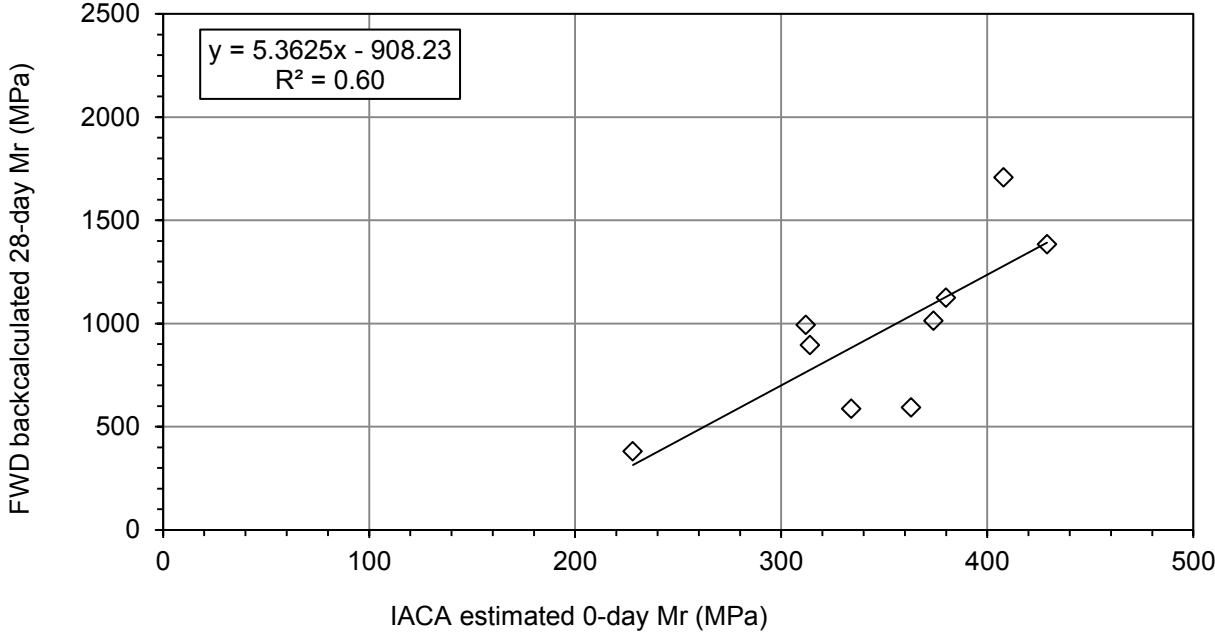


Figure 26. Correlation between FWD backcalculated 28-day moduli and IACA predicted 0-day M_r .

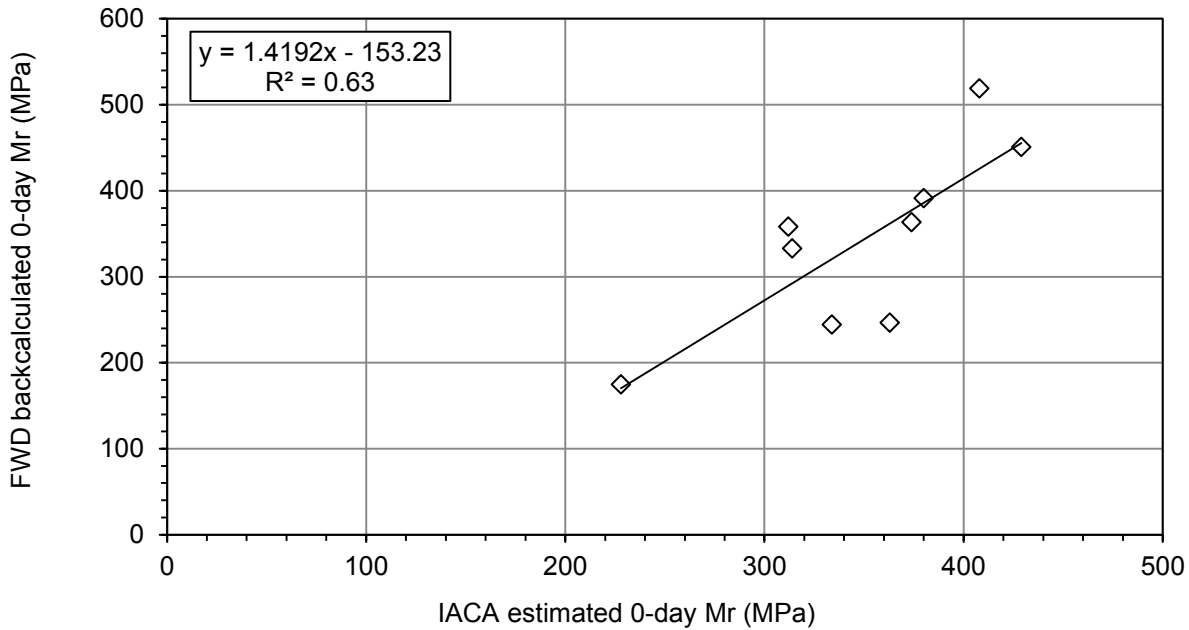


Figure 27. Correlation between FWD backcalculated 0-day Moduli and IACA estimated 0-day M_r .

Station wise comparisons of IACA estimated M_r and FWD backcalculated modulus

Figure 28 shows the station wise comparison between the FWD modulus and IACA estimated M_r . It is very interesting to see that the FWD backcalculated modulus and IACA estimated M_r follows a similar trend with the minimum modulus being recorded at Station M6. Good correlation between the IACA predicted M_r and FWD back calculated modulus shows that the IACA is able to estimate the degree of compaction of the soil subgrade during the compaction process.

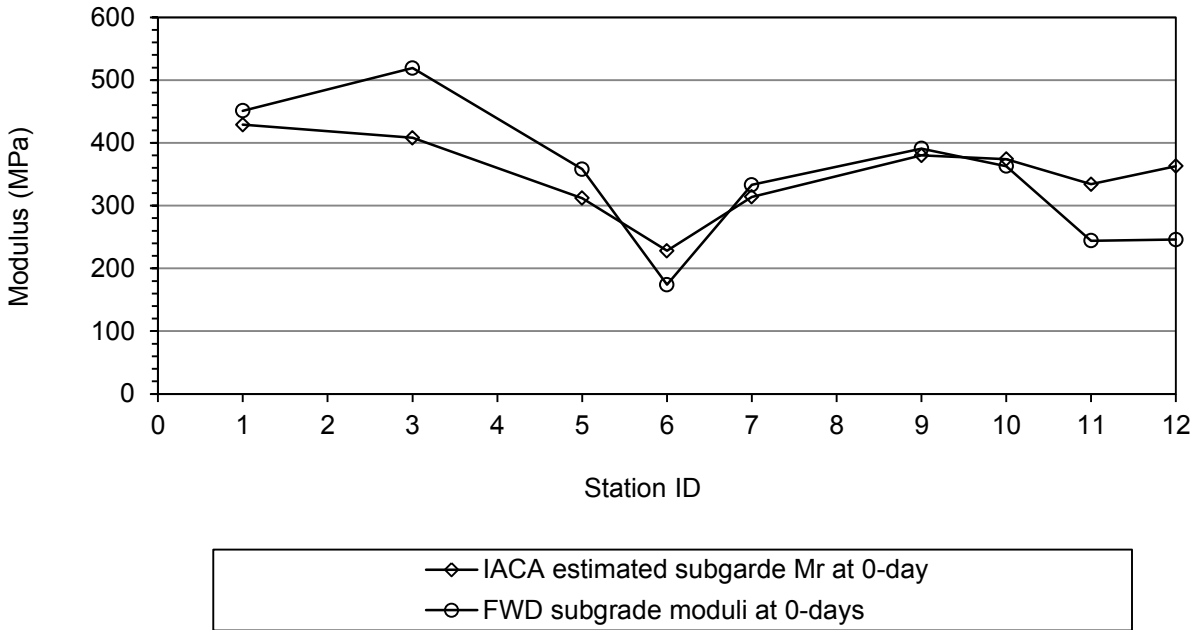


Figure 28. IACA estimated M_r and FWD backcalculated moduli of subgrade at 0-day at different stations.

4.4 Apple Valley, Oklahoma City, OK

The fourth site selected for evaluating the IACA was located in Apple Valley, Edmond, OK. A 0.7-mile (2 lanes) long full-depth asphalt pavement was constructed on Apple Valley Road (State Project STP-155B (813) AG). The subgrade was stabilized by mixing 10% CKD to a depth of 304.8 mm (12 inches). In this project, the base layer was constructed in two separate lifts. Each lift was a 76.5 mm (3 inches) thick asphalt layer. Also the asphalt mixture was the same for both the lifts. Approximately, 26 percent 1" (25 mm) rock, 25 percent manufactured sand, 22 percent screenings, 12 percent sand, and 15 percent RAP and 4.3 percent PG 70-28 OK binder were used in the mix. The surface course was a 50.8 mm (2 inches) thick S4 PG70-28OK mix. This mix in the surface course contained with an approximately 35 percent 5/8" (15.6 mm) chips, 25

percent manufactured sand, 13 percent C-33 screenings, 12 percent screenings, and 15 percent sand, with 4.9 percent PG 70-28 OK binder.

Laboratory and Filed Investigation

The subgrade soil at this site primarily consists of Stephenville-Darsil-Newalla complex, with 3 to 8% slopes. (Soil Survey of Oklahoma County, Oklahoma, 2003) Typically, the top layer of the existing soil consists of fine sandy loam and loamy fine sand (CL-ML, SM, ML, SC-ML, ML-CL) and is about 254 mm (10 inches) thick. The LL and PI of the top layer vary between 0 to 26% and NP to 7%, respectively. The subsoil is fine sandy loam, sandy clay loam, silty clay loam and clay loam (CL, SC, SC-SM, CL-ML, SC) and is about 254 mm (10 inches) deep below the top layer. The LL and PI of the subsoil vary between 20 to 60% and 7 to 34%, respectively. Below the subsoil, clay and silty clay soil (CL, CH) exist up to a depth of 508 mm (20 inches). The soil in this region has LL and PI in the range of 0-60% and NP-34%, respectively. Figure 29 shows the particle size distribution of collected soil. This soil is classified as SM and is characterized as a non-plastic soil. Figure 30 and Figure 31 present the relationship between moisture content and dry density for the collected raw soil and CKD stabilized soil, respectively. The OMC for the raw soil was found to be 12.1 %, whereas, it was 12.7 % for CKD stabilized soil. The maximum dry density (MDD) of raw soil and CKD mixed soil were 18.9 and 18.3kN/m³, respectively.

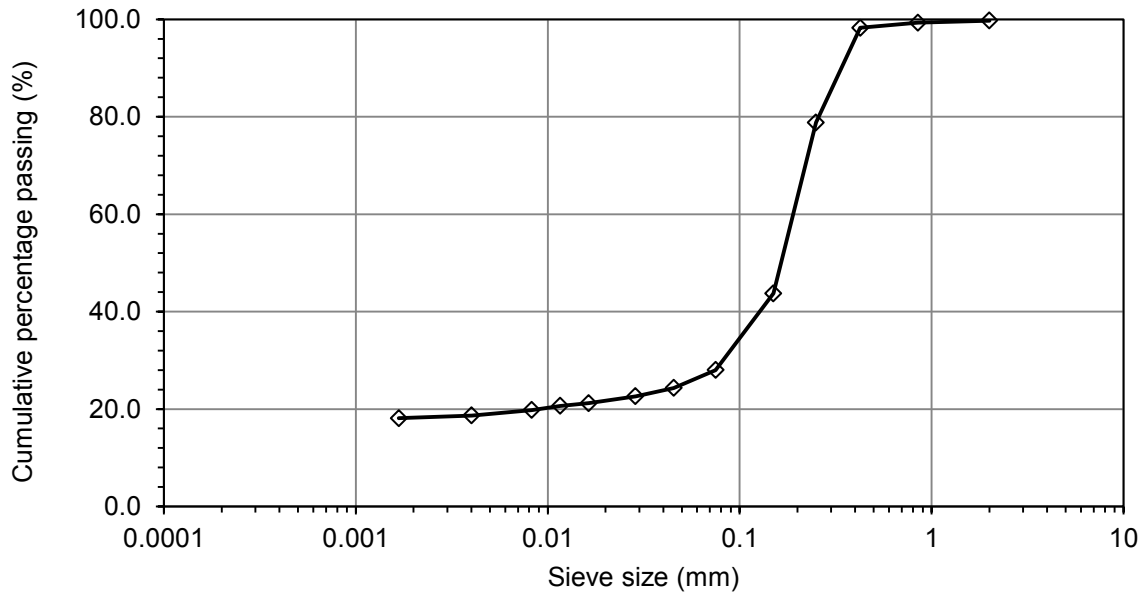


Figure 29. Particle size distribution of soil.

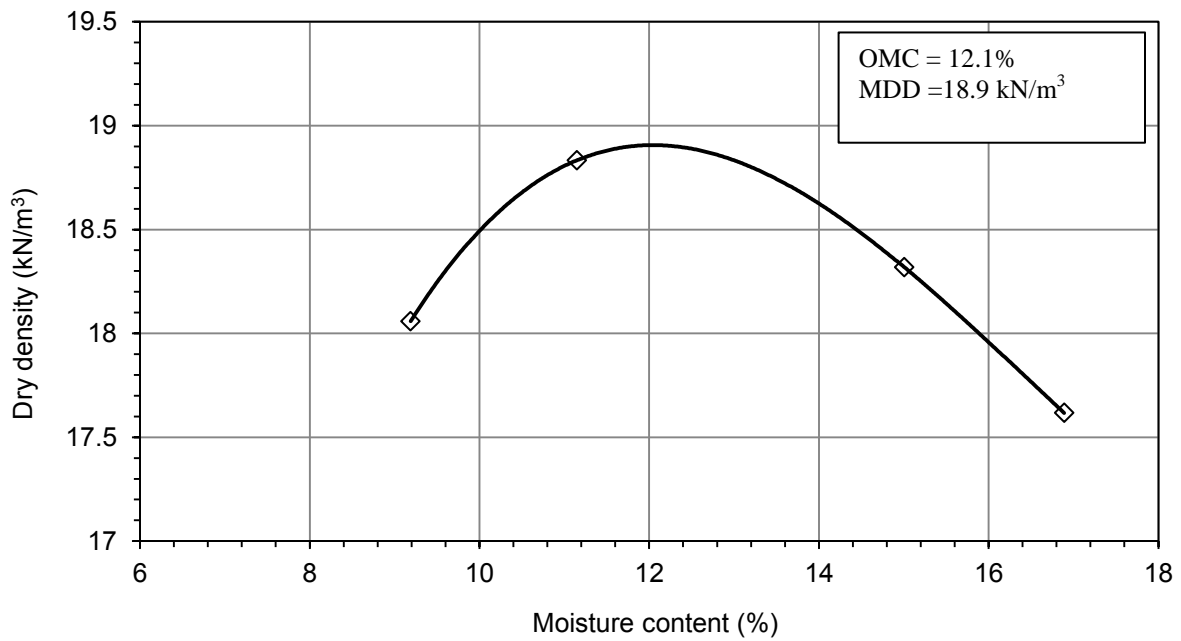


Figure 30. Moisture content and dry density relationship for raw soil.

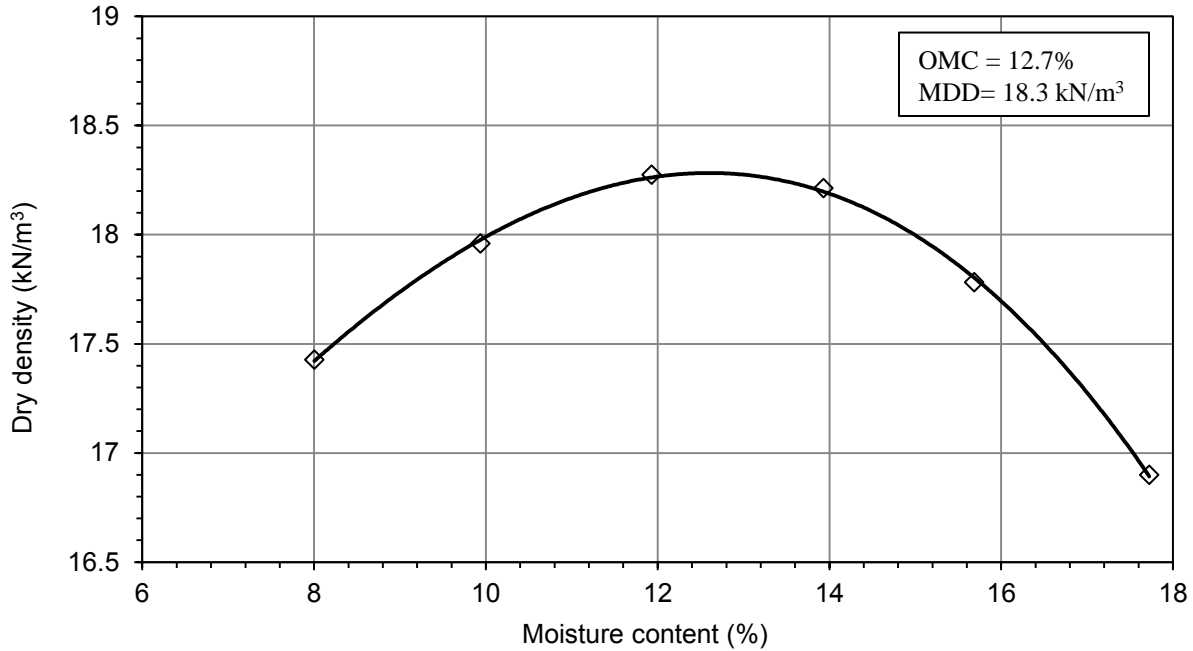


Figure 31. Moisture content and dry density relationship for CKD mixed soil.

Density and Moisture Content Measured in the Field

After blending the cKD with the virgin soil and compacting it with padfoot rollers was complete, twelve different stations (M1 through M12) were marked on the CKD-stabilized subgrade layer, at an approximately 15.24 m (50 feet) interval. Using a nuclear density gauge, the degree of compaction at each test station was determined by first measuring the laboratory determined MDD for CKD-stabilized soil (i.e., 18.3kN/m³) and the measured dry density. The degree of compaction and the measured field moisture content at the twelve stations are presented in Table 9. It can be seen that the degree of soil compaction ranged between 100 to 108.2%, while the moisture content ranged between 9.3 to 12.8% while the OMC was determined as 12.7%.

Table 9. Moisture contents, dry densities and degree of compaction at 12 stations in the field.

Test stations	Moisture content (%)	Dry density (kN/m ³)	Degree of compaction (% of MDD)
M1	11.4	19.4	106.0
M2	11.7	19.2	104.9
M3	10.4	19.0	103.8
M4	12.6	18.6	101.6
M5	12.8	19.0	103.8
M6	12.4	19.0	103.8
M7	9.7	19.4	106.0
M8	10.6	19.0	103.8
M9	10	19.8	108.2
M10	10.7	19.2	104.9
M11	9.9	18.3	100.0
M12	9.3	18.5	101.1

Laboratory Resilient Modulus

Similar to the 60th street project, the resilient modulus test was performed on six specimens. To match with the composition of the subgrade in the field, resilient modulus samples were prepared with 10% CKD, by weight of the soil. Out of six specimens, three specimens were prepared at OMC and the other three were prepared at OMC-2%. Resilient modulus test was conducted at both 0-day and 28-day curing periods. Table 10 lists the moisture content, dry density and degree of compaction for each compacted specimen.

Table 10. Moisture content, dry density and degree of compaction for the resilient modulus test specimens.

Specimen No.	Moisture content (%)	Dry density (kN/m ³)	Degree of compaction (% of MDD)
1	10.8	18.1	98.9
2	10.8	18.3	100.0
3	10.6	18.3	100.0
4	12.6	18.5	101.1
5	12.8	18.3	100.0
6	11.4	18.6	101.6
OMC = 12.7% , MDD = 18.3 kN/m ³			

Figure 32 through Figure 35 show that the effect of deviatoric stress and confining pressure on the M_r values for 0-day cured specimens for Apple Valley project. Two

out of six specimens were discarded because of outlying results. It can be seen that the increment in deviatoric stress results in reduction in M_r . The slope of reduction in M_r due to increase in deviatoric stress is steeper for lower deviatoric stresses. As expected, for a given deviatoric stress, the higher confining pressure results in a higher M_r .

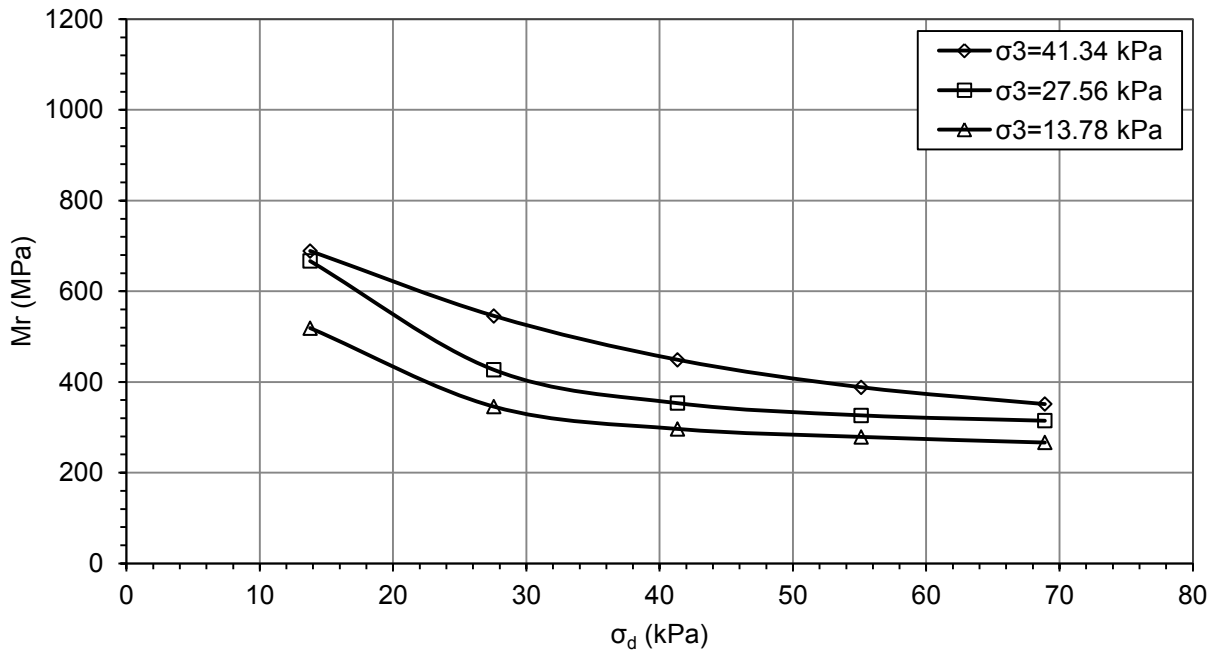


Figure 32. M_r as a function of stress state at moisture content = OMC-2%, Specimen No.1.

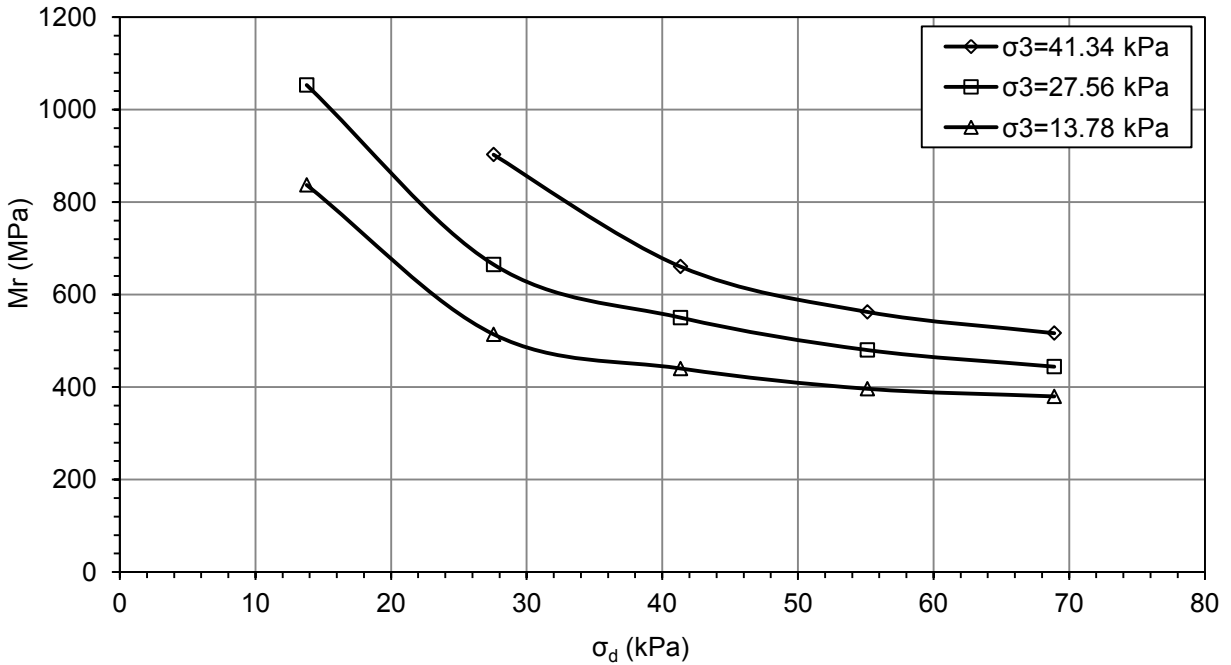


Figure 33. M_r as a function of stress state at moisture content = OMC-2%, Specimen No.2.

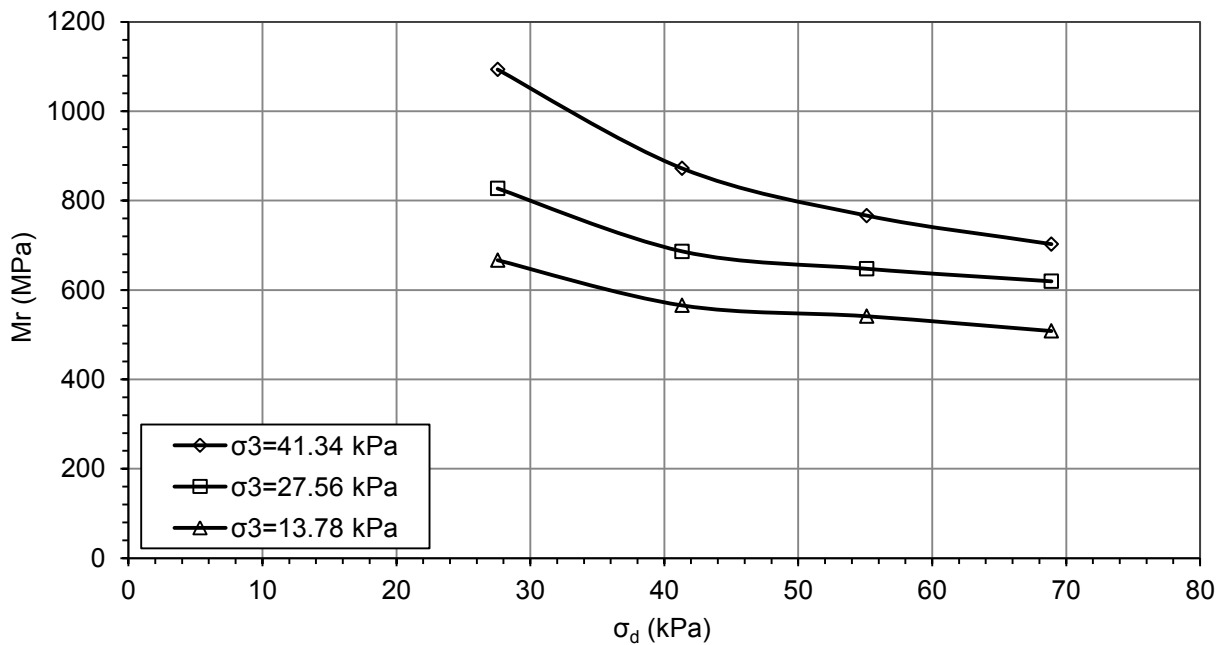


Figure 34. M_r as a function of stress state at moisture content = OMC-2%, Specimen No.3.

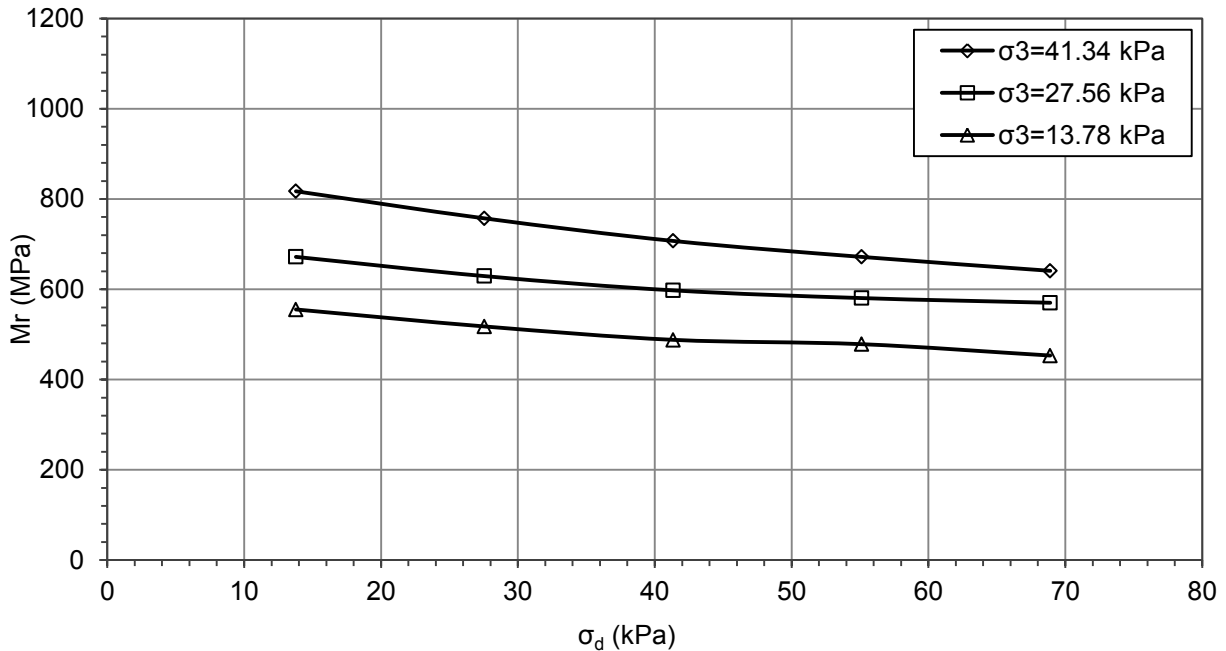


Figure 35. M_r as a function of stress state at moisture content = OMC, Specimen No.4.

Figure 36 through Figure 41 show the effect of deviatoric stress and confining pressure on the 28-day M_r . Results from all the six specimens are incorporated in this case. The M_r values of the 28-day cured specimens are significantly higher than that of the 0-day cured specimens. Also, it can be seen in these six graphs that the M_r does not show a considerable dependency on the confining pressure. The variation of M_r , both at 0- and 28-day curing periods, with respect to the bulk stress (θ) has also been studied. The Appendix A of this report includes the plots showing the variation M_r as a function of bulk stress and confining stress. The trend of the variation of the M_r over bulk stress in the Apple Valley project is similar to that of the 60th street project.

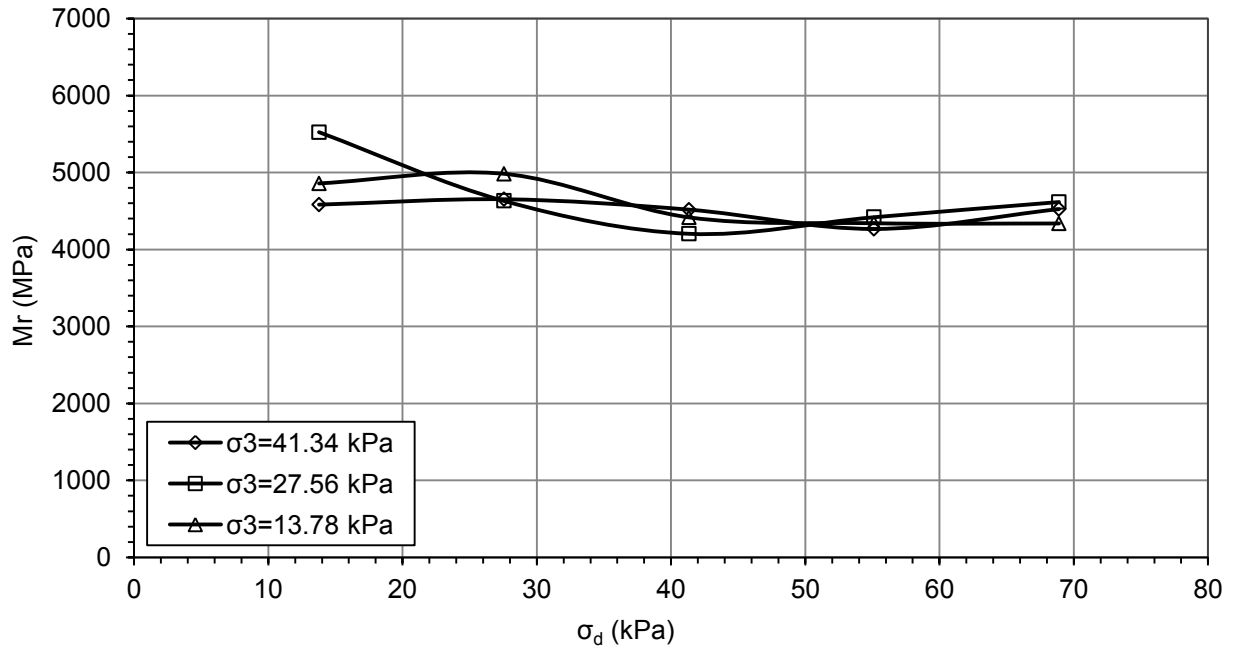


Figure 36. M_r as a function of stress state at moisture content = OMC-2%, Specimen No.1.

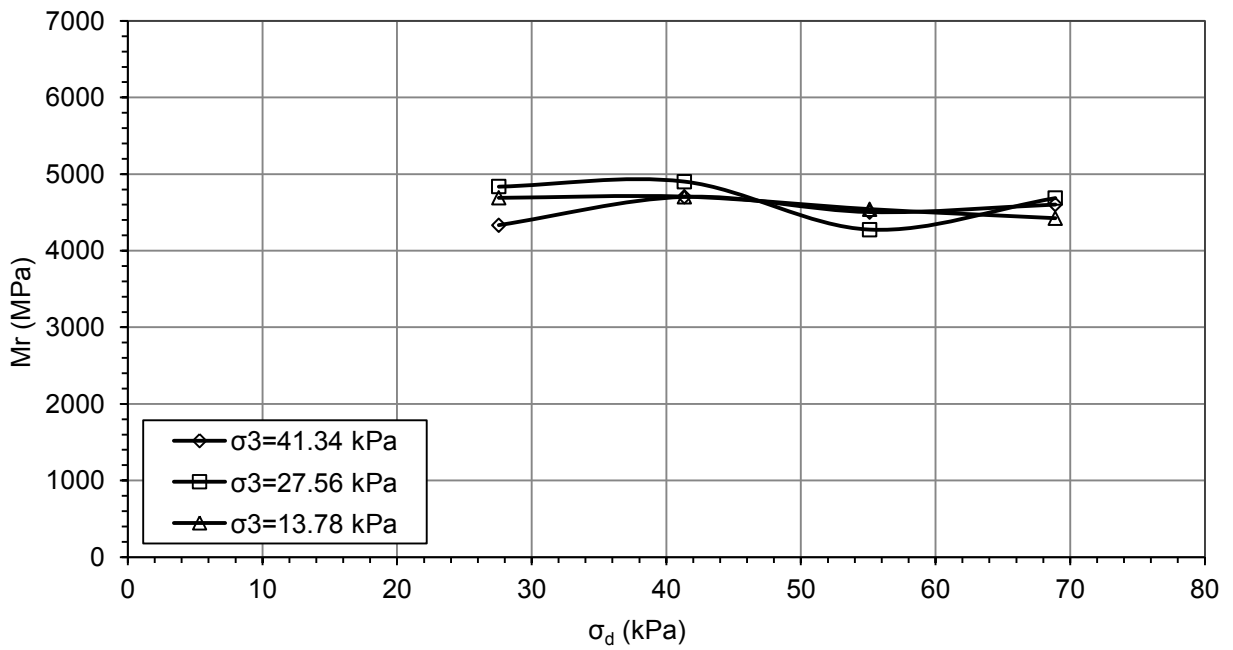


Figure 37. M_r as a function of stress state at moisture content = OMC-2%, Specimen No.2.

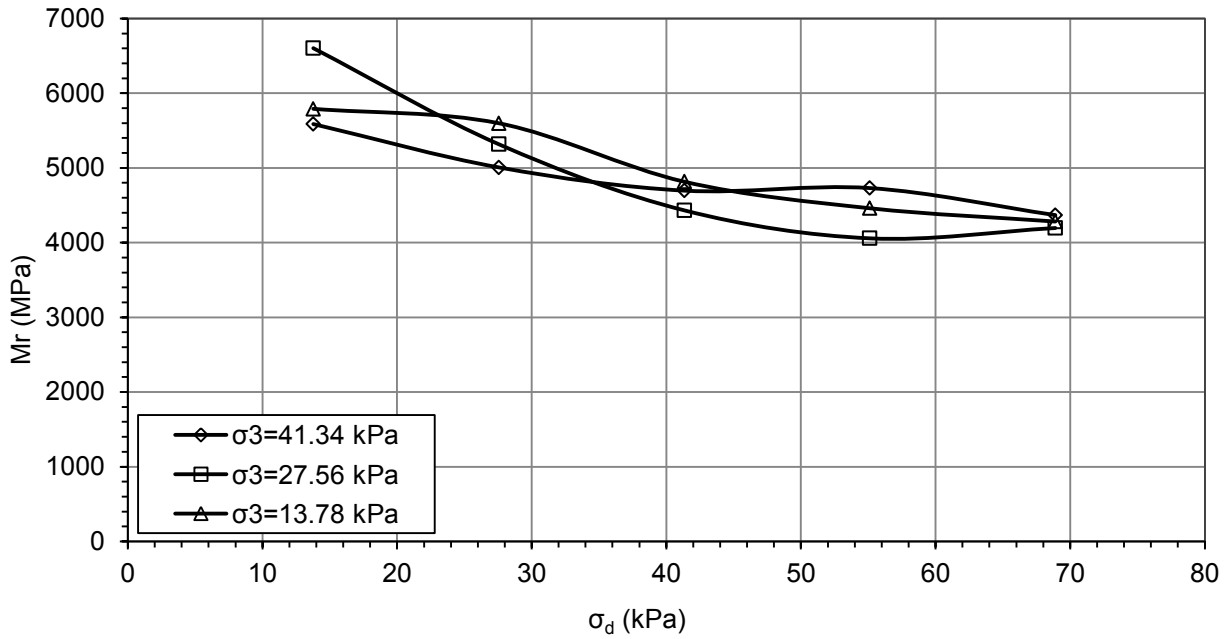


Figure 38. M_r as a function of stress state at moisture content = OMC-2%, Specimen No.3.

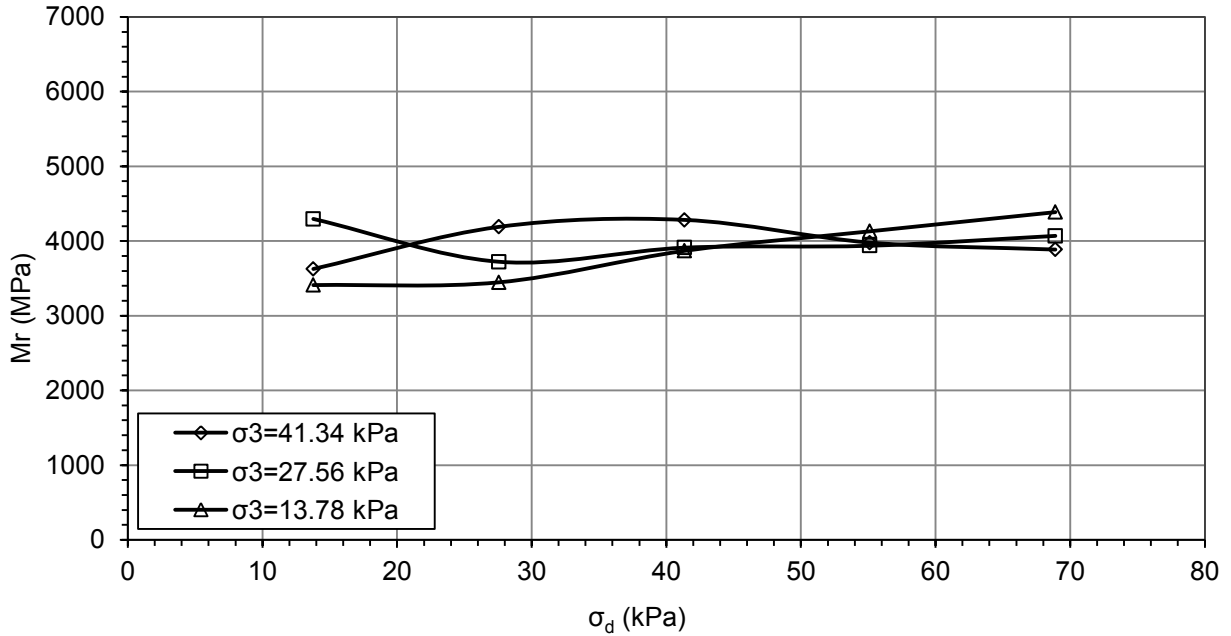


Figure 39. M_r as a function of stress state at moisture content = OMC, Specimen No.4.

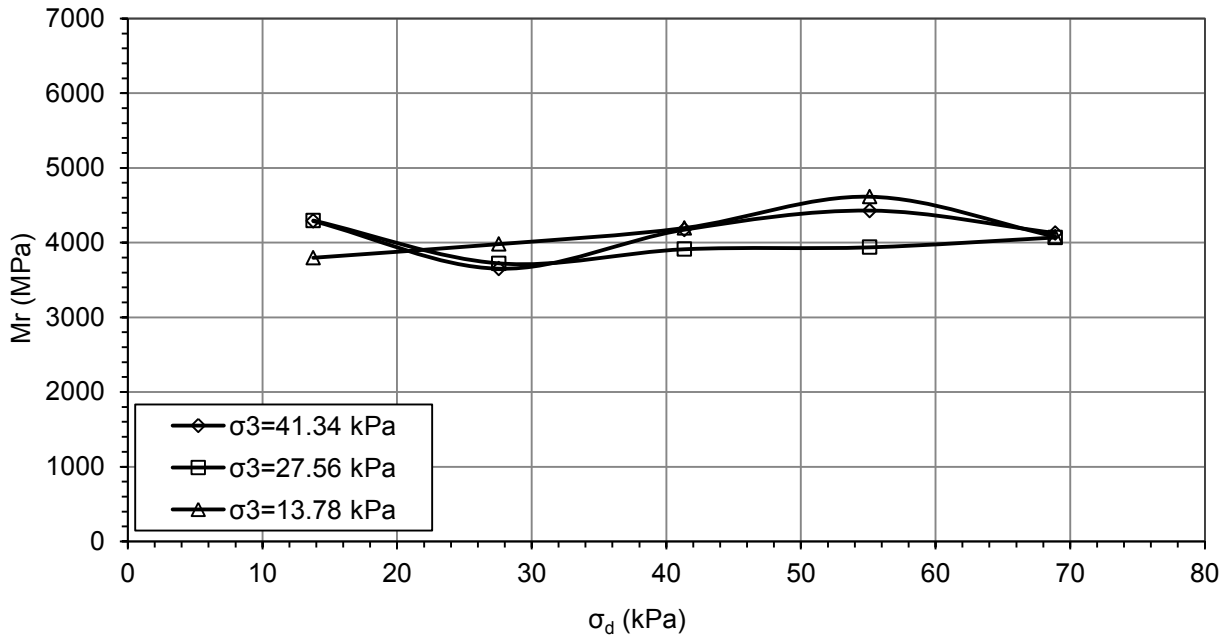


Figure 40. M_r as a function of stress state at moisture content = OMC, Specimen No.5.

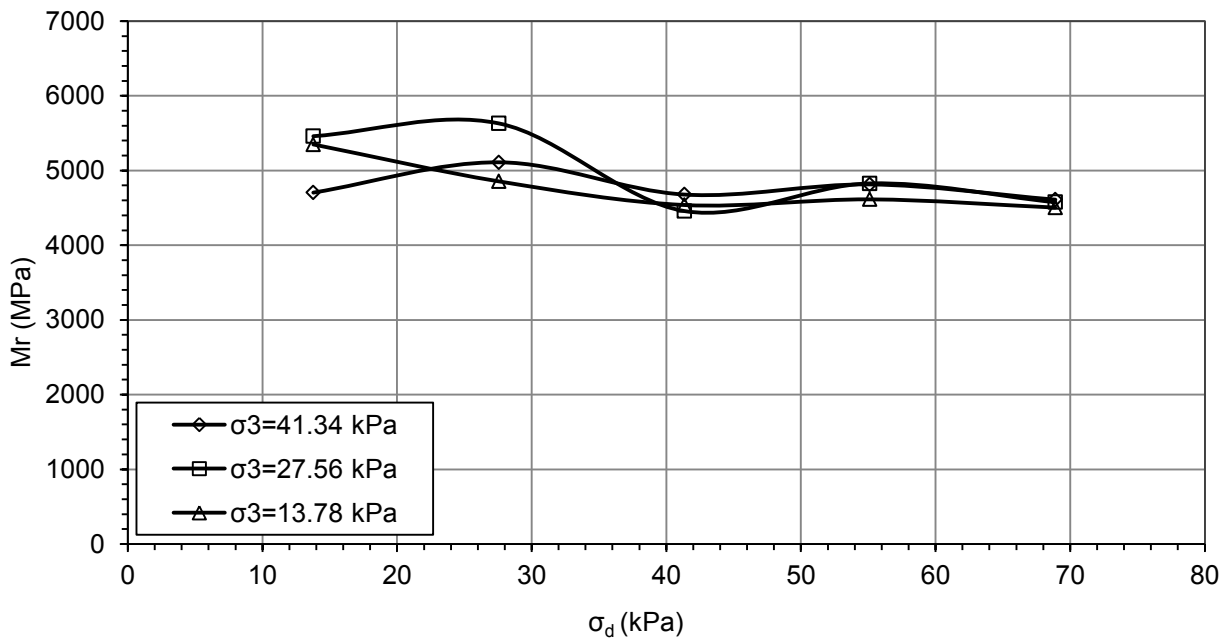


Figure 41. M_r as a function of stress state at moisture content = OMC, Specimen No.6.

Regression models for the empirical determination of resilient modulus

Table 12 shows the regression coefficients for 0-day and 28- days curing periods, respectively. Utilizing the coefficients k_1 , k_2 and k_3 presented in Table 11 and Table 12, regression equations were developed as a function of moisture content and dry density of specimens. Eighty percent of the laboratory M_r data was used in the development of the model. The remaining 20% of the data was used for validation. These regression equations are given in Equation 10 to Equation 15 for both the 0-day and 28-day of curing periods.

Table 11. Value of the coefficients in the constitutive model for 0-day curing.

Specimen No.	k_1	k_2	k_3
1	2055.8	0.427715	-0.5646
2	2809.6	0.480939	-0.65774
3	3900.86	0.570671	-0.54251
4	4218.12	0.48827	-0.26049

Table 12. Value of the coefficients in the constitutive model for 28-day curing.

Specimen No.	k_1	k_2	k_3
1	43609.1	-0.00339	-0.0327
2	43347.8	0.04376	-0.07368
3	39877.5	-0.02893	-0.1692
4	37817.5	0.045445	-0.05661
5	41754	0.100398	0.014232
6	41798.9	0.050764	-0.12664

Models for regression coefficients k_1 , k_2 and k_3 at 0 day curing:

$$k_1 = -116808.633 - 200.155 MC + 6676.181(\gamma_d) \quad \text{Equation 10}$$

$$k_2 = -11.509 - 0.109 MC + 0.722(\gamma_d) \quad \text{Equation 11}$$

$$k_3 = 2.867 + 0.223 MC - 0.321(\gamma_d) \quad \text{Equation 12}$$

Models for regression coefficients k_1 , k_2 and k_3 at 28days curing:

$$k_1 = 127792.503 - 835.980(MC) - 4183.115(\gamma_d) \quad \text{Equation 13}$$

$$k_2 = -0.880 + 0.035 MC + 0.028(\gamma_d) \quad \text{Equation 14}$$

$$k_3 = 3.662 + 0.055 MC - 0.238(\gamma_d) \quad \text{Equation 15}$$

Figure 42 and Figure 43 show the predictability of the regression models developed for 0-day and 28-day curing periods, respectively. In these two figures, the actual and predicted resilient moduli are compared. In each figure, the resilient moduli data used for developing (80% data) and validating (20% data) the models are also presented. The value of R^2 is 0.84 for the 0-day M_r predicting model, while it is 0.65 for 28-day M_r predicting model. It can be seen that the predictability is quite good, with less than 20 and 15% errors in the 0- and 28-day M_r prediction, respectively.

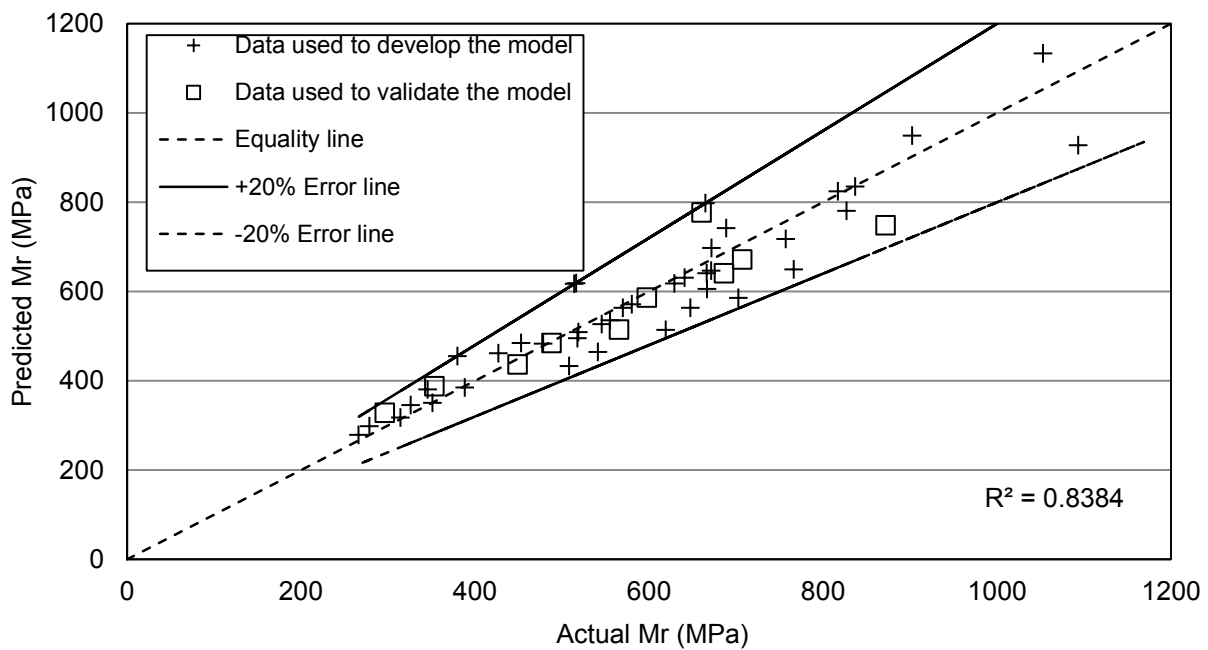


Figure 42. Predicted vs actual M_r values at 0-day curing period.

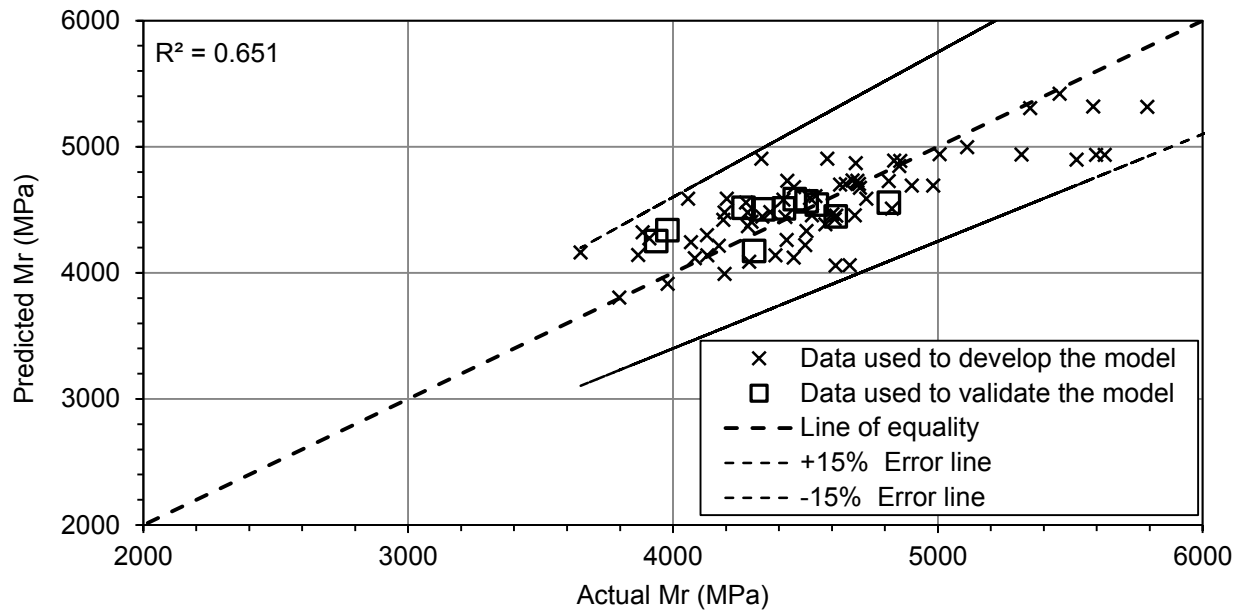


Figure 43. Predicted vs actual M_r values at 28-day curing period.

Relationship between 0- and 28-day Predicted Resilient Moduli

Relationship between the 0-day and 28-day M_r values was established through a regression model. As similar to 60th street project, the ratio of 28-day M_r to 0-day M_r , denoted as y , is expressed as a function of moisture content, dry density, stress state and M_r at 0-day. *Equation 16* shows the regression relationship. The 28-day M_r can be determined from the knowledge of 0-day M_r , and the vice versa.

$$y = -0.90497 MC + 1.56633(\gamma_d) - 0.00312996(\theta) - 0.0168001(Mr_{0-day}) \quad \text{Equation 16}$$

where MC is moisture content, γ_d is dry density, θ is bulk stress (sum of three principal stresses) and Mr_{0-day} is the 0-day M_r . Figure 44 shows the relationship for the predicted 0-day M_r (using *Equation 16*) and actual lab measured 0-day M_r . It can be seen that the model can predict the M_r with an error less than $\pm 15\%$.

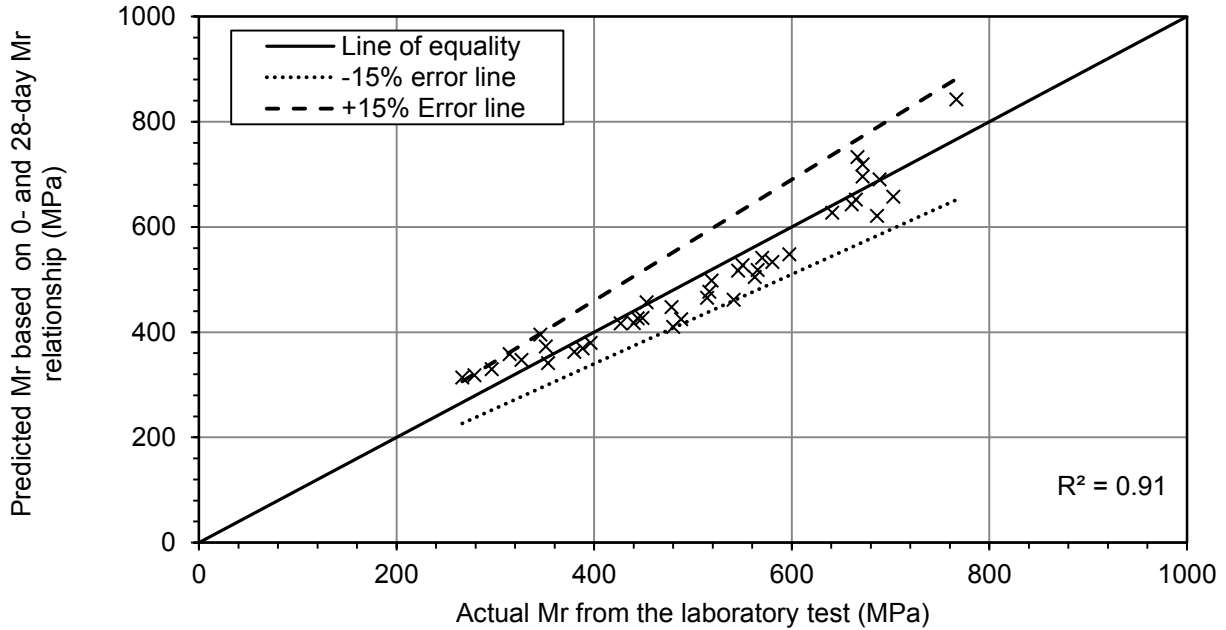


Figure 44. Predictability of the regression model developed for relating the 0-day M_r and 28-day M_r .

Estimation of stiffness (M_r) at the test locations during compaction of the subgrade

Twelve stations were marked in the field to record the IACA readings. Moisture contents and dry densities were also collected at those 12 stations as was already listed in Table 9. Using the equations for k_1 , k_2 and k_3 , resilient modulus of subgrade at each station (with the corresponding moisture contents and dry densities) can be calculated

$$M_r = k_1 p_a \left(\frac{\theta}{p_a} \right)^{k_2} \left(\frac{\sigma_d}{p_a} \right)^{k_3}$$

according to the constitutive model expressed in

Equation 2. The maximum stress state applied on the resilient modulus test specimen was used in estimating the resilient moduli. The coefficients k_1 , k_2 and k_3 and predicted 28-day M_r at 12 stations are listed in Table 13. It may be mentioned here that the dry density attained in the field was well above the dry density that was achieved in the lab. Therefore, the developed model for 0-day M_r could not directly be used to predict the M_r at all the 12 stations with a reasonable accuracy. It may also be mentioned that the 28 days M_r were not too sensitive, and a reasonable prediction could

be made by using the developed 28-day model. Therefore the 0-day resilient moduli for the 12 stations were backed out by using the 0-day and 28-day relationship (Equation 16). The M_r values are presented in Table 14.

Table 13. Predicted 28-day resilient modulus at the twelve stations.

Test stations	k_1	k_2	k_3	Predicted M_r (MPa)
M1	37148.39	0.060	-0.325	4431
M2	37677.53	0.065	-0.264	4405
M3	39544.25	0.014	-0.291	4521
M4	39264.98	0.081	-0.081	4323
M5	37537.90	0.099	-0.158	4306
M6	37872.29	0.085	-0.180	4342
M7	38569.55	0.000	-0.419	4589
M8	39377.05	0.021	-0.280	4503
M9	36758.87	0.021	-0.491	4558
M10	38513.51	0.030	-0.319	4496
M11	43082.01	-0.024	-0.141	4536
M12	42803.65	-0.040	-0.219	4596

Table 14. Predicted 0-day resilient modulus at the twelve stations.

Test stations	Predicted 0-day M_r (MPa)
M1	846
M2	794
M3	866
M4	580
M5	658
M6	700
M7	967
M8	851
M9	995
M10	871
M11	795
M12	869

IACA Measured Modulus

Table 15 shows the IACA estimated 0-day resilient modulus at 12 stations. IACA was calibrated using the maximum (995 MPa) and minimum (580 MPa) M_r values obtained at Stations M9 and M4, respectively. Then for validation purpose, the 0-day M_r values

for the remaining 10 stations were estimated. The vibration data collected at all the 12 stations were processed and 0-day modulus was estimated (Table 15).

Table 15. IACA measured modulus for the 12 test stations.

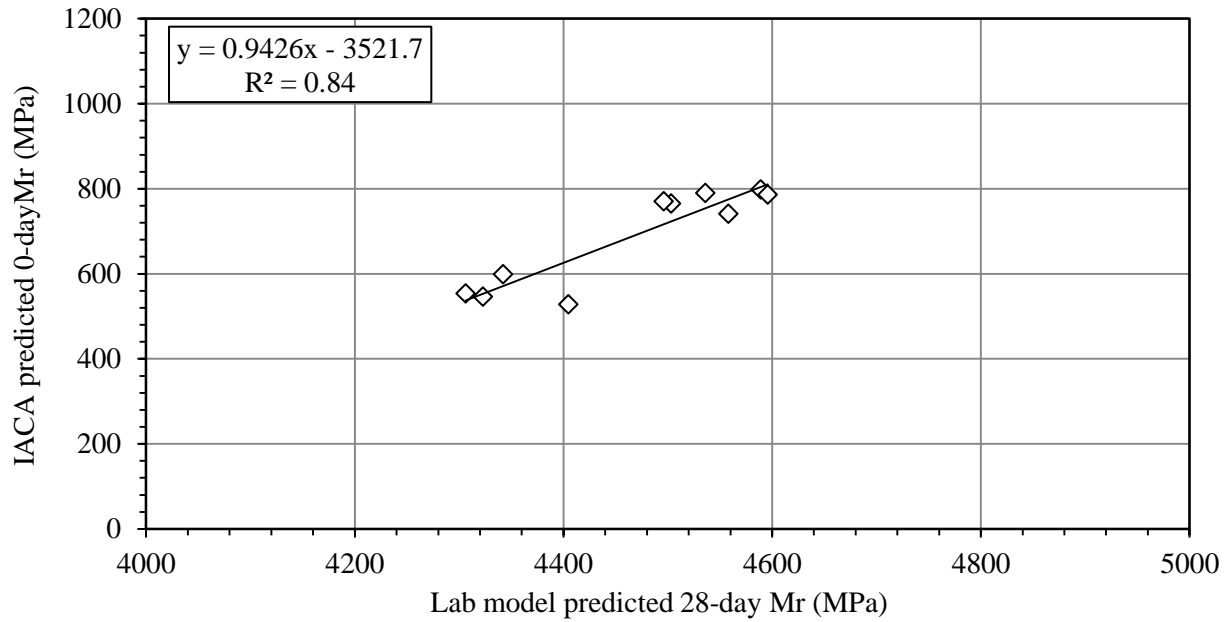
Test stations	IACA Predicted 0-day M_r (Mpa)
M1	561
M2	528
M3	501
M4	546
M5	553
M6	599
M7	798
M8	765
M9	740
M10	770
M11	790
M12	786

Comparison of the laboratory model predicted M_r and IACA estimated M_r

Table 16 provides a comparison of the M_r values estimated through the different methods, discussed in this report. Figure 45 shows the relationship between the IACA estimated 0-day M_r and lab predicted 28-day M_r . It can be seen that the IACA estimated M_r values have a very good correlation with 28-day lab predicted M_r values. The coefficient of determination (R^2) is 0.84 for this correlation. Figure 46 shows the relationship between the IACA estimated 0-day M_r and lab predicted 0-day M_r . The correlation is also very good with R^2 equal to 0.60.

Table 16. Comparison of the moduli obtained through different methods.

Test stations	Laboratory predicted 28-day M_r (MPa)	Lab predicted 0-day M_r (MPa)	IACA estimated M_r (MPa)
M2	4405	794	528
M4	4323	580	546
M5	4306	658	553
M6	4342	700	599
M7	4589	967	798
M8	4503	851	765
M9	4558	995	740
M10	4496	871	770
M11	4536	795	790
M12	4596	869	786



Note: A different scale was used for the lab predicted 28-day M_r .

Figure 45. Correlation between the IACA estimated 0-day M_r and laboratory model predicted 28-day M_r .

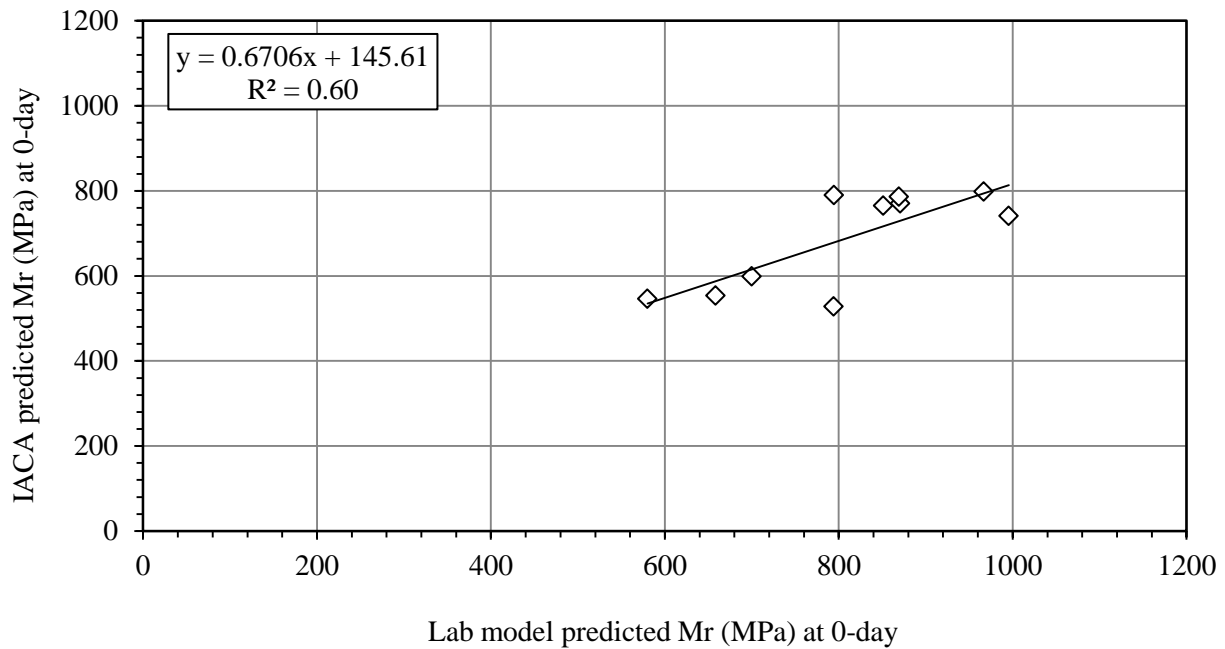


Figure 46. Correlation between the IACA estimated 0-day M_r and laboratory model predicted 0-day M_r .

Station wise comparisons between IACA estimated M_r with laboratory model predicted M_r

Figure 47 shows the station wise comparison between the laboratory model predicted M_r and IACA estimated M_r . It can be seen that in most of the stations, the laboratory model predicted M_r and IACA estimated M_r are well in agreement. This finding also encourages that the IACA can predict the subgrade resilient modulus with a reasonable accuracy.

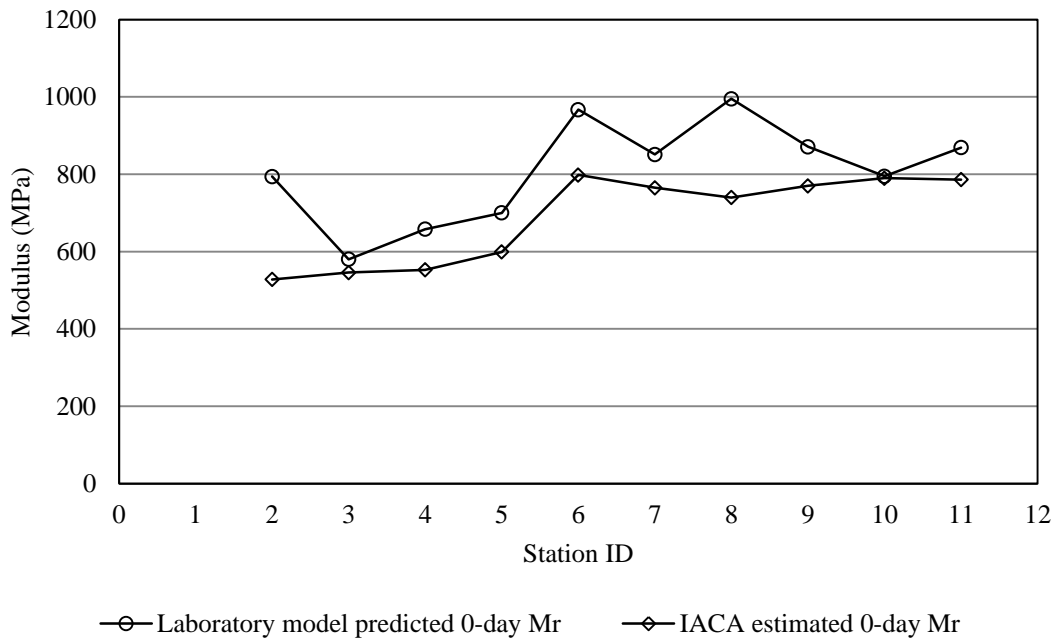


Figure 47. IACA estimated M_r and laboratory model predicted M_r at different stations.

The analysis of the results from the Apple Valley project shows that the IACA can be calibrated with the M_r values predicted by the laboratory M_r models. The M_r models were developed based on the laboratory M_r results. If the measured dry densities and moisture contents in the field are reliable and the laboratory achieved compaction level matches with the field compaction level, then a good correlation between the laboratory predicted M_r and IACA estimated M_r can be achieved. Accurate measurement of moisture content and dry density of the stabilized soil in the field will aid in the estimation of resilient modulus with a low error.

4.5 Generic Regression Models

The laboratory models developed for predicting the resilient moduli for both 60th Street and Apple Valley projects are general in nature. The application of those models is limited to the soil types that were actually used in stabilizing the subgrade in those two projects. Further, only one percentage of a particular additive (10% CKD) was used in stabilizing the subgrade. Therefore, an attempt was made to develop generic models for predicting M_r values for any type of soil, additive, and percentage of stabilizing agent. Because of the limitation of the database in the present work, data available in the literature was used to develop generic models. Solanki et al. (2010) and Zahid et al. (2011) considered a large number of soil and additive types in developing regressions models for predicting 28-day M_r . However in their models, the percent fines (P_{200} - percentage passing through ASTM sieve No. 200) were not considered. As this is a very important parameter, the present study took into consideration this parameter in the development of predictive models for M_r .

Prior results in the literature considered 28-day M_r test results as a function of stress state, atmospheric pressure, soil type, additive type and percentage, moisture contents and dry densities. In this study, a database was developed using four different soils collected from four different locations in the state (one silty clay with sand, two lean clays and one fat clay) and three different types of stabilizers (lime, class C fly ash and CKD). Seventy five percent of the total data was used to develop the model and the remaining 25% was used to validate the model. 75% data was plugged into AASHTO

$$M_r = k_1 p_a \left(\frac{\theta}{p_a} \right)^{k_2} \left(\frac{\sigma_d}{p_a} \right)^{k_3}$$

1993 M_r predicting constitutive model (

Equation 2) for backing out the coefficients k_1 , k_2 and k_3 as a function of the above mentioned variables. Then an individual regression model was developed for each of the three coefficients as a function physical properties of soil, chemical properties of soil and properties of additive etc. **Error! Reference source not found.** to

$$k_3 = c_0 \log \left(\frac{UCS}{P_a} \right) + c_1 \log(MC) + c_2 \log \left(\frac{DUW}{\gamma_w} \right) + c_3 \log(PI) + c_4 \log(SA) + c_5 \log(A) + c_6 \log(CaO)$$

$$+ c_7 \log(FL) + c_8 \log(LOI) \quad \text{Equation 19}$$

presents the generic models for k_1 , k_2 and k_3 coefficients.

$$\log(k_1) = a_0 + a_1 \log\left(\frac{UCS}{P_a}\right) + a_2 \log(MC) + a_3 \log\left(\frac{DUW}{\gamma_w}\right) + a_4 \log(PI) + a_5 \log(SSA) + a_6 \log(Al_2O_3) + a_7 \log(P_{325}) \quad \text{Equation 17}$$

$$k_2 = b_0 \log\left(\frac{UCS}{P_a}\right) + b_1 \log(pH_s) + b_2 \log(PA) + b_3 \log(P_{200}) \quad \text{Equation 18}$$

$$k_3 = c_0 \log\left(\frac{UCS}{P_a}\right) + c_1 \log(MC) + c_2 \log\left(\frac{DUW}{\gamma_w}\right) + c_3 \log(PI) + c_4 \log(SSA) + c_5 \log(PA) + c_6 \log(CaO) + c_7 \log(FL) + c_8 \log(LOI) \quad \text{Equation 19}$$

where UCS is the 28-day unconfined compressive strength (kPa); P_a is the atmospheric pressure (101.283 kPa); γ_w is the density of water (9.81 kN/m³); PI is the plasticity index; SSA is the specific surface area of soil (m²/g); Al₂O₃ = alumina content of additive (%); P₃₂₅ is the percentage passing No. 325 sieve for additive (%); pH = pH of pure soil; PA is the additive content in specimen (%); CaO is the calcium oxide content of additive (%); FL is the free lime content of additive (%); LOI is the loss on ignition of additive (%); MC is molding moisture content (%) and DUW is the molding dry unit weight (kN/m³). The parameters a_0 to a_7 , b_0 to b_3 and c_0 to c_8 are the regression coefficients, the value of each of them are given Table 17. Figure 48 shows the predictability of the generated generic model. The data used to validate the model are included in the graph. It can be seen that the predictability of the model is quite good with R² equal to 0.78.

Table 17. Comparison of the moduli obtained through different methods.

k ₁		k ₂		k ₃	
a ₀	-4.547	b ₀	-0.59206	c ₀	0.245309
a ₁	1.210	b ₁	0.398808	c ₁	0.355379
a ₂	1.265	b ₂	0.34705	c ₂	-6.28843
a ₃	1.426	b ₃	-0.07653	c ₃	0.161071
a ₄	0.127			c ₄	-0.22804
a ₅	-0.449			c ₅	-0.26732
a ₆	0.099			c ₆	0.647208

a_7	3.171		c_7	-0.32259
			c_8	0.169303

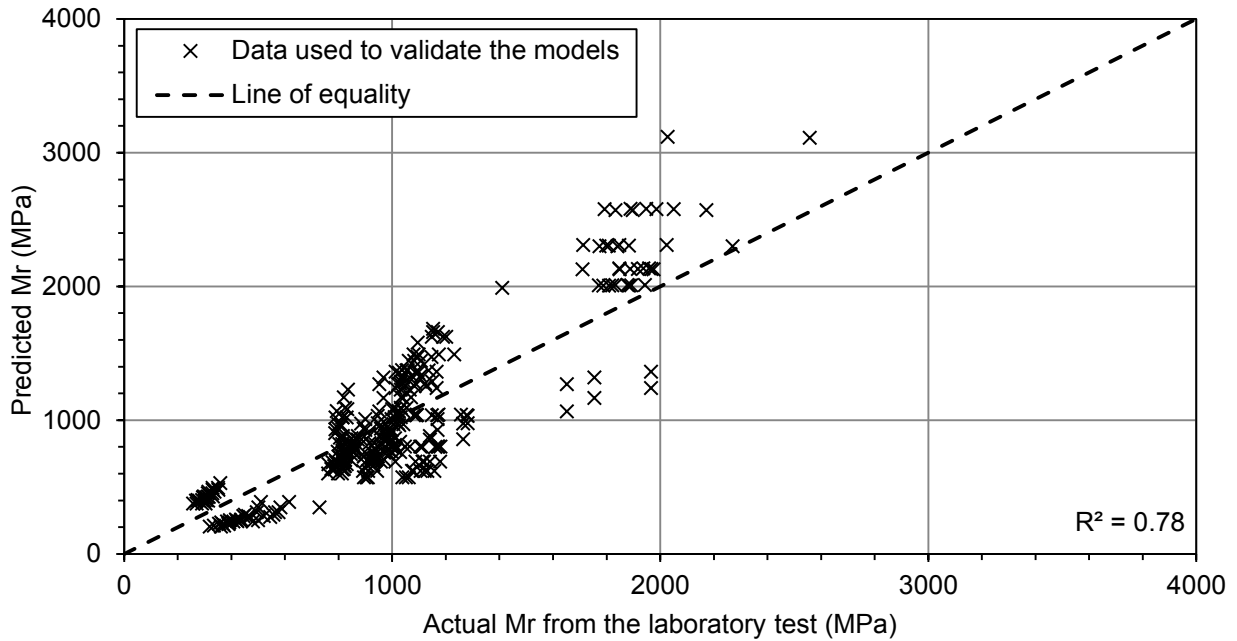


Figure 48. Validation of the generic regression model for 28-day M_r .

The study reported in this section indicates that generic empirical models can be used to estimate the resilient modulus of the com compacted subgrade soil if the maximum dry density and moisture content at the test location on the compacted subgrade are known. Such empirical models are especially useful if it is not possible to carry out detailed resilient modulus tests in the laboratory prior to the construction.

5. OUTCOMES OF THE RESEARCH AND CONCLUSIONS

The use of the Intelligent Asphalt Compaction Analyzer (IACA) to estimate the resilient modulus (M_r) of cementitiously stabilized subgrade soils in real-time during their compaction was evaluated in this research. Preliminary feasibility studies were carried out at two different sites in Year One of the study. These results were then used to develop calibration and estimation procedures for the IACA. The validation of the IACA was carried out at two different project sites in Year Two of the study. Virgin soil and additives from each of these sites were first collected and their properties were studied in the laboratory. Regression models were then developed to analyze the dependence of the subgrade stiffness (M_r) on the soil properties and level of compaction. Tests using Falling Weight Deflectometer (FWD) and Nuclear Density Gauge (NDG) were conducted at select locations on the stabilized subgrade after compaction. IACA estimated M_r values were then compared with FWD backcalculated moduli and M_r values predicted using the regression models. The results of these tests reveal that the calibrated IACA can be used to estimate the resilient modulus of the soil in real time during compaction with an accuracy that is suited for quality control applications.

Each of the four projects contributed to our understanding of the effect of moisture content and dry density on the stiffness of the stabilized subgrade and to our understanding the applicability of the IACA for soil compaction. The first two projects verified that the IACA could detect changes in the vibrations of the compactor during operation and that these changes were a direct result of changing stiffness of the subgrade soil. The next two projects included a compressive study for investigating the ability of the IACA in predicting the M_r . The new mechanistic pavement design method such as MEPDG (ARA 2004) requires the M_r as the design input. An effort was thereby made in both the 60th Street and Apple valet projects to investigate the capability of the IACA in determining the in-situ M_r during the construction of the subgrade. Following are a few conclusions that could be drawn from the results of the research.

- The regression model developed from the laboratory M_r test results can be used to predict the M_r in the field as a function of dry density and moisture content and soil properties. However, accurate representative measurements of moisture content and dry density in the field are required to obtain accurate prediction of the modulus.
- It was found that the IACA can estimate the resilient modulus with reasonable accuracy and comparable with the FWD-backcalculated subgrade modulus ($R^2 = 0.63$; error = $\pm 15\%$) and laboratory measured resilient modulus ($R^2 = 0.59$; error = $\pm 15\%$).
- It is understood that it is not feasible to conduct FWD tests in all the projects. In such instances, M_r models based on the laboratory results can be used to calibrate the IACA as well to verify the IACA estimated modulus.
- Lastly, in real time quality control work for a given project, subgrade samples can be collected beforehand to conduct the resilient modulus test. Based on the M_r test results M_r predicting models can be developed. Then during the field work, field moisture contents and dry densities can be collected at a few calibration points, which can then be used to determine the calibration coefficients for the IACA. This would greatly simplify the process of calibration and reduce the time required for installation and calibration of the IACA.

5. RECOMMENDATIONS AND SCOPE FOR FUTURE WORK

The primary goal of the project described in this report is the extension of the Intelligent Asphalt Compaction (IACA) Technology to the compaction of stabilized soil subgrades and to demonstrate its use during field compaction. The IACA prototype developed in this study was shown to be rugged, easily installable on any vibratory compactor, and is suitable for its use as a quality control device during the compaction of cementitious stabilized soil subgrades. While the technology is mature, there still has to be a significant education of the workforce before the technology can find widespread use. The following are the major findings and recommendations of the study.

- The IACA is suitable for use as a quality control tool during the compaction of soil subgrades.
- The IACA can reduce quality control personnel making spot checks behind the roller during the compaction process. This would have tremendous consequence on the work place safety and will be likely to increase the productivity of the crew.
- While the technology has been successfully demonstrated, significant education of the contractor and DOT personnel is required before Intelligent Compaction technologies can find wide spread use.
- The results reported in this study substantiate the ability of the IACA technology to provide continuous estimates of the stiffness of the soil during its compaction. Such continuous estimates can enable the operator to identify deficiencies (under compaction / soft spots) during compaction. Remediation of such deficiencies can improve the stiffness and quality of the subgrades and have direct impact on the quality of asphalt pavements constructed on top of the compacted subgrade.
- The IACA estimates reflect the stiffness of the subgrade during its construction. For the first time, IC reported values were shown to correlate with in-situ measurements. Contrary to other IC technologies, the IACA reports estimates of the resilient

modulus of the subgrade and not some arbitrary machine specific value. While MEPDG guidelines recommend the use of resilient modulus to determine the quality of compaction of stabilized subgrades, quality assurance / acceptance criteria used by different state and federal agencies do not explicitly require the determination of the modulus either over the entire extent or at randomly selected locations on the constructed subgrade. QA specifications in terms of stiffness will greatly aid in the early acceptance of IC technologies by the contractors.

In this study the researchers demonstrated the ability of the IACA to estimate the stiffness of cementitiously stabilized soil during compaction. The tests were performed by the project staff under controlled set of conditions. In the next few years, the PIs plan to conduct several independent trials to study the accuracy of the estimated resilient modulus of the soil subgrade.

The demonstrations in this study were limited to the compaction of subgrade soils stabilized using CKD. The compaction of soils stabilized using Fly Ash or lime and the compaction of unmodified soils were not addressed in this research. Further, at this time, the IACA technology only provides real-time feedback of the compaction quality to the operator. The use of this information in the closed-loop control of the compactor is one of the goals of future research.

7. TECHNOLOGY TRANSFER SUCESESSES

The IACA technology has been patented and licensed to Volvo Construction Equipment (VCE). VCE has partnered with OU in the enhancement of the IACA technology and is committed to providing 51% of all the development costs pertaining to this technology. Since 2008, VCE has contributed over \$1.2M towards royalty payments and for refining the IACA technology. This has also resulted in additional leveraged funding of \$831,119 over the same period. VCE is currently supporting the OU Research team in the systematic evaluation of the IACA for estimating the stiffness of asphalt pavements as well as the stiffness of modified soils and soil subgrades (OTCREOS 10.1-11: Real-time measurement of quality during the compaction of subgrade soils). VCE and OU are collaborating to introduce the IACA technology to the market in the near future.

8. REFERENCES

1. AASHTO (1993). "Guide for Design of Pavement Structures." AASHTO, National Research Council, Washington, D.C.
2. AASHTO T 307 (1999). "Standard Method of Test for Determining the Resilient Modulus of Soils and Aggregate Materials." AASHTO Standards, Washington, DC.
3. AASHTO (2004). "Guide for Mechanistic-Empirical Design of New and Rehabilitated Pavement Structures." Final Report prepared for National Cooperative Highway Research Program (NCHRP), Transportation Research Board, National Research Council, Washington D.C.
4. AASHTO M 145 (2008). "Practice for Classification of Soils and Soil-Aggregate Mixtures for Highway Construction Purposes". AASHTO Standards, Washington, D.C.
5. AASHTO T-166 (2010). "Standard Method of Test for Bulk Specific Gravity of Compacted Hot Mix Asphalt (HMA) Using Saturated Surface-Dry Specimens." AASHTO Standards, Washington, DC.
6. Andrei, D., Witczak M. W., Schwartz C. W., and Uzan J. (2004). "Harmonized Resilient Modulus Test Method for Unbound Pavement Materials." In Transportation Research Record: Journal of the Transportation Research Board, No. 1874, Transportation Research Board of the National Academies, Washington, D.C., pp. 29–37.
7. ARA, Inc., ERES Consultants Division (2004). "Guide for Mechanistic-Empirical Design of New and Rehabilitated Pavement Structures." NCHRP Project 1-37A. Transportation Research Board of the National Academies, Washington, D.C.
8. Camargo, F., Larsen, B., Chadbourn, B., Roberson, R., and Siekmeier, J. (2006). "Intelligent Compaction: A Minnesota Case History," Proc., 54th Annual University of Minnesota Geotechnical Conf., St. Paul, MN.
9. Commuri, S., and Zaman, M. (2008). "A Novel Neural Network-Based Asphalt Compaction Analyzer." International Journal of Pavement Engineering, 9(3), pp. 177-188.

10. Commuri, S., and Zaman, M. (2010). "Method and Apparatus for Predicting the Density of Asphalt." U.S. Patent No. 7-669-458.
11. Hoffman, O., Guzina, B. and Drescher, A. (2004). "Stiffness Estimates Using Portable Deflectometers," Transportation Research Record, 1869, Transportation Research Board, National Research Council, Washington D. C., 59-66.
12. Hossain, Z., Zaman, M., Doiron, C., & Cross, S. (2011). "Development of Flexible Pavement Database for Local Calibration of MEPDG-Volume 1" No. FHWA-OK-11-06 (1).
13. Lambe, T. W., and Whitman, R. V. (1969). "Soil Mechanics." John Wiley and Sons, New York.
14. Little, D. N. (1996). "Evaluation of Resilient and Strength Properties of Lime-Stabilized Soils for the Denver, Colorado Area." Report for the Chemical Lime Company.
15. Mooney, M. A. and Rinehart, R. V. (2007). "Field Monitoring of Roller Vibration during Compaction of Subgrade Soil," Journal of Geotechnical and Geoenvironmental Engineering, 133(3), 257-265.
16. Nazarian, S., Yuan, D. and Williams, R. B. (2003). "A Simple Method for Determining Modulus of Base and Subgrade Materials," Proceedings of Symposium on Resilient Modulus Testing for Pavement Components, Salt Lake City, 152-164.
17. NCHRP (1997). "Laboratory Determination of Resilient Modulus for Flexible Pavement Design." NCHRP Web Document 14 for Project 1-28. Transportation Research Board, Washington, D.C.
18. OHD L-50 (2009). "Soil Stabilization Mix Design Procedure." Oklahoma Highway Department Procedure, <http://www.okladot.state.ok.us/materials/pdfs-ohdl/ohdl50.pdf>, Last Accessed: June 06, 2011.
19. Petry, T. M. and Little, D. N. (2002). "Review of Stabilization of Clays and Expansive Soils in Pavements and Lightly Loaded Structures – History, Practice, and Future." Journal of Materials in Civil Engineering, 14(6), 447-460.

20. Siekmeier, J. A., Young, D. and Beberg, D. (2000). "Comparison of the Dynamic Cone Penetrometer with other Tests During Subgrade and Granular Base Characterization in Minnesota." Nondestructive Testing of Pavement and Backcalculation of Moduli, ASTM STP 1375, 3, West Conshohocken, P.A.
21. Soil Survey of Cleveland County, Oklahoma (1987). conducted by the United States Department of Agriculture Soil Conservation Service, in cooperation with Oklahoma Agricultural Experimental Station, pp. 63-64.
<http://soildatamart.nrcs.usda.gov/Manuscripts/OK027/0/Cleveland.pdf>
22. Soil Survey of Oklahoma County, Oklahoma (2003). conducted by the United States Department of Agriculture Soil Conservation Service, in cooperation with Oklahoma Agricultural Experimental Station, pp. 149-150, 200.
23. Solanki, P., Zaman, M. M., & Dean, J. (2010). "Resilient Modulus of Clay Subgrades Stabilized with Lime, Class C Fly Ash, and Cement Kiln Dust for Pavement Design." Transportation Research Record: Journal of the Transportation Research Board, 2186(1), 101-110.
24. TRB (2009). "Development of an In-Situ Test that will Measure Performance Properties of Sub-Grade Soils Stabilized with Cementitious Materials." TRB Research Needs Statements, <http://rns.trb.org/dproject.asp?n=12637>, Last Accessed: October, 2009.

APPENDIX A

Resilient Modulus as a function of bulk stress and confining stress

60th street project

0-day curing

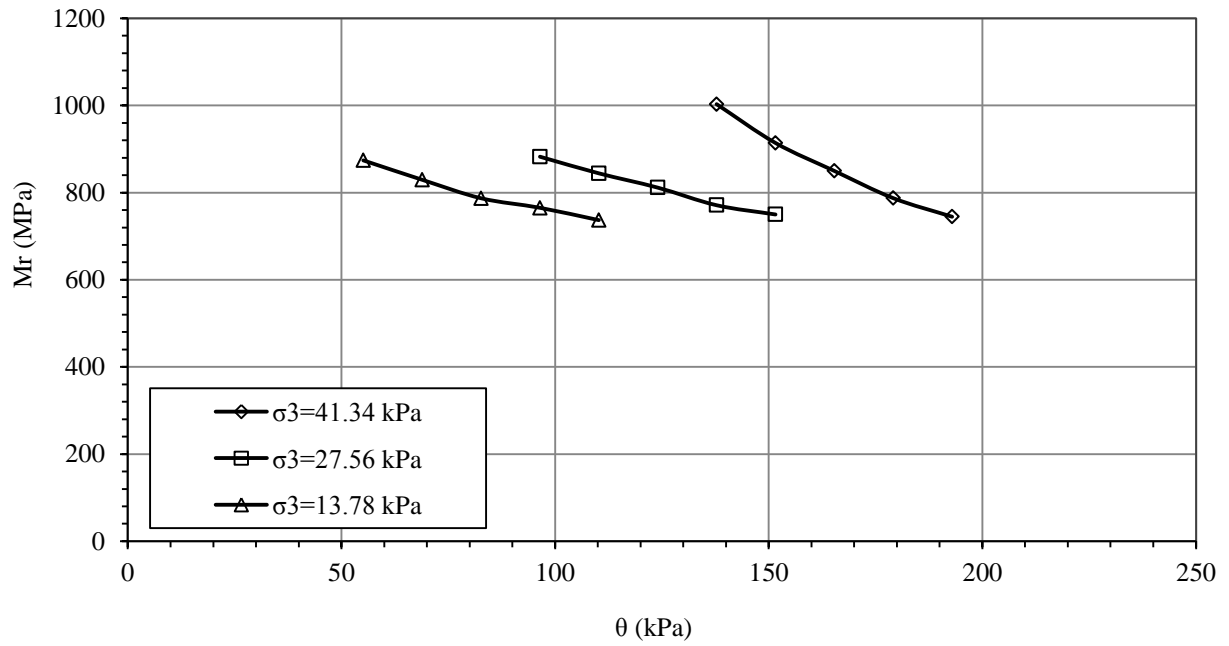


Figure A-1. M_r as a bulk stress at MC = OMC-2%, Specimen No.1.

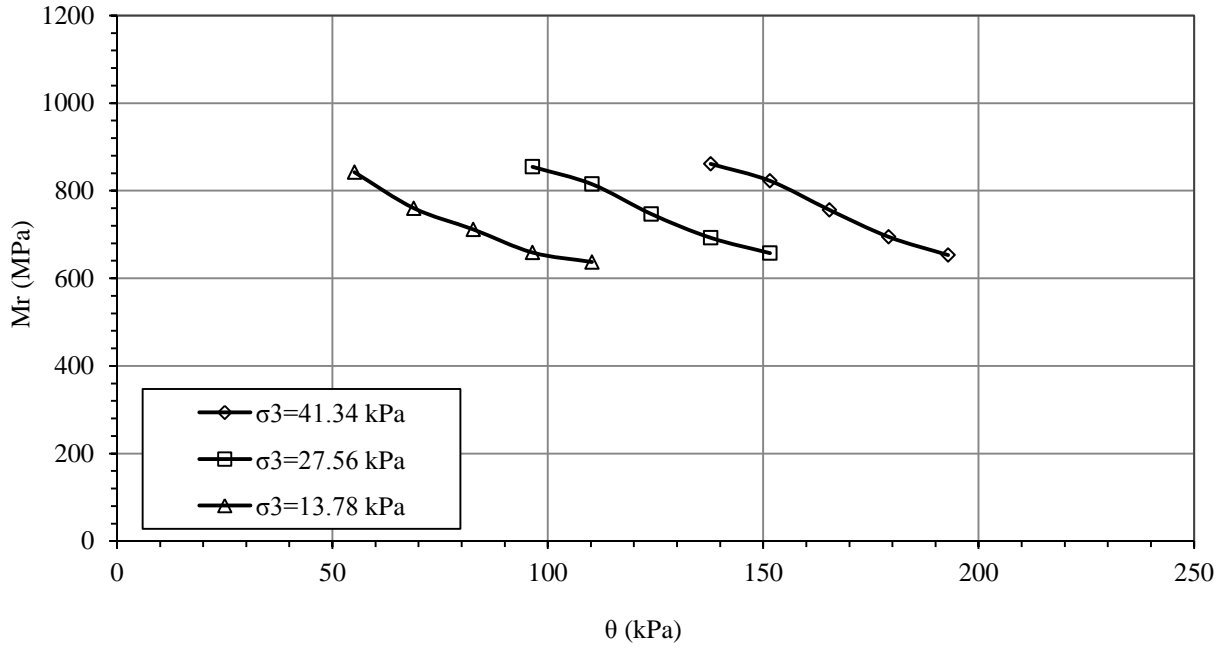


Figure A-2. M_r as a bulk stress at MC = OMC-2%, Specimen No.2.

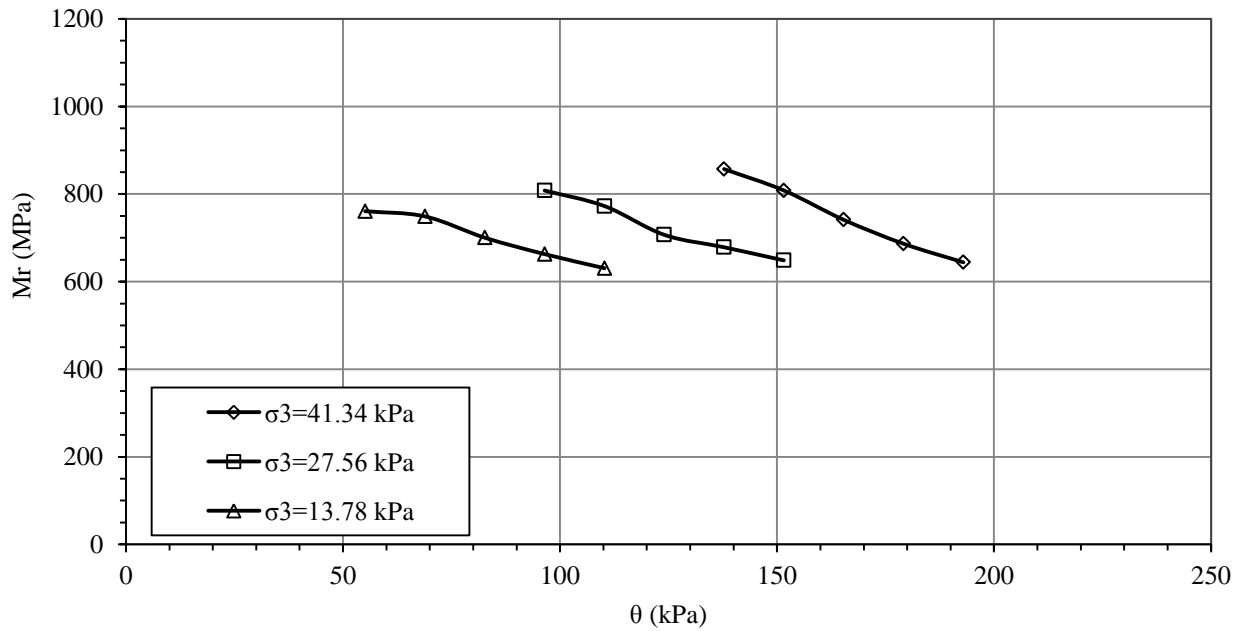


Figure A-3. M_r as a bulk stress at MC = OMC-2%, Specimen No.3.

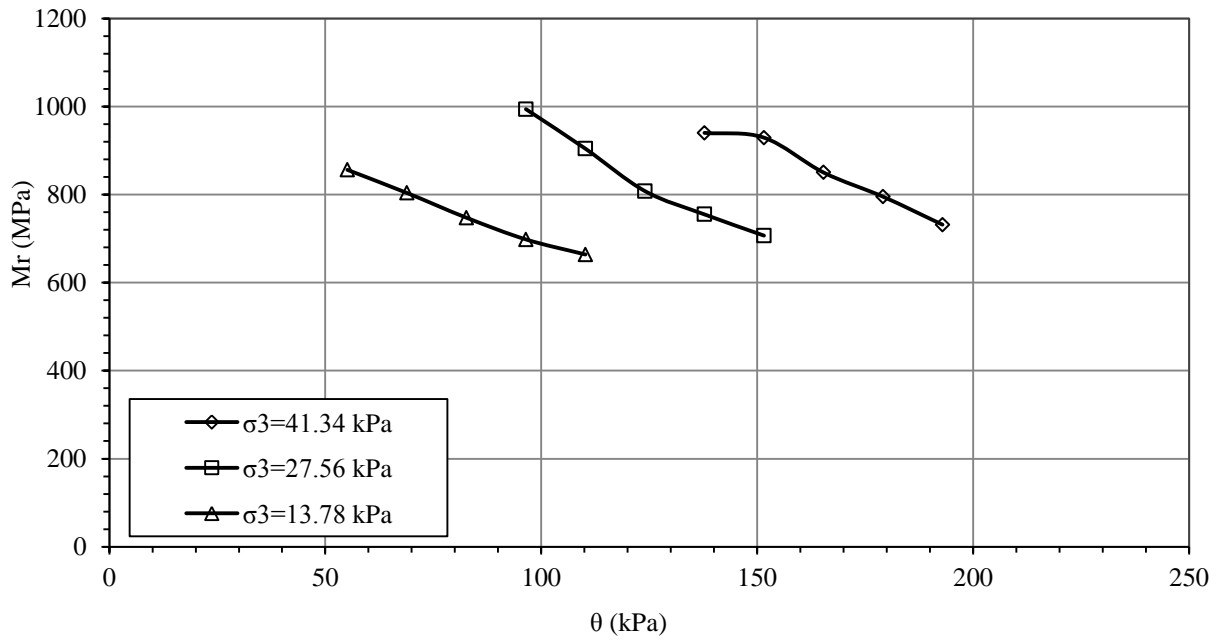


Figure A-4. M_r as a bulk stress at MC = OMC, Specimen No.4.

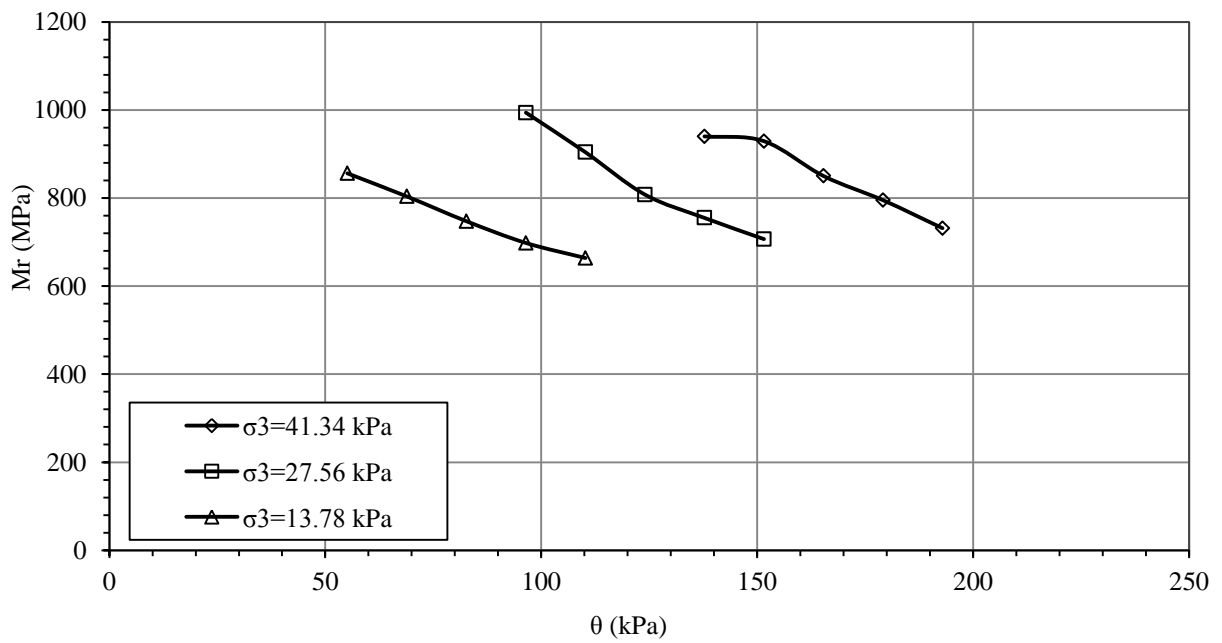


Figure A-5. M_r as a bulk stress at MC = OMC, Specimen No.5.

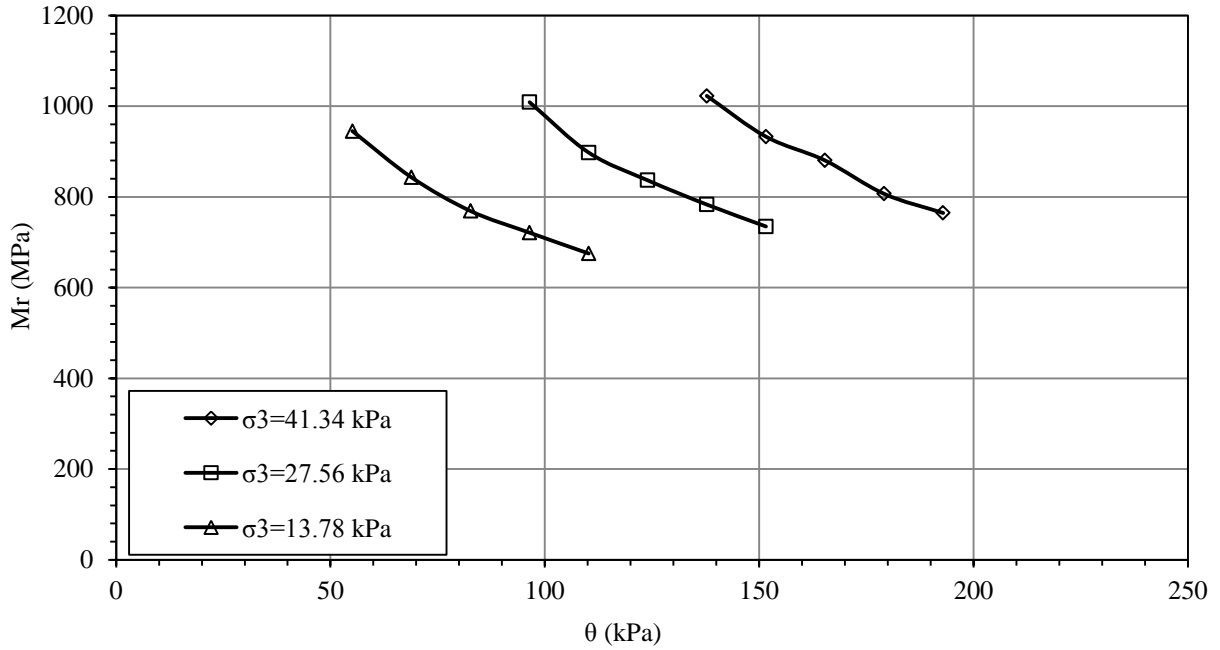


Figure A-6. M_r as a bulk stress at MC = OMC, Specimen No.6.

28-day curing

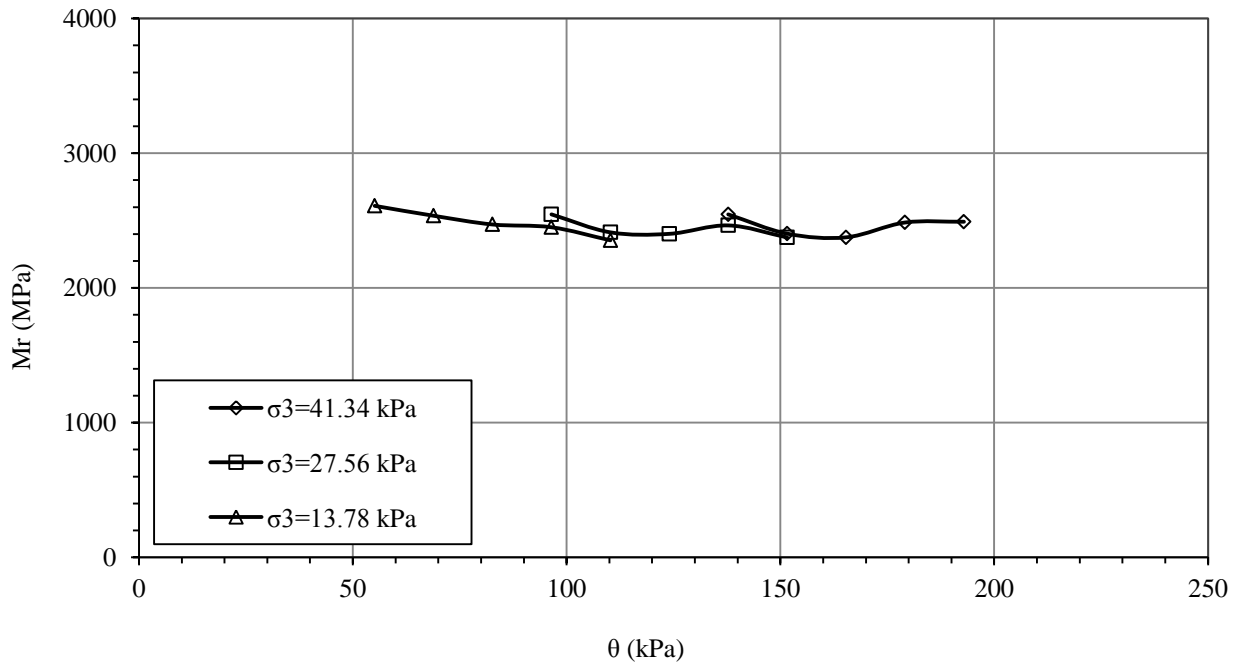


Figure A-7. M_r as a bulk stress at MC = OMC-2%, Specimen No.1.

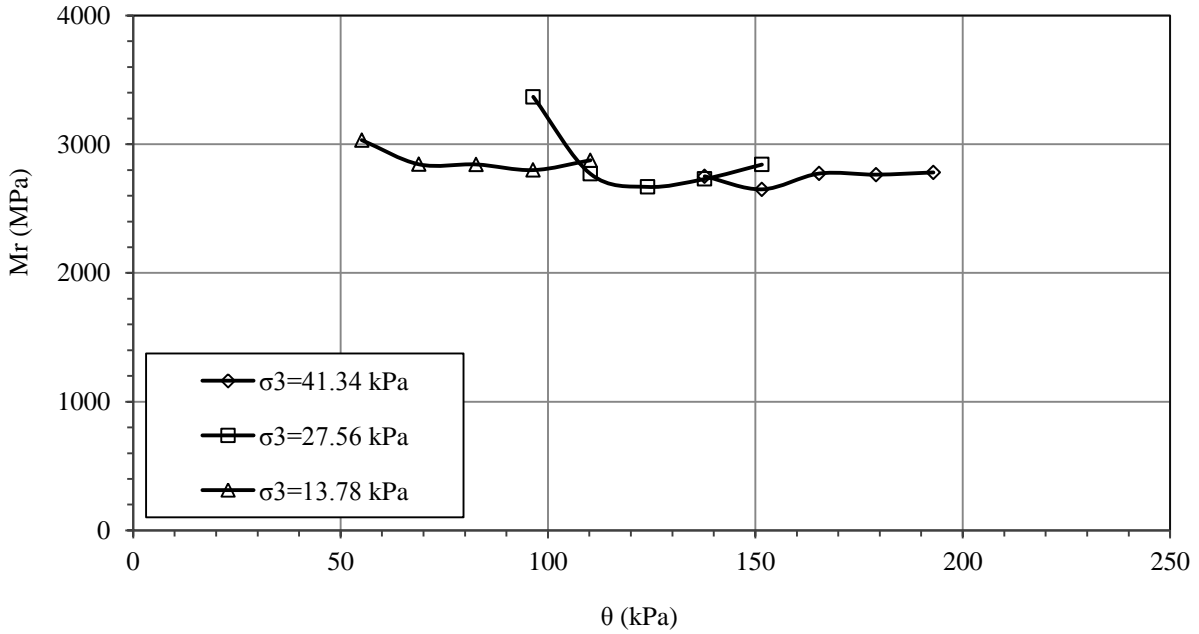


Figure A-8. M_r as a bulk stress at $MC = OMC - 2\%$, Specimen No.2.

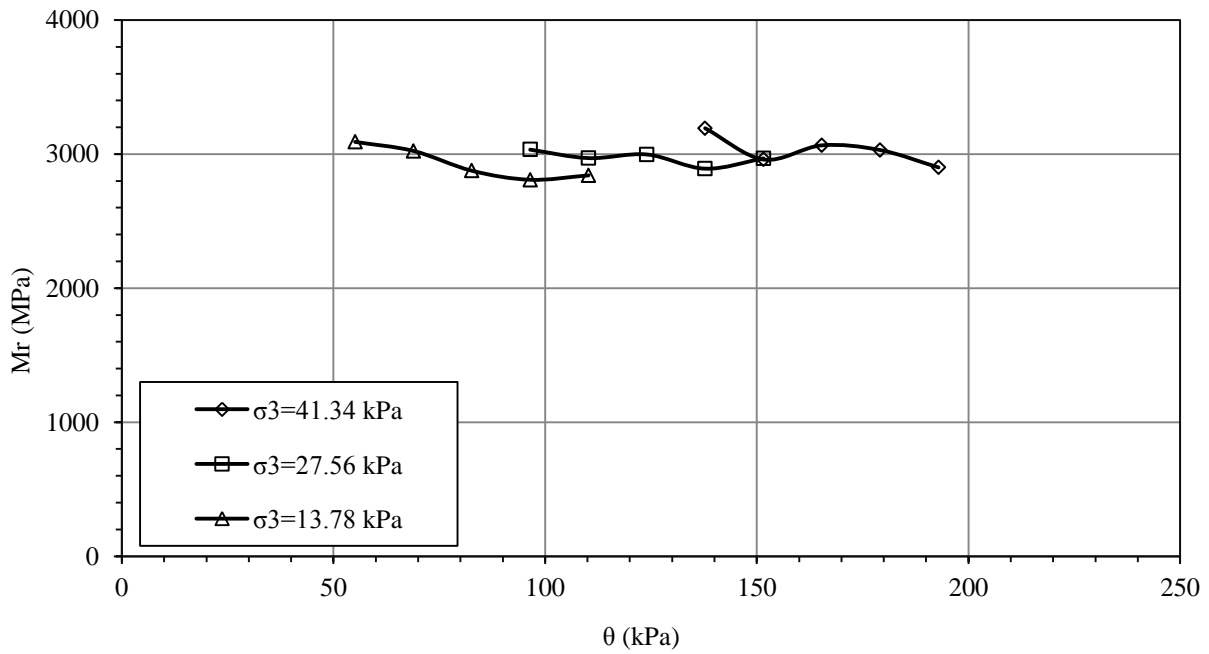


Figure A-9. M_r as a bulk stress at $MC = OMC - 2\%$, Specimen No.3.

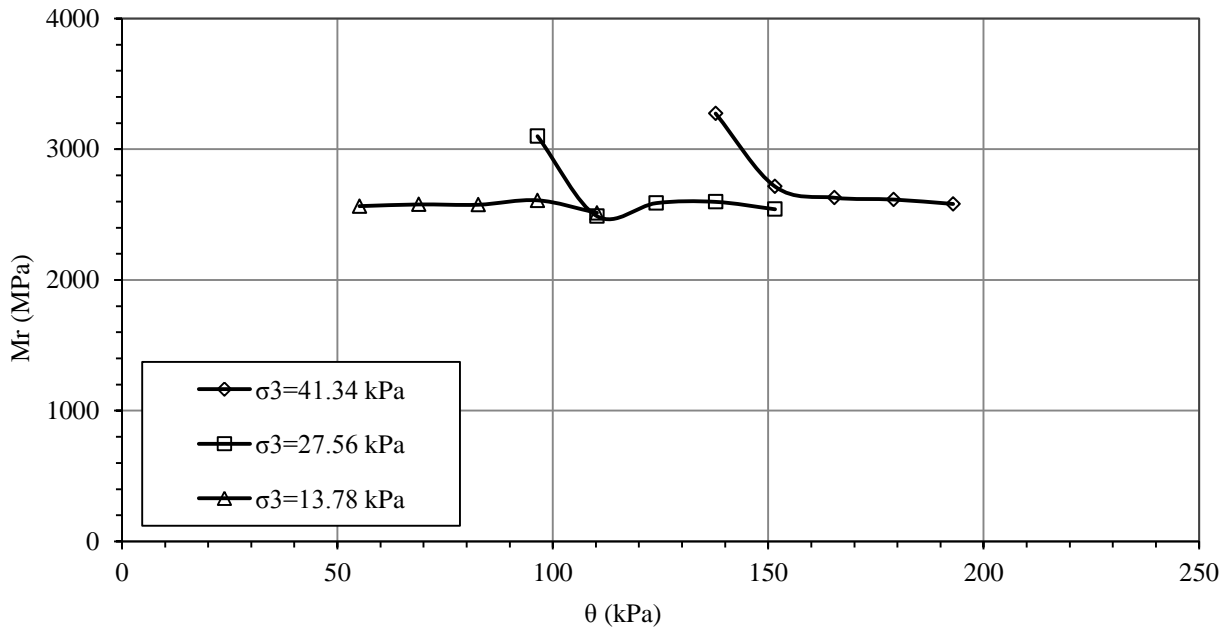


Figure A-10. M_r as a bulk stress at MC = OMC, Specimen No.4.

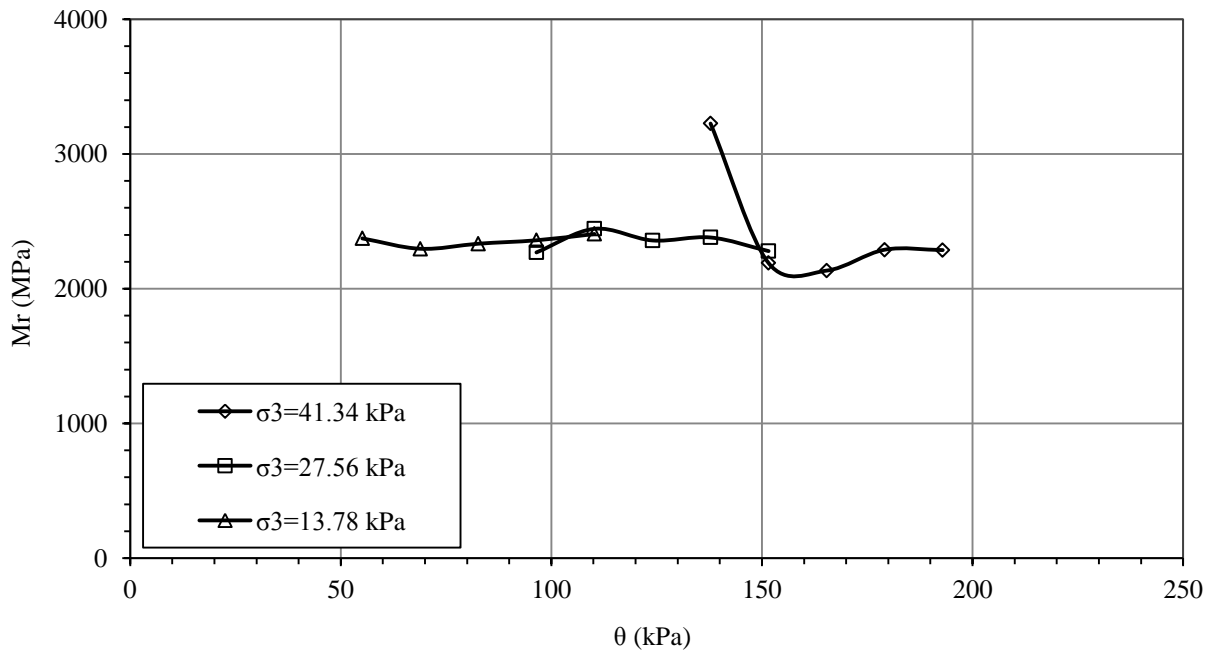


Figure A-11. M_r as a bulk stress at MC = OMC, Specimen No.5.

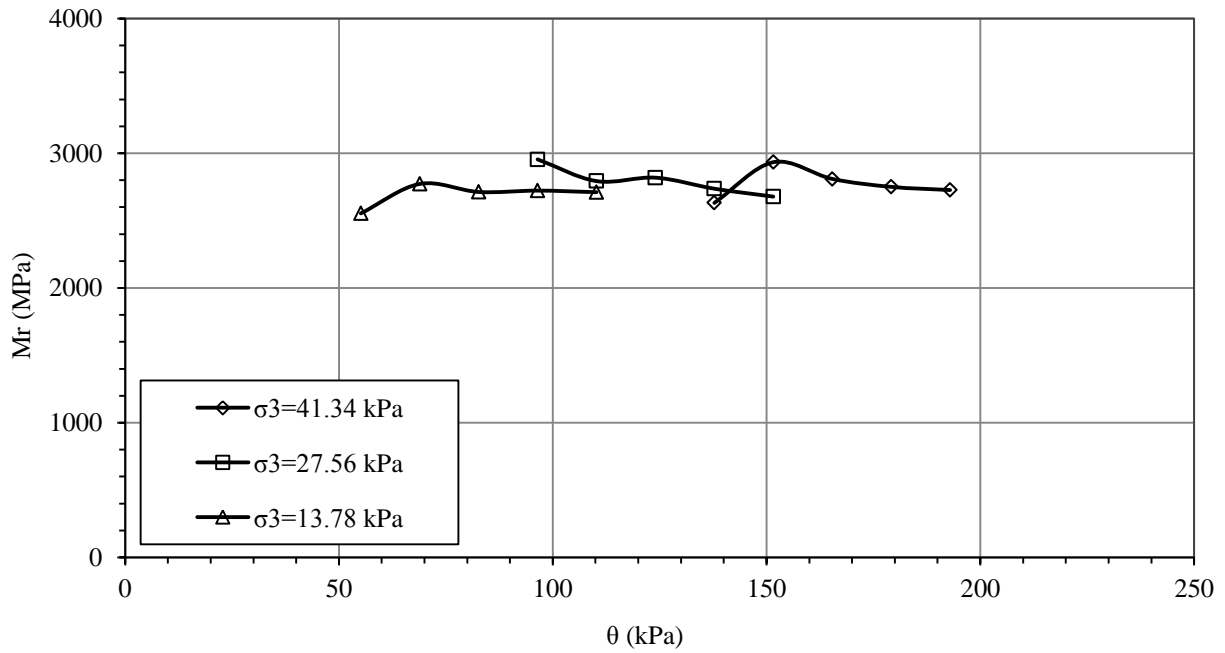


Figure A-12. M_r as a bulk stress at MC = OMC, Specimen No.6.

Apple Valley
0-day Curing

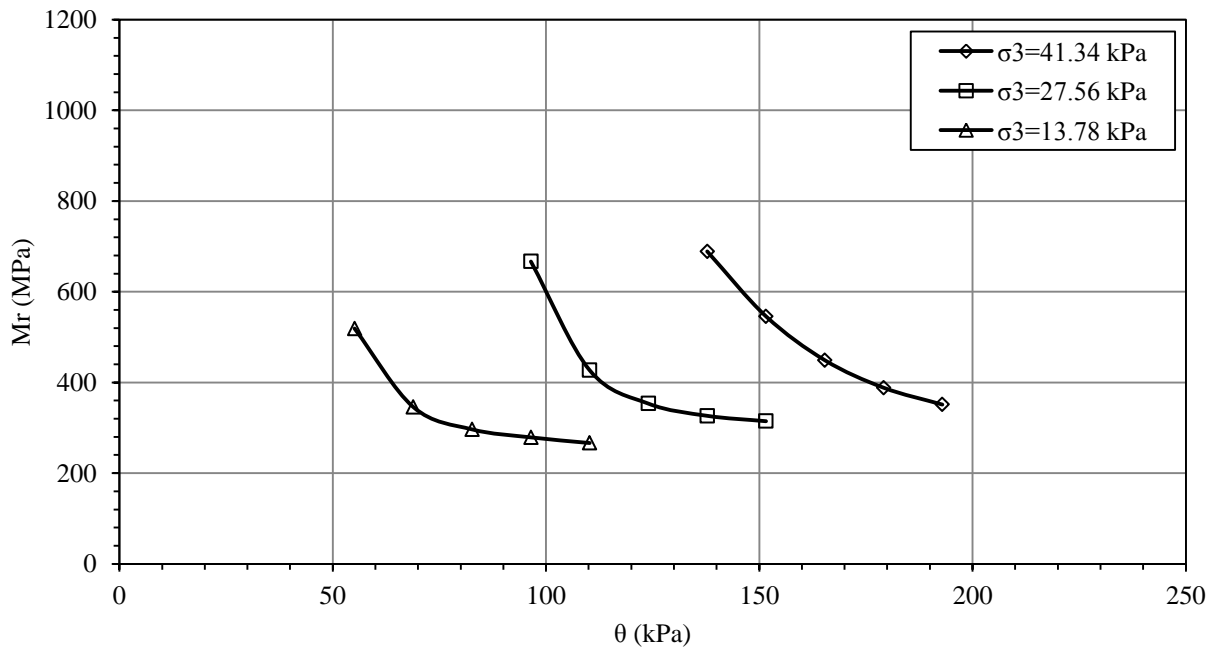


Figure A-13. M_r as a bulk stress at MC = OMC-2%, Specimen No.1.

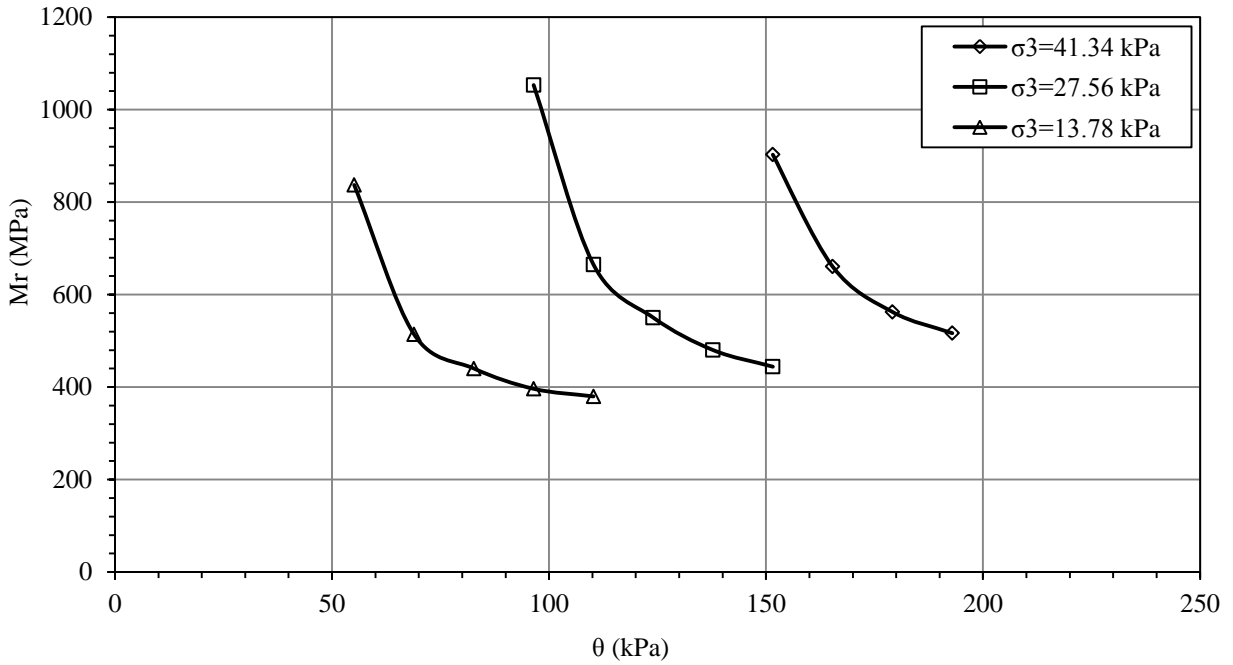


Figure A-14. M_r as a bulk stress at MC = OMC-2%, Specimen No.2.

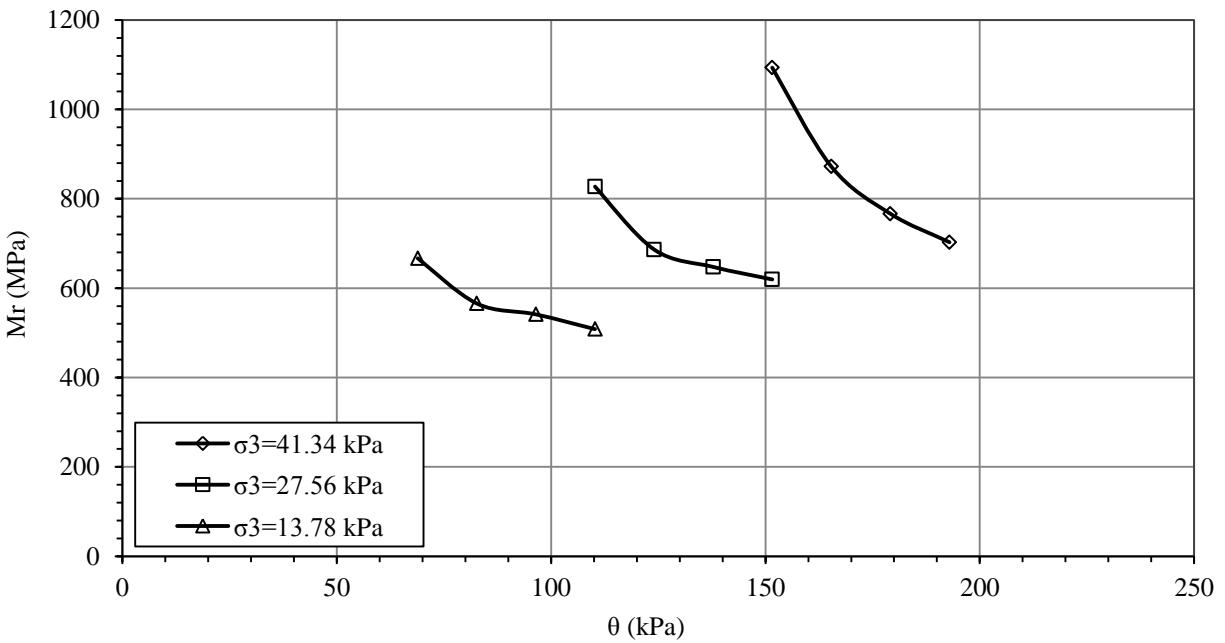


Figure A-15. M_r as a bulk stress at MC = OMC-2%, Specimen No.3.

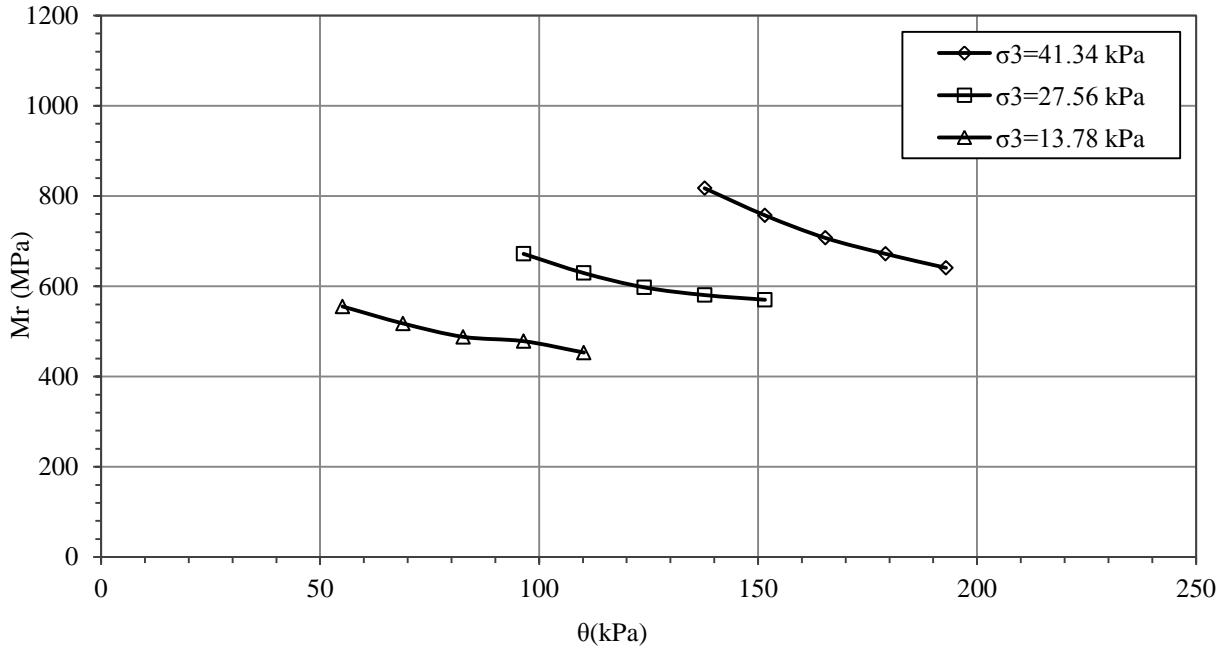


Figure A-16. M_r as a bulk stress at MC = OMC, Specimen No.4.

28-day Curing

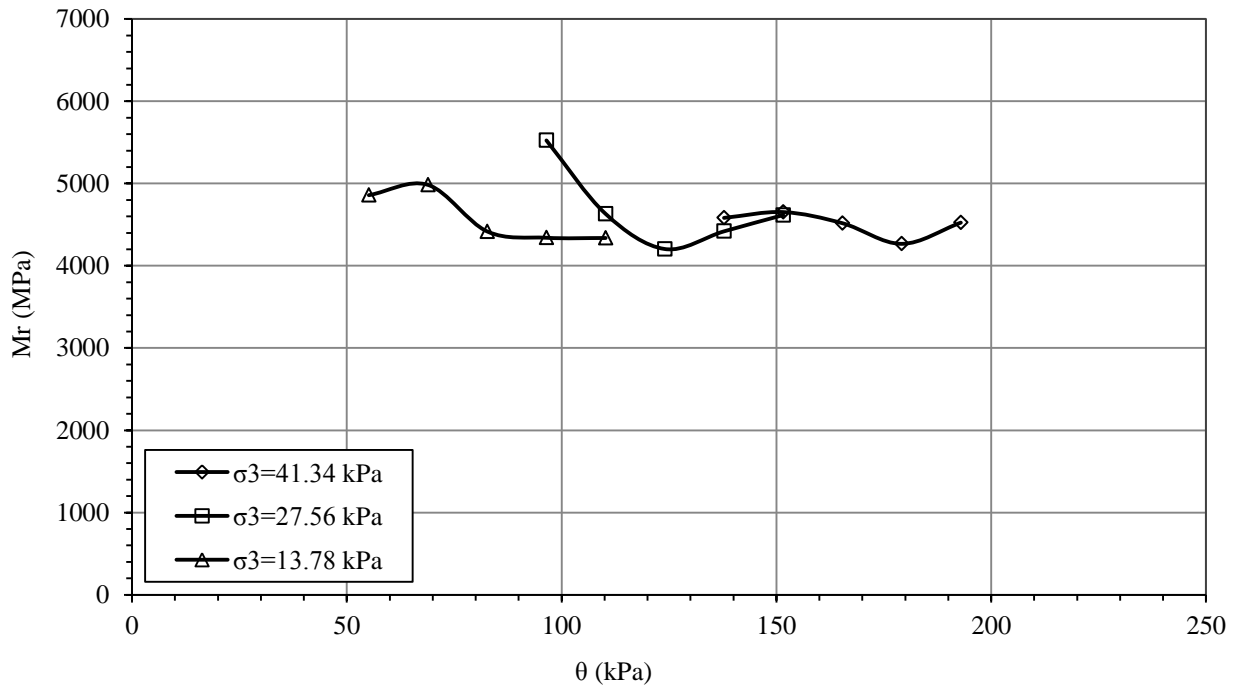


Figure A-17. M_r as a bulk stress at MC = OMC-2%, Specimen No.1.

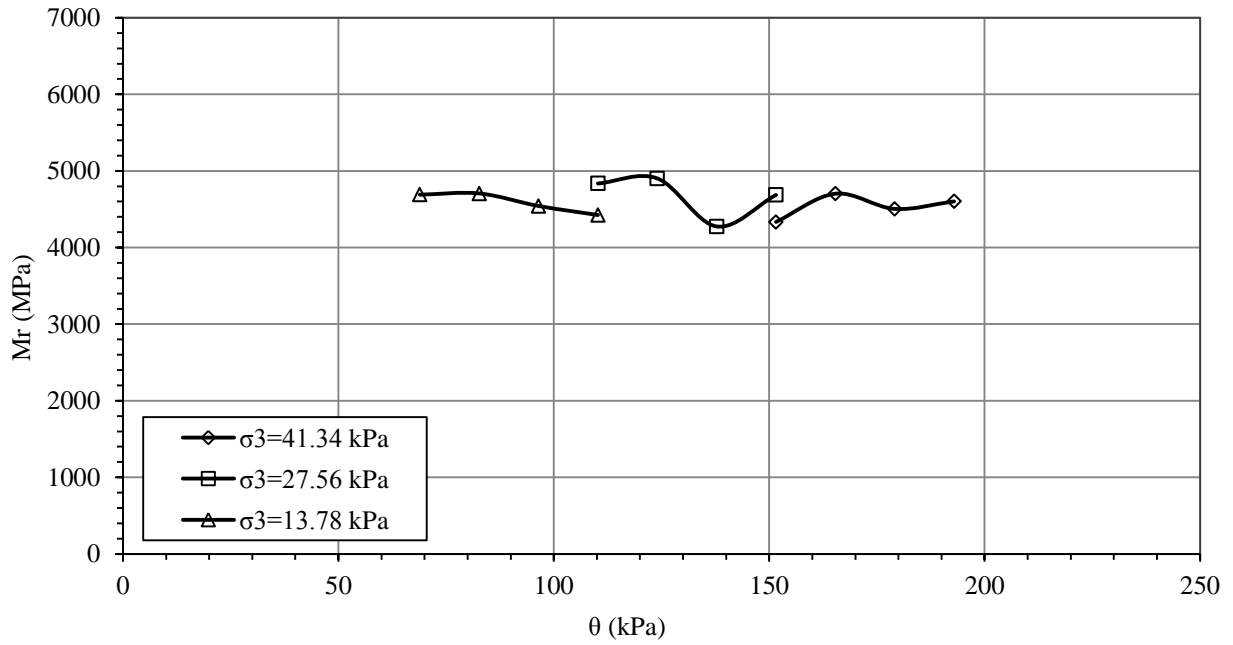


Figure A-18. M_r as a bulk stress at MC = OMC-2%, Specimen No.2.

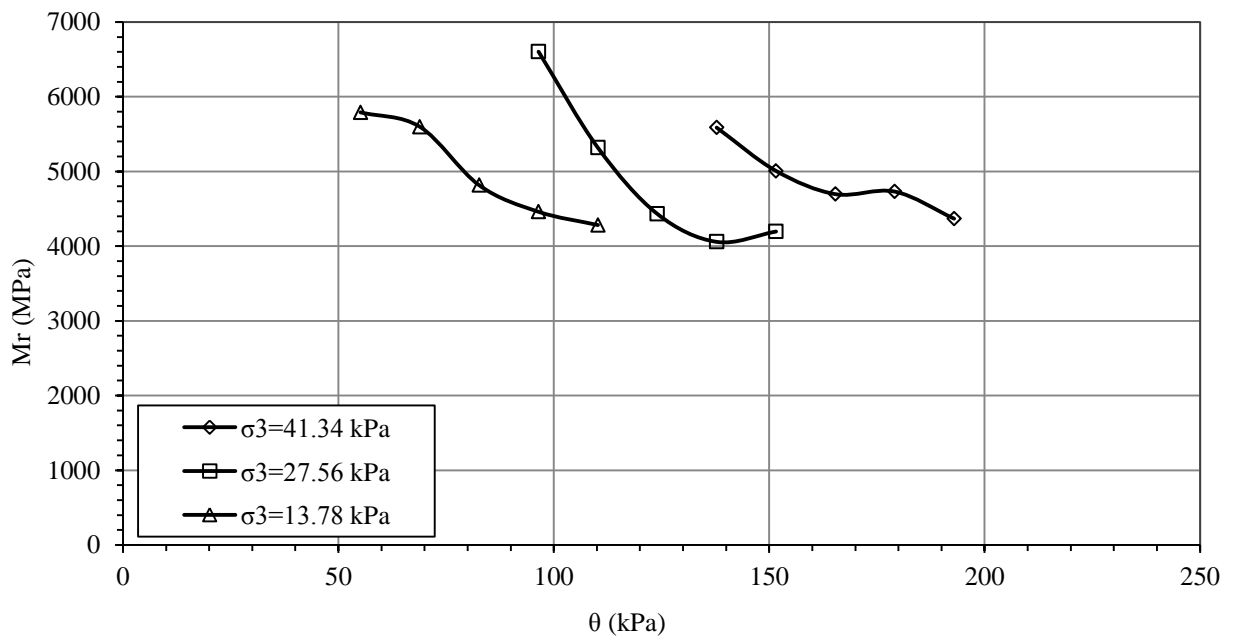


Figure A-19. M_r as a bulk stress at MC = OMC-2%, Specimen No.3.

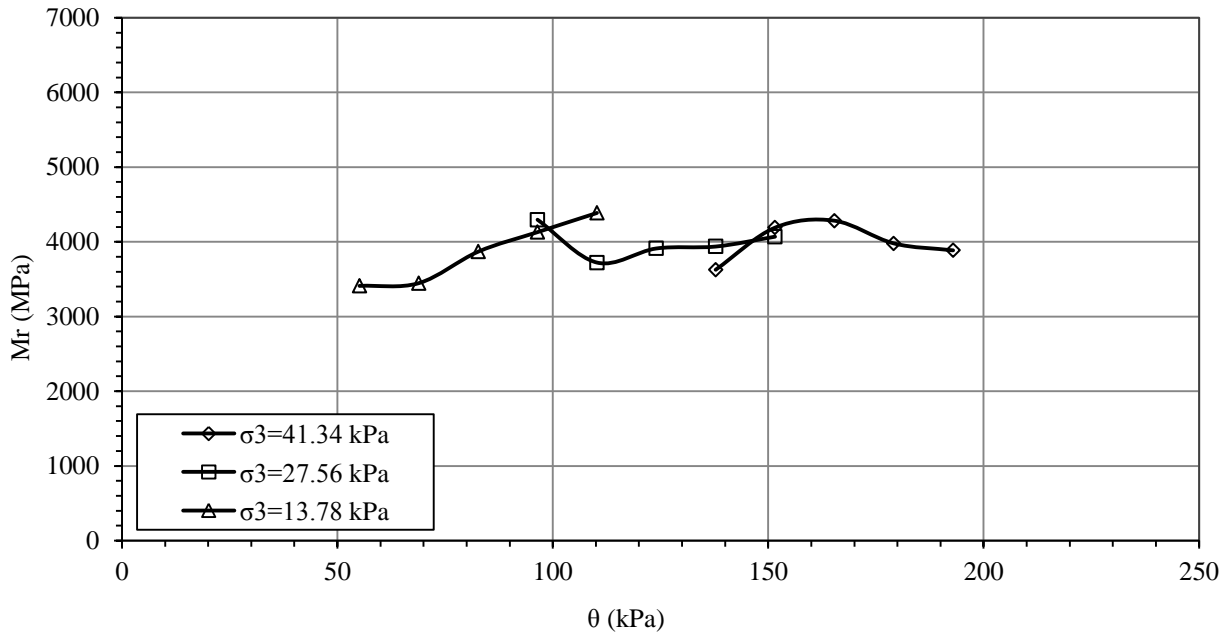


Figure A-20. M_r as a bulk stress at MC = OMC, Specimen No.4.

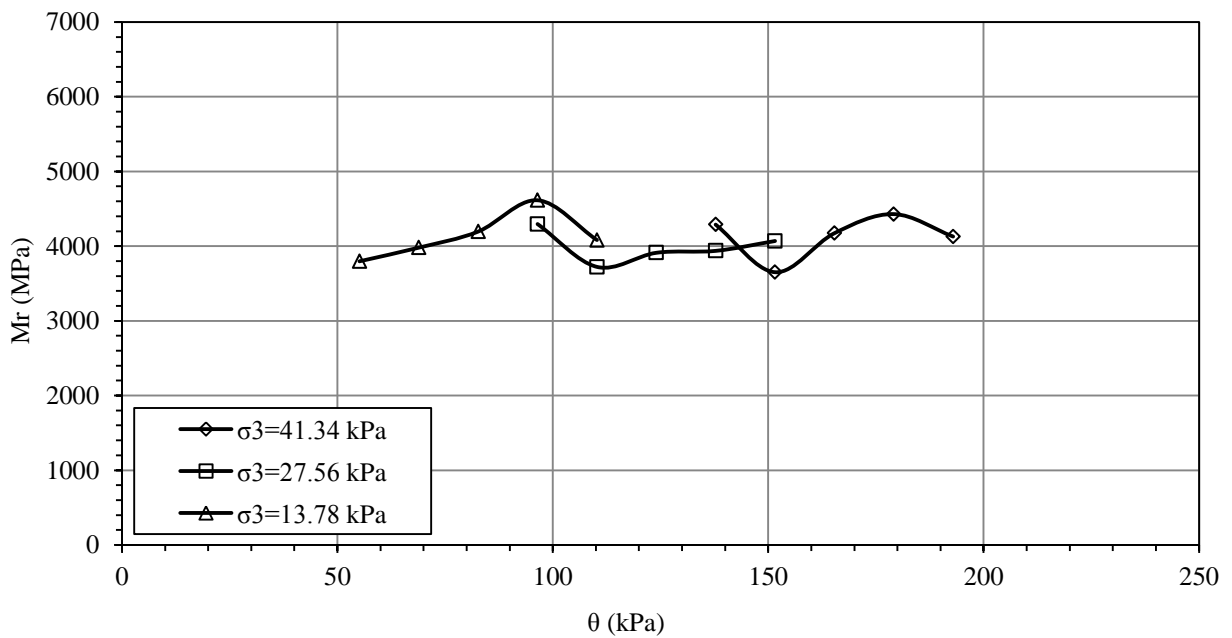


Figure A-21. M_r as a bulk stress at MC = OMC, Specimen No.5.

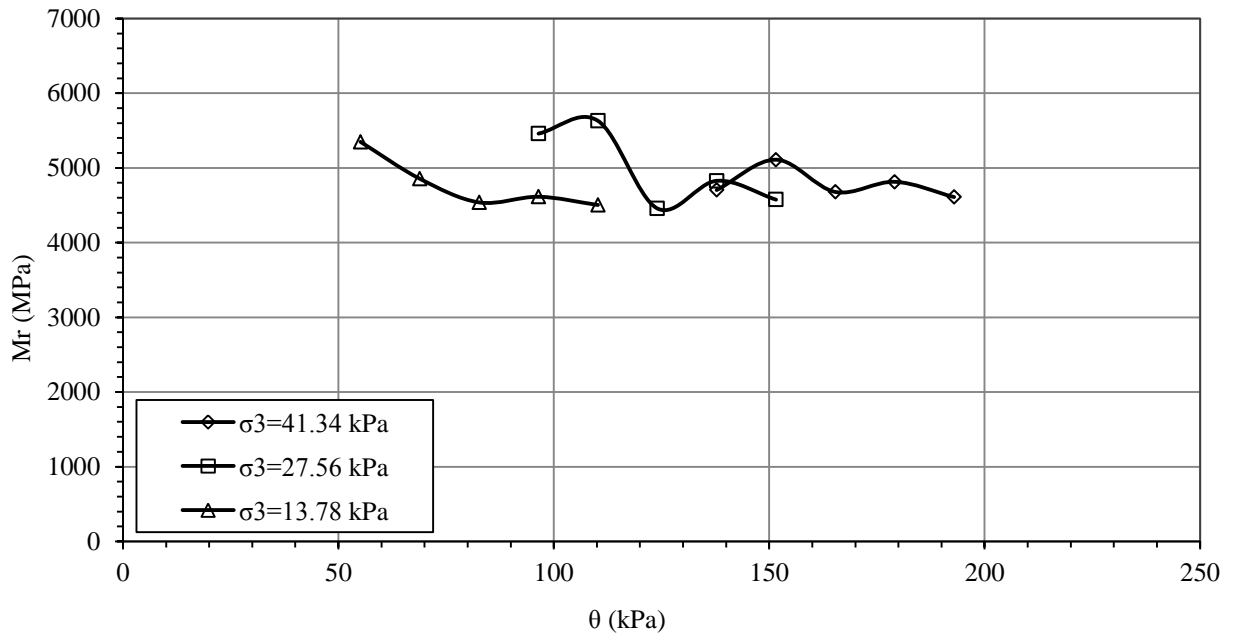


Figure A-22. M_r as a bulk stress at MC = OMC, Specimen No.6.